6th International Conference
on Stability and Handling of Liquid Fuels
Vancouver, B. C., Canada
October 13-17, 1997

MEASUREMENT OF DISSOLVED AND TOTAL WATER CONTENT IN ADVANCED TURBINE ENGINE FUELS WITH A GAS-LIQUID CHROMATOGRAPHIC OTC TECHNIQUE

Steven D. Anderson[1], Wayne A. Rubey*[2], and Richard C. Striebich[2]

[1]Wright Laboratories, POSF, 1790 Loop Road North, Wright-Patterson AFB, OH 45433-7103.
[2]Environmental Sciences and Engineering Laboratory, Research Institute, University of Dayton, 300 College Park, Dayton, OH 45469-0132.

ABSTRACT

Significant capabilities have been developed over the past quarter century for detecting extremely trace quantities of organic compounds in water. However, accurate and precise analyses for water in complex organic mixtures continues to be an analytical challenge. Water is omnipresent and a thin film of adsorbed moisture usually coats every type particle and surface. The analysis for water content in a complex turbine engine fuel is complicated by water sorption onto fine particulate matter and also the presence of numerous fuel additives, e.g., corrosion inhibitors, fuel system icing inhibitors, static dissipators, metal deactivators, detergents, dispersants, etc. Many of these additives affect the interfacial surface tension and the water coalescing properties of the bulk fuel. Instrumental approaches for measuring water content in complex organic mixtures include titration techniques, optical spectroscopy, humidity sensing devices, diode lasers, light emitting diodes, liquid chromatography, and gas chromatography. There has been a real need for a laboratory technique that can provide appropriate water content measurements for turbine engine fuels which contain extensive additive packages. Accordingly, we pursued the gas chromatographic approach for measuring dissolved and free water. Initially, a reaction gas chromatography (RGC) technique was investigated in which water was converted to acetylene by way of a temperature controlled calcium carbide reactor. Although this RGC procedure exhibited considerable sensitivity via detecting water as acetylene using hydrogen flame ionization detection, significant irreproducibility was encountered. Accordingly, various gas-solid chromatographic (GSC) and gas-liquid chromatographic (GLC) scenarios were investigated. It was found that when a modified high-temperature splitter injector assembly is used in conjunction with a highly deactivated and low β value GLC open tubular column, that water can be well-behaved (symmetrical zone profile) and separated from other constituents. Measurement of water content in a variety of turbine engine fuels while using a modulating thermal conductivity detector was found to be both precise and sensitive, even into the sub-ppm region. Using standard addition procedures along with an internal standard, it is anticipated that this GLC analytical method can be simplified for eventual field-scale testing.

INTRODUCTION

Many analytical techniques have been developed for measuring trace levels of organic substances *in water*. Some of these instrumental procedures can measure certain organic constituents at the sub part-per-trillion level.[1,2] The situation is significantly different for measuring *water in* an organic mixture, as analytical techniques only have measurement capabilities down to the low ppm or high ppb measurement regions. Much of this difference in analytical capability is due to ease of contamination and the difficulty in quantitatively transporting trace quantities of water, particularly in various chromatographic scenarios.

With respect to advanced turbine engine fuels, dissolved and total water content represent important information with respect to transferring and refueling aircraft under a severe range of atmospheric conditions. There are many additives in advanced turbine engine fuels which can adversely affect the interfacial tension and the water coalescing properties of the bulk hydrocarbon fuel. They can also form emulsions or micelles as depicted in Figure 1. Example additives are fuel system icing inhibitors, static dissipators, metal deactivators, detergents, corrosion inhibitors/lubricant improvers, dispersants, etc. There has been a pressing need for a laboratory technique that can provide appropriate dissolved and total contained water measurements for turbine engine fuels, along with other complex organic mixtures which contain extensive additive packages.

Background. Under our earthly atmospheric conditions, water is omnipresent. Accordingly, precise measurement of water content is complicated by the physical and chemical nature of the various materials. A thin film of adsorbed moisture usually coats every type of particle and surface. In addition, water is present as a dissolved or dispersed contaminant in practically every organic mixture sample. Consequently, accurate measurement of low concentrations of water in an organic matrix needs to be accomplished with a minimum of atmospheric exposure, sample transfer, and further contamination.

There are a variety of instrumental techniques for measuring water in specific samples. However, an urgent need exists for a general technique which can address a wide range of organic matrices and particularly samples which contain fine particulate matter, assorted additives, and other interfering materials. The Karl Fischer titration procedure[3] has long been used for analyses where water can be liberated and reacted. Also, a variety of spectroscopy

procedures have found wide acceptance when water can be truly isolated from related materials, such as, alcohols, ketones, etc. A gas chromatographic technique was desired which could rapidly separate and detect low ppm concentrations of water in advanced turbine engine fuels. Initially, a precise laboratory procedure was desired in support of fuel research activities for high-performance aircraft. However, a field-portable unit would also be advantageous for monitoring fuel status at flight line facilities.

INSTRUMENTAL APPROACH

For several decades, ppm levels of water have been measured with a reaction gas chromatographic (RGC) procedure. Our laboratory and other research facilities have had considerable success measuring low levels of water using RGC techniques whereby water vapor is passed through a heated calcium carbide reactor.[4] This quantitatively converts the highly adsorbed water to acetylene which is thereafter readily transported and detected by a hydrogen flame ionization detector. High ppb levels of water in jet fuel can be measured using such a procedure. Even so, as the block diagram of the RGC system in Figure 2 shows, there are many stages involved in transporting water, acetylene, and the various associated inert and organic compounds through such an analytical system. It was found that significant and unpredictable error was associated with this particular multi-stage transport and RGC measurement procedure. Different forms of gas-solid chromatography (GSC) were also investigated and found to be unacceptable with respect to quantitatively transporting trace-levels of water. Consequently, a more straight forward gas-liquid chromatographic (GLC) analytical approach was pursued whereby inertness (relative to water) of the chromatographic flowpath was of primary concern.

Modified GLC-OTC Approach. Recent advances in column technology have permitted a different analytical approach for separating and measuring low levels of water. This instrumental approach utilized a modified GLC system which employed a highly deactivated and very thick film polydimethylsiloxane open tubular column (OTC). Detection was with the modulating thermal conductivity detector, although a variety of detection devices could be used, e.g., AED, PDID, etc. A special high-temperature splitter injector[5] was used for injecting approximately two microliters of fuel sample. This high- temperature split assembly used an inerted injector insert (with deactivated glass wool) which needed to be replenished after

approximately 50 injections. A high capacity, but coarse, in-line charcoal trap was used in the vent line of the injector.

The column specifics were the key to obtaining a separation of water from the other trace eluting constituents of the organic mixtures. Although the OTC was deactivated, the thick film of polydimethylsiloxane contributed significantly to the good symmetry of the emerging water zone. The importance of generating symmetrical solute zones is related to both the quantitative precision and accuracy. Specifically, Figure 3 presents a description of the various statistical moments that are associated with generating chromatographic zones. For this type of trace-water analysis, the third statistical moment describes the major criterion. The symmetry (or extent of asymmetry) that exists with an emerging zone is of extreme importance as the initiation and termination of the integration process is determined by the behavior of the extremities of the solute zone. Thus, symmetrical zone profiles always provide far better quantitative measurements in chromatography.

EXPERIMENTAL

We have a strong preference for the GLC separation mode. When chromatography is performed properly in the GLC mode, symmetrical elution profiles are generated.[6] Figure 4 shows a high resolution GC-MS tracing of a typical JP-8 fuel. Consequently, when water can be transported and eluted without skew (like these organic solutes) and analytically separated by GLC, then considerable instrumental simplifications can be obtained. Previously, most gas chromatographic procedures that involved a water separation (particularly the GSC methods) also included extensive solute zone "tailing", which would be extremely detrimental for precise quantitation of the trace amount of water.

The sample introduction mode is of major importance to a laboratory GLC analytical procedure. Two different procedures were investigated; an on-column injection technique, and a high-temperature split injection procedure. In both cases, an extremely thick film GLC-OTC was used as it has two distinct advantages for separating water from other constituents. By having a very thick film column, the water could be slightly retained relative to inert gases that would be dissolved in the jet fuel. Also, the thick film of stationary phase provides further deactivation of the fused silica OTC wall surface. Eventually, we decided upon the modified

high-temperature injector assembly shown in Figure 5. The instrumental arrangement for conducting water-in-fuel analyses consisted of a modified Hewlett Packard 5890 gas chromatograph with a reporting integrator (HP-3390A). This GC instrument had highly filtered helium as the carrier gas. With the splitter injector and a 15 meter megabore OTC having a polydimethylsiloxane substrate (of low phase ratio, or β value), water could be eluted with near-perfect symmetry (see Figure 6). Such an instrumental arrangement allowed water to be easily separated from the other constituents, and Figure 7 shows a typical chromatogram of a JP-8+100 fuel. Figure 8 also shows the early portion of chromatograms for other similar types of turbine engine fuels. These separations were performed with a GLC column temperature of 35°C. The only co-eluting species or interferent in this analysis scenario was propane. Consequently, a series of different jet fuels were analyzed for propane content using the highly sensitive hydrogen flame ionization detector, and here it was found that only extremely small quantities of propane (approximately 0.01 ppm) were encountered.

As water is an omnipresent contaminant, it was found that different syringe needles sorbed differing quantities of water. For example, while under laboratory conditions, a polyimide-clad fused silica needle could contain up to 100 nanograms of water, while a simple #26 stainless steel syringe needle sorbed approximately 10 nanograms of water. Recent information has shown that a special Silcosteel treated needle is especially inert with respect to water sorption, and only miniscule amounts of water have been detected using this syringe needle in conjunction with JP-8+100 fuels.

RESULTS

This particular gas-liquid chromatographic open tubular column method has been able to analyze a variety of turbine engine fuels. Thus far, measurements of water content have ranged from 33 to 144 ppm, by weight. The calibration procedure that is associated with this GLC method utilized a standard addition technique. The precision for the water measurement was found to be 2.48% RSD. It appeared that the largest source of error with the present method is associated with sample delivery. An automatic sampler or a digital syringe should reduce this error.

Water settling time has been observed to be a variable in high water-content analyses. The size of the formed water droplets appears to be especially important. Experiments are

planned for examining several aspects further. Investigations are underway to determine water settling time at different fuel temperatures and water/fuel equilibrium properties with various additive packages.

CONCLUSIONS

The measurement of water content in JP-8+100 fuel can be accomplished with precision using near-conventional GLC technology. Trace levels of water can behave well in an appropriate open tubular column and be measured to sub-ppm concentrations with the use of on-column injection. In this type of analytical work, precautions are needed for dealing with surface adsorbed water. Accurate calibrations for water are achievable using special standard addition procedures. With backflush capabilities, this measurement technique can be scaled down for field testing.

ACKNOWLEDGEMENTS

This work was supported by the Fuels Branch of the US Air Force Wright Laboratory. Part of this effort was performed under the Combustion and Heat Transfer Studies Program, F33615-87-C-2767.

REFERENCES

(1) Grob, K. *J. Chromatogr.* **1973**, *84*, 255-273.

(2) Tomkins, B. A. Griest, W. H., and Higgins, C. E. *Anal. Chem.* **1995**, *67*, 4387-4395.

(3) Fischer, K. *Angew. Chem.* **1935**, *48*, 394-399.

(4) Knight, H. S., and Weiss, F. T. *Anal. Chem.* **1962**, *34*, 749-751.

(5) Sandra, P. *Sample Introduction in Capillary Gas Chromatography: Volume 1*, Huthig: Heidelberg, 1985.

(6) Giddings, J. C. *Unified Separation Science*, Wiley: New York, 1991.

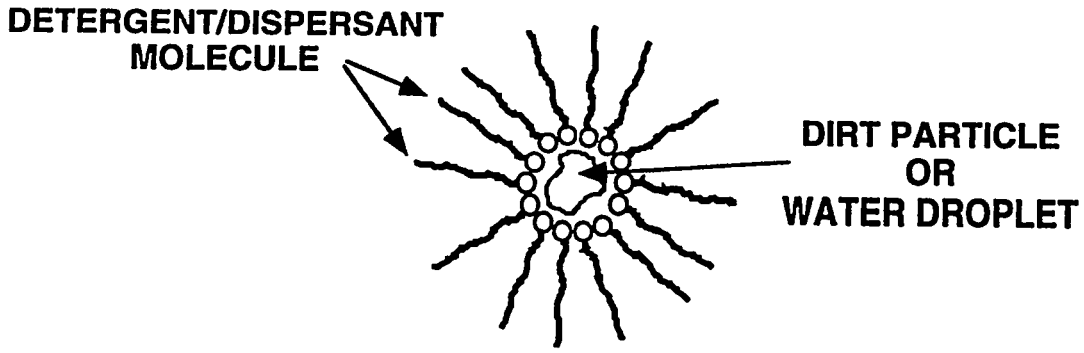

Figure 1. Detergent/dispersant additives can form micelles around dirt particles and water droplets. This prevents agglomeration of particles needed for removal in current filter/coalescer media.

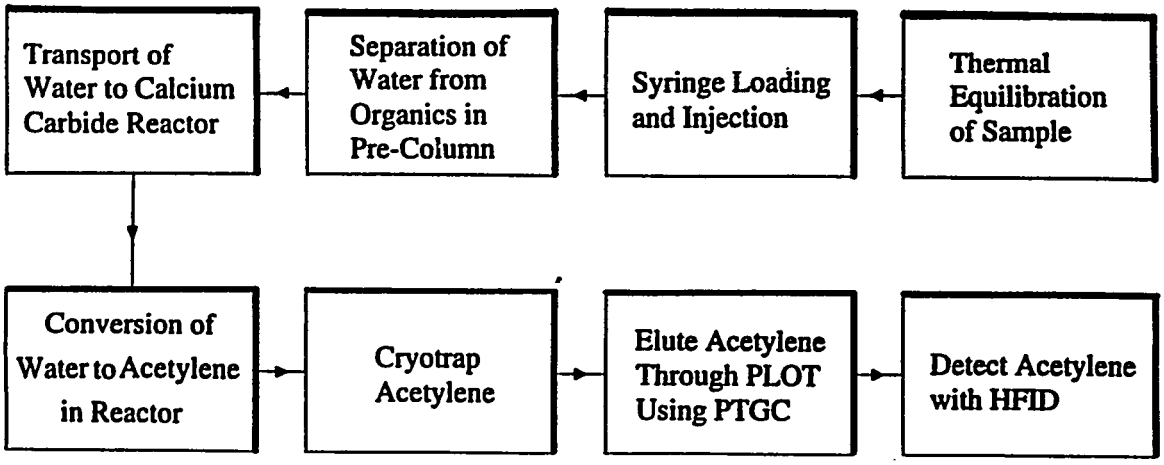

Figure 2. Block diagram of reaction gas chromatographic (RGC) procedure.

$$\bar{m}_k = \frac{\int_0^\infty c(\tau)(\tau - m_1)^k d\tau}{\int_0^\infty c(\tau) d\tau}$$

m_0 = zone area

m_1 = zone retention time

$\bar{m}_2$ = zone time variance

$\bar{m}_3$ = zone skew, or asymmetry

$\bar{m}_4$ = zone kurtosis, or flattening

Figure 3. Statistical moments of emerging GC solute zones.

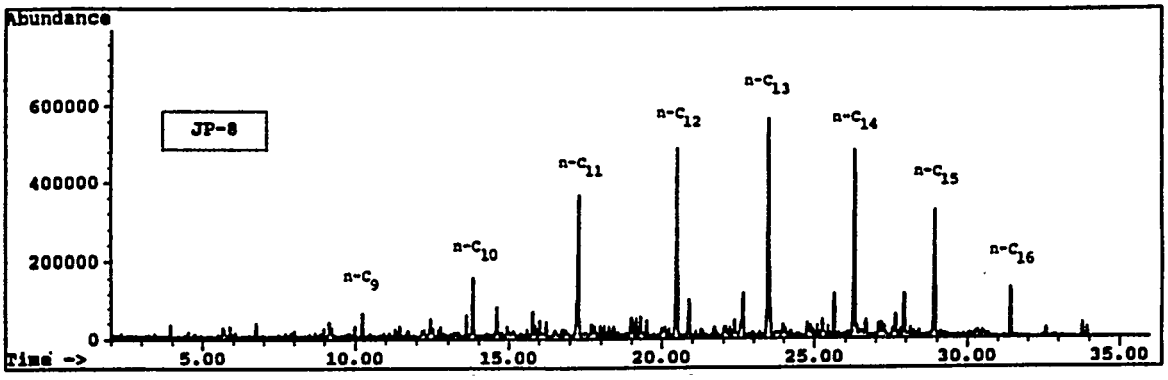

Figure 4. GC-MS output signal for a JP-8 fuel.

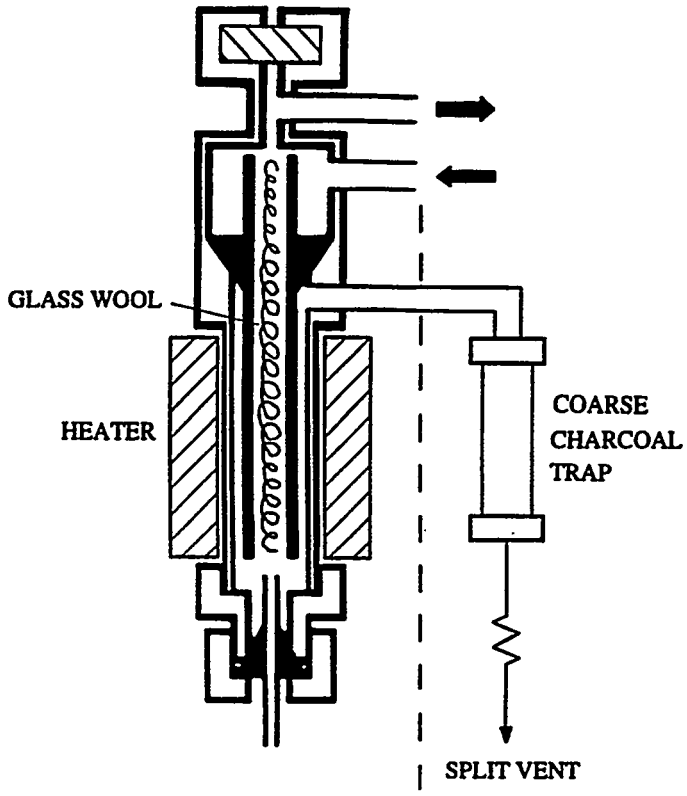

Figure 5. Modified high-temperature splitter injector assembly.

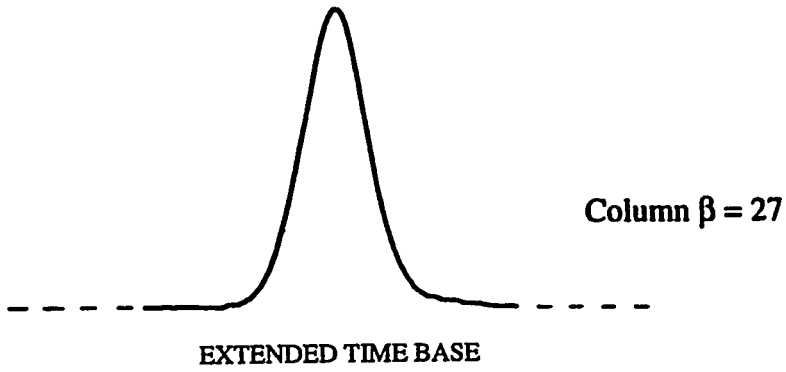

Figure 6. Near-perfect symmetry of water elution zone.

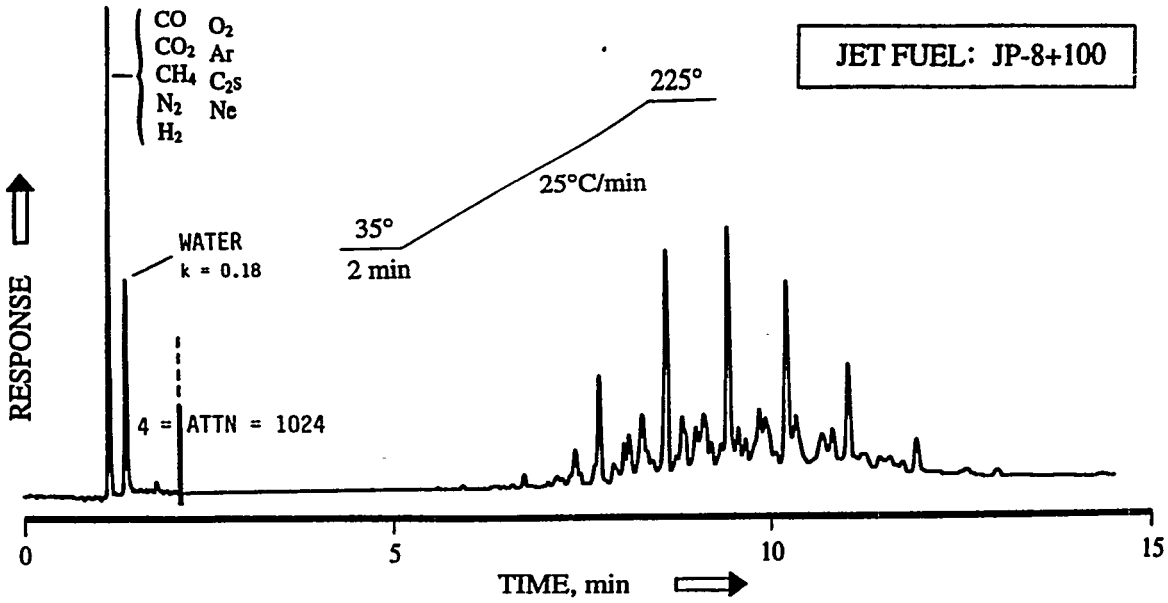

Figure 7. Typical GLC chromatogram of a JP-8+100 fuel.

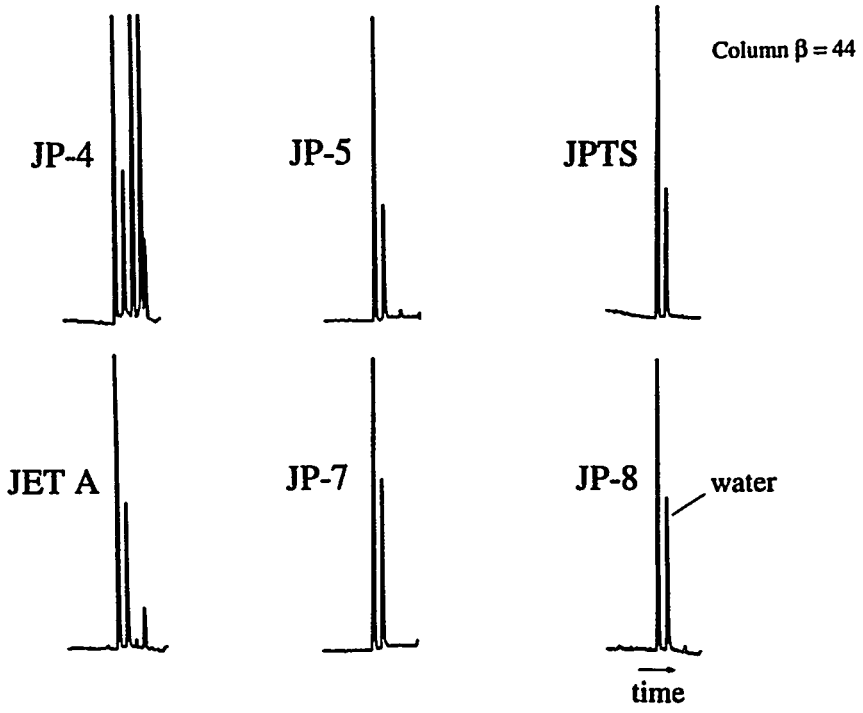

Figure 8. Early elution portion of GLC chromatograms of other types of jet fuels.

6th International Conference
on Stability and Handling of Liquid Fuels
Vancouver, B.C., Canada
October 13-17, 1997

AVIATION FUEL HANDLING: NEW MECHANISTIC INSIGHT INTO THE EFFECT OF SURFACTANTS ON WATER COALESCER PERFORMANCE

Victor B. Hughes

Shell Research & Technology Centre, Thornton, P.O. Box 1, Chester, CH1 3SH, U.K.

Aviation fuels may contain trace polar materials of a type and at a concentration sufficient to impair the performance of filter-water-coalescers in the removal of dispersed droplets of free water from the fuel. This process, commonly called "coalescer disarming" may cause the transmission of unacceptable levels of free water. There are a number of proposed mechanisms for this phenomenon, one of which invokes a change in "(water-)wettability" of the coalescer fibres as a result of surfactant adsorption. In this paper the results of fibre wettability changes observed using an Environmental Scanning Electron Microscope (ESEM) are presented. Bundles of fibres may be observed in the ESEM whilst the water vapour pressure is varied. Precipitation of water droplets onto the fibres may be induced by cooling the stage holding the fibres and increasing the water vapour pressure. Thence the contact angles made by water droplets may be assessed for fibres exposed to fuels with and without potent surfactants. Droplet growth may also be observed until coalescence occurs. Surprisingly the observations reveal that the trend in fibre wettability as a function of surfactant exposure does not go the way expected from considerations of currently proposed mechanisms. Fibres exposed to surfactants appear to be prone to water swamping rather than becoming hydrophobic. The implications of this observation will be discussed in terms of macroscopic coalescer performance observations.

1. Introduction

Water can become entrained in jet fuels as very finely divided droplets, often <40 μm in diameter. In this finely divided state, water will not readily settle out of the fuel under gravity alone. The Stokesian settling rate for 20 μm droplets in a typical jet fuel is approximately 15 mm/min. For even finer droplets gravity settling becomes totally ineffective as Brownian motion dominates.

The exclusion or removal of water from jet fuel is of major importance to the distribution and supply industry in order to guard against the delivery of contaminated fuel into-plane and the consequent potential catastrophic consequences of an in-flight failure. Increasing the droplet

size of fine water dispersions by fibre bed coalescence is one of the currently adopted solutions.

1.1. Filter/Water Separators

These devices (complying with an API 1581 specification) contain two types of element (Fig. 1). Firstly the fuel passes through a combined filtration and water coalescence element (in-to-out) where dirt particles >1μm in diameter are filtered out and finely dispersed water droplets are coalesced into larger droplets which easily settle out of the fuel under gravity. Secondly the fuel passes through a separator element (out-to-in) which is usually a simple hydrophobic (water-repelling) screen. Coalesced water drops settle out of the fuel rapidly and accumulate in the sump whence bulk water can be drained off. Vessels usually contain more than one of each element type. Each element has a maximum recommended flow rate and this value is used to calculate the numbers of elements needed for a particular flow rate.

2. Dispersed water coalescence:

Definition: "The process of joining together two or more bodies of the same fluid, separated by another immiscible fluid. One of the fluids must be a liquid, the other can be a liquid or a gas."

2.1. Coalescence Mechanisms.

Droplet-droplet coalescence (AUTOCOALESCENCE) may occur if the number population of water droplets is high enough and if there are no antagonistic components in the fuel.

The Hazlett model[1] for coalescence processes in a fibrous bed has remained unchallenged for many years. The model (Fig. 2) comprises four main steps:

- Approach of a droplet to a fibre,
- Attachment of the droplet to the fibre,
- Coalescence of droplets on the fibre and
- Release of enlarged droplets from the downstream side of the fibre bed.

In summary: PROXIMITY, INTERCEPTION, GROWTH, RELEASE.

Of the interception mechanisms, inertial, direct collision and diffusional, Hazlett considers that direct collision is the most likely and inertial impaction the least likely (on hydrodynamic

grounds). Diffusion is only likely to contribute with the smallest droplets and at low velocities. On this premise Hazlett developed a Langmuirian model for the interception of droplets at a single isolated fibre, derived from purely hydrodynamic considerations and for superficial velocities less than a critical value of about 1.5 cm/sec.:

$$E_S = \frac{1}{2(2-\ln N_R)}\left[2(1+r)\ln(1+r)-(1+r)+\frac{1}{(1+r)}\right] \qquad 1)$$

where: E_S = interception efficiency (%) i.e., the efficiency of collection by a single fibre from a fluid stream of a width equal to the diameter of the fibre,

N_R = Reynold's No. = $v\, d_f \rho / \mu$

v = superficial velocity,

d_f = fibre diameter,

d_p = droplet diameter,

$r = d_p / d_f$

However this model takes no account of any non-hydrodynamic effects which may reduce interception efficiency and assumes that every droplet/fibre interception is 100% successful. Hughes and Foulds[2] introduced an empirical correction factor, σ, to account for coalescence systems which failed to conform to the Hazlett model, when:

$$E'_S = \sigma E_S \qquad 2)$$

For aqueous emulsions σ was related to electrostatic effects only. In the jet fuel system, a similar factor could be related more comprehensively to both electrostatic and steric repulsion effects. More importantly Hughes and Foulds extended the Hazlett model to a number of non-interacting fibres in a fibre bed based on sequential probabilities of interception:

$$E_B = \left(1-E'_S\right)^n \qquad 3)$$

where: E_B = Coalescence Efficiency of the whole bed,

$$n = 2(1-\varepsilon)\left(\frac{d}{d_f}\right)$$

ε = porosity of the bed,

d = bed depth.

Not much is known about the subsequent stages of coalescence but in an effectively operating fibrous bed coalescer, water appears to be released from specific "active" sites on the downstream side. The coalesced dispersed phase has been observed to accumulate in the upstream part of the fibrous bed and to feed threads of liquid through the bed, bridging fibre-

to-fibre. Release of large coalesced drops of water remains "black-art" with most coalescer manufacturers providing a relatively coarse weave cotton "sock" as the final release medium.

2.2. Coalescer Disarming.

Experiments on a full-sized test rig have shown a dramatic reduction in coalescer efficiency in the presence of a model fuel surfactant (Aerosol OT, which is a sulphosuccinate). The results of these experiments are shown in Fig.3. The coalescer was subjected to a fuel in which 1% volume of water had been finely dispersed. The base fuel with no surfactants or additives transmitted only 5 ppmv water maximum during an extended test period. However, as can be seen in Fig.3, increasing the concentration of surfactant in the fuel caused increasing levels of water transmission.

Sodium naphthasulphonate (SNS) has long been known in the industry to produce the same effect at levels of only 0.4 ppm. Recent work commissioned by the Institute of Petroleum and carried out on the test facility at Thornton indicate the potency of this material in causing disarming (Table 1). Neither SNS nor AOT are likely components of jet fuel but are representative of those that are and as such can be used in laboratory and rig investigations of disarming.

Coalescer failures of this type are known as "coalescer disarming" and are thought to be the result of surfactant adsorption onto the glass fibre coalescer surfaces and also onto the hydrophobic water separator element altering the water-wetting properties of those surfaces in an adverse way. Jet Fuels may occasionally contain surfactants as a result of the type of crude oil used by a refinery or deficiencies in the processing steps. These can be quite potent in causing coalescer disarming and in the field many examples have been encountered. Additives which contain surfactant material such as Static Dissipators when used at their normal working dosage rates are not known to cause problems.

2.3. Proposed Mechanisms for "Disarming"

The two theories currently being advanced to explain coalescer disarming are based on droplet size and fibre wettability considerations respectively.

2.3.1. Droplet Size.

The Hazlett model clearly indicates that the smaller the droplet size for a given fibre diameter the less the probability for interception. Droplet size is related to mechanical shearing but also to the interfacial properties of the fuel/water interface. The lower the interfacial tension then the smaller the droplet size for a given shear regime. Interfacial tension (IFT) measurements for water and fuels containing either SNS or AOT indicate subtle differences in their behaviour (Fig.4). AOT is very effective in reducing IFT and has been extensively reported in literature to be a very powerful emulsifier. The IFT data for SNS indicates this material to be potentially much less effective as an emulsifier. This is very interesting in terms of coalescer disarming because it suggests that the disarming seen with AOT is much more likely to arise from a droplet size effect whilst for SNS, and materials of similar IFT response, another mechanism must be sought.

Conclusion: Surfactant materials active at the fuel/water interface are most likely to produce coalescer failure because of the smaller water droplet size produced by shear in such systems. This effect is purely hydrodynamic and is predicted by the Hazlett model. In the field, fuels behaving in this way could be identified by a simple water haze stability measurement.

2.3.2. Fibre "wettability".

The glass fibre medium used in conventional filter-coalescer elements presents a surface which has both hydrophilic (silicate) and hydrophobic (organic resin) regions. It is commonly thought that water interception and growth occurs at the hydrophilic sites. Surfactant adsorption can also occur at the hydrophilic sites because surfactants have polar groupings within the molecule. Such a process will alter the surface properties of the glass fibre. For many years it has been the view of many in the industry that the process produces a fibre surface with hydrophobic properties with the result that water droplets are not intercepted but migrate without coalescence through the media.

Conclusions: Surfactants especially active at the solid/fuel interface might be expected to dominate this disarming process. In the field, fuels behaving in this way would require a more

sophisticated and controlled method for identification, one in which the coalescer fibres have adequate exposure to the potent fuel components.

3. Characterisation of Fibre Surfaces by ESEM

To explore further the surface properties of glass-fibres used in water coalescence media a new approach was taken. The development of Environmental Scanning Electron Microscopy[3,4] in which a sample can be examined in a vapour space saturated with water (25 millibar at room temperature) permits the condensation of free water onto the specimen fixed to a cold mount. Further, the samples can be studied without the need for coating because the controlled environment ensures that surface charging is neutralised (Fig.5).

3.1. Experimental:

Dry coalescer fibres were taken from a Velcon Filters Inc. filter coalescer Model 85. Fibres were then immersed for 24 hours in either a clay-treated Jet A-1 fuel or the same fuel to which had been added 1%v/v Petronate L (Sodium Naphthasulphonate - supplied by Witco). The samples were allowed to dry and then glued to a conventional SEM stub.

The ESEM was operated with a water vapour pressure of 6-7 millibars and the sample was maintained at ambient temperatures during normal data aquisition. To initiate water droplet formation on the fibres the stage was cooled to 8°C and the water vapour pressure increased to saturation at 11 millibars.

Real time video imaging of the fibres was carried out during droplet formation and evaporation.

3.2. Results:

3.2.1. Fibres soaked in clay-treated Jet A-1

Condensing water formed discrete droplets on specific sites (Fig.6). Evaporation of the droplets followed by another condensation cycle resulted in the formation of water droplets on the same sites as previously observed. This indicated that the fibres possessed "islands" of hydrophilic surfaces within a hydrophobic "sea". Back-scattered X-rays (EDX) indicated the hydrophobic sites to be resinous and containing carbon and oxygen (CKa, OKa). To further verify that the droplets seen were water, an electron beam was focussed on individual droplets which then rapidly evaporated. Focussing the same beam on resinous structures had no effect

on the structure. As the condensed water increased, coalescence of adjacent droplets was observed and if the droplet size reached some critical size the drop fell off the fibre.

Conclusion: Water droplet interception and attachment occurs on specific sites in resin-coated fibre-glass media used in filter-coalescer elements.

3.2.2. Fibres soaked in Jet A-1 containing a sodium naphthasulphonate (SNS).

The dry fibres appeared structurally similar to those soaked in clay-treated Jet A-1.

In the first condensation cycle, no droplets formed on the fibre surfaces, instead thin films of water were observed to bridge across fibres (Fig.7). All fibre surfaces were wetted by the water, i.e. THE FIBRE SURFACES WERE COMPLETELY HYDROPHILIC. These water films ruptured on the evaporation cycle or when the film was subjected to a focussed beam of electrons. This observation was a complete surprise being in complete contradiction of commonly held theories of coalescer disarming. The observation does however explain one specific feature of coalescer disarming, viz. "Graping". Graping is the occurrence of released water structures comprising a fuel drop surrounded by a "skin" of water. Such structures have a near-neutral boyancy in a fuel continuous phase and are frequently observed in disarmed coalescers. Spontaneous rupture of the skin results in the formation of large numbers of extremely small (~1μm) droplets. Water films formed across a fibre framework could produce such structures when flowing fuel moves against the framework in an analogous manner to blowing soap-film bubbles (Fig.8).

Conclusion: Surfactant coated fibres prevent the normal interception and attachment of discrete water droplets. Instead, a continuous spontaneously spreading water film is produced suggesting that the fibres have become completely hydrophilic. This observation entirely contradicts currently held theories which suggest an increasing hydrophobicity on exposure to such surfactants but does explain the formation of some structures seen in cases of coalescer disarming which current theories do not. Further it suggests that the observed coalescer failures are in this case involves the droplet release stage rather than interception.

4. Conclusions

- Surfactants which are highly interfacially active at the water/fuel interface can cause filter-coalescer failure by producing fine water droplets. These remain on streamlines and cannot be intercepted by glass-fibres effectively.
- Some surfactants are not as highly interfacially active at the fuel/water interface but are active at the solid/fuel interface. Such surfactants also cause coalescer disarming, but by a mechanism which this work shows to be at variance with commonly held theories. Features of this mechanism are:

  (i) Rather than becoming hydrophic the fibres become completely hydrophilic.

  (ii) Water droplets intercepted by such fibres spontaneously spread to form water films.

  (iii) The water drop release stage is the more likely cause of the perceived coalescer performance failure.
- At least one disarming phenomenon, graping, can be explained by this new mechanism.

5. Acknowledgements

P.D.Rugen for the Interfacial Tension Measurements and the full scale rig coalescer performance data.

D. Park who for many years heralded the introduction of ESEM and who finally set up the contact with University of Manchester Institute of Science and Technology (UMIST) and who together with Mike Macknay and the technicians at UMIST conducted the ESEM study.

6. References

1. Hazlett, R.N., *Ind. Eng. Chem. Fundam.*, **1969,** *8*, 625, and **1970,** *9,* 520 and with Carhart, H.W., *Filt. Sep.*, **1972,** *9*, 456.
2. Hughes, V.B.; Foulds, A.W., *Proc. 4th World Filtration Congress*, **1986.**
3. Danilatos, G.D., *J.Microsc.*, **1991,** *162*, 391-402
4. Danilatos, G.D., *Microscopy Research & Technique,* **1993,** *25,* 529-534.

	FUEL TYPE	% Water (Inlet)	Facet CA 14-3SB	Velcon I614-85TB	Faudi F7-362
RUN 1	1.0 mg/l Stadis 450 + 2.9 mg/l Hitec 580 + 0.4 mg/l Petronate L	0.01	Fail	Fail	Not available
		3.0	Fail	Fail	for testing
RUN 2	1.0 mg/l Stadis 450 + 0.4 mg/l Petronate L	0.01	Fail	Fail	Pass
		3.0	Pass	Fail	Fail
RUN 3	4.5 mg/l Stadis 450	0.01	Pass	Pass	Not available
		3.0	Pass	Pass	for testing
RUN 4	2.9 mg/l Hitec 580	0.01	Pass	Pass	Not available
		3.0	Pass	Pass	for testing
RUN 5	1.0 mg/l Stadis 450 + 2.9 mg/l Hitec 580	0.01	Pass	Pass	Pass
		3.0	Pass	Pass	Pass
RUN 6	4.5 mg/l Stadis 450 + 2.9 mg/l Hitec 580	0.01	Pass	Not	Not
		3.0	Pass	Tested	Tested
RUN 7	0.4 mg/l Petronate L	0.01	Fail	Fail	Pass
		3.0	Fail	Fail	Fail

Table 1. Examples of commercial coalescer failures in fuels containing various additives including SNS (Petronate L). Failure is defined as the transmission of >15ppm free water downstream of the coalescer. Fuels containing approved additives such as Stadis 450 (a static dissipator additive) and/or Hitec 580 (a corrosion inhibitor) are not disarmed. The inclusion of only 0.4 mg/l SNS in the fuel causes failure at one or both of the inlet water addition rates.

Figure 1. Filter-Water Separator (schematic)

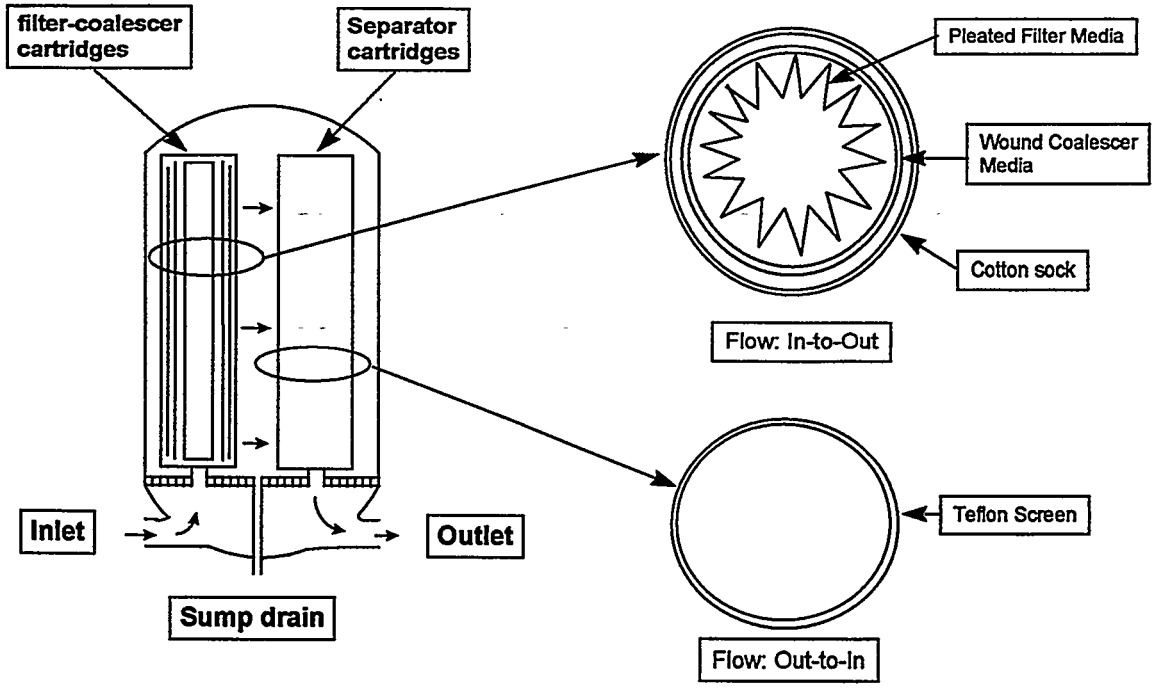

Figure 2. Dispersed Water Coalescence:

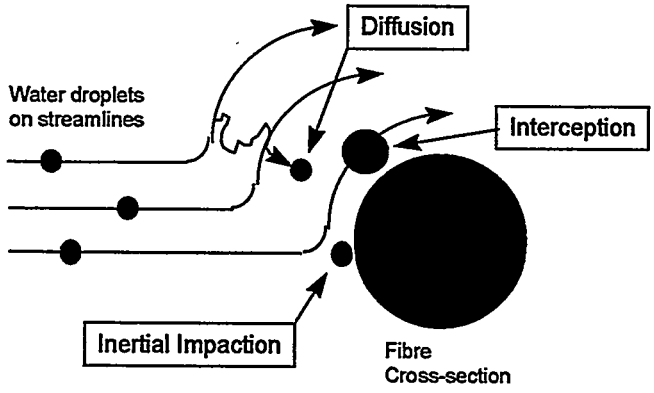

(Hazlett Theory)

PROXIMITY

INTERCEPTION

GROWTH

RELEASE

$$E_S = \frac{1}{2(2-\ln N_R)}\left[2(1+r)\ln(1+r) - (1+r) + \frac{1}{(1+r)}\right]$$

E_s = interception efficiency (%)

$r = d_p / d_f$

N_R= Reynold's No.

Figure 3. Effect of fuel surfactant level on the water coalescence performance of a commercial filter-coalescer, model Velcon 85.

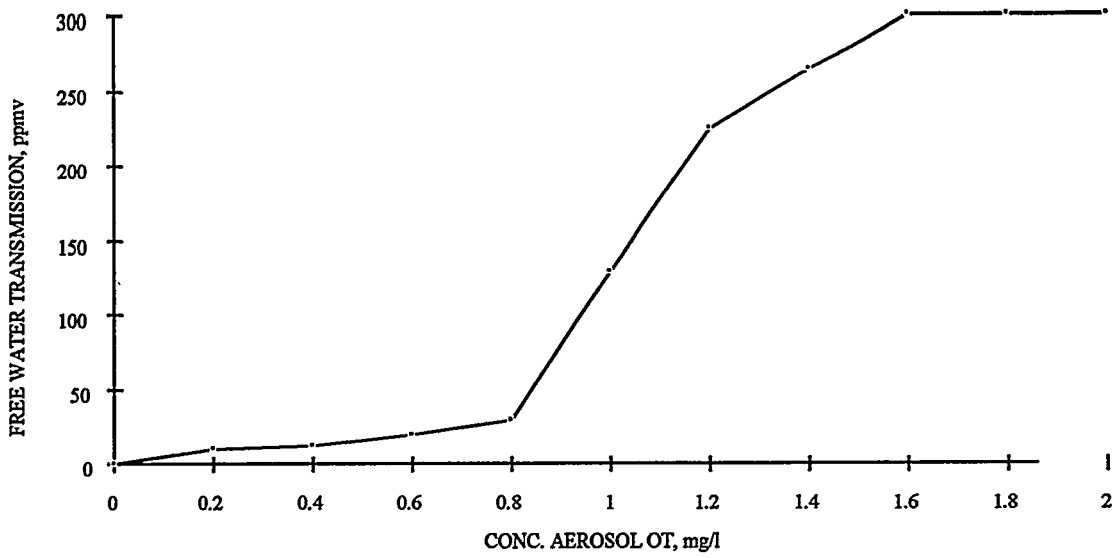

Figure 4. Water/Jet fuel Interfacial tension values for fuel containing AOT and SNS

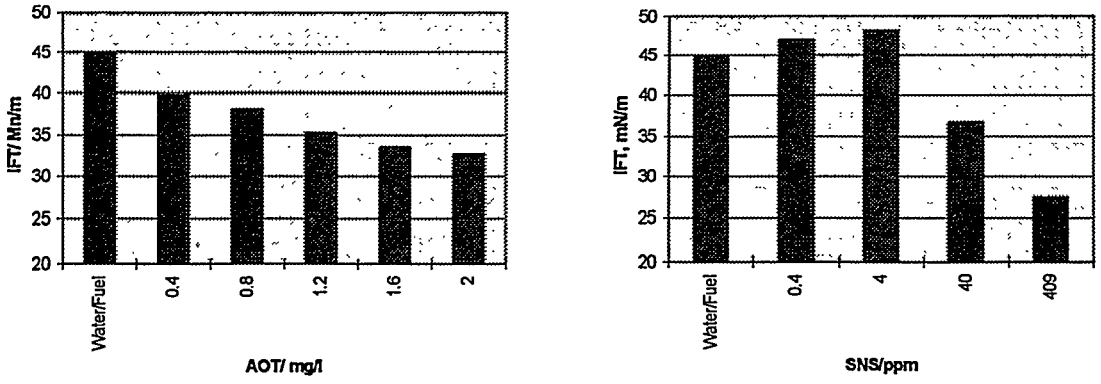

Figure 5. UMIST ElectroScan ESEM Model 20

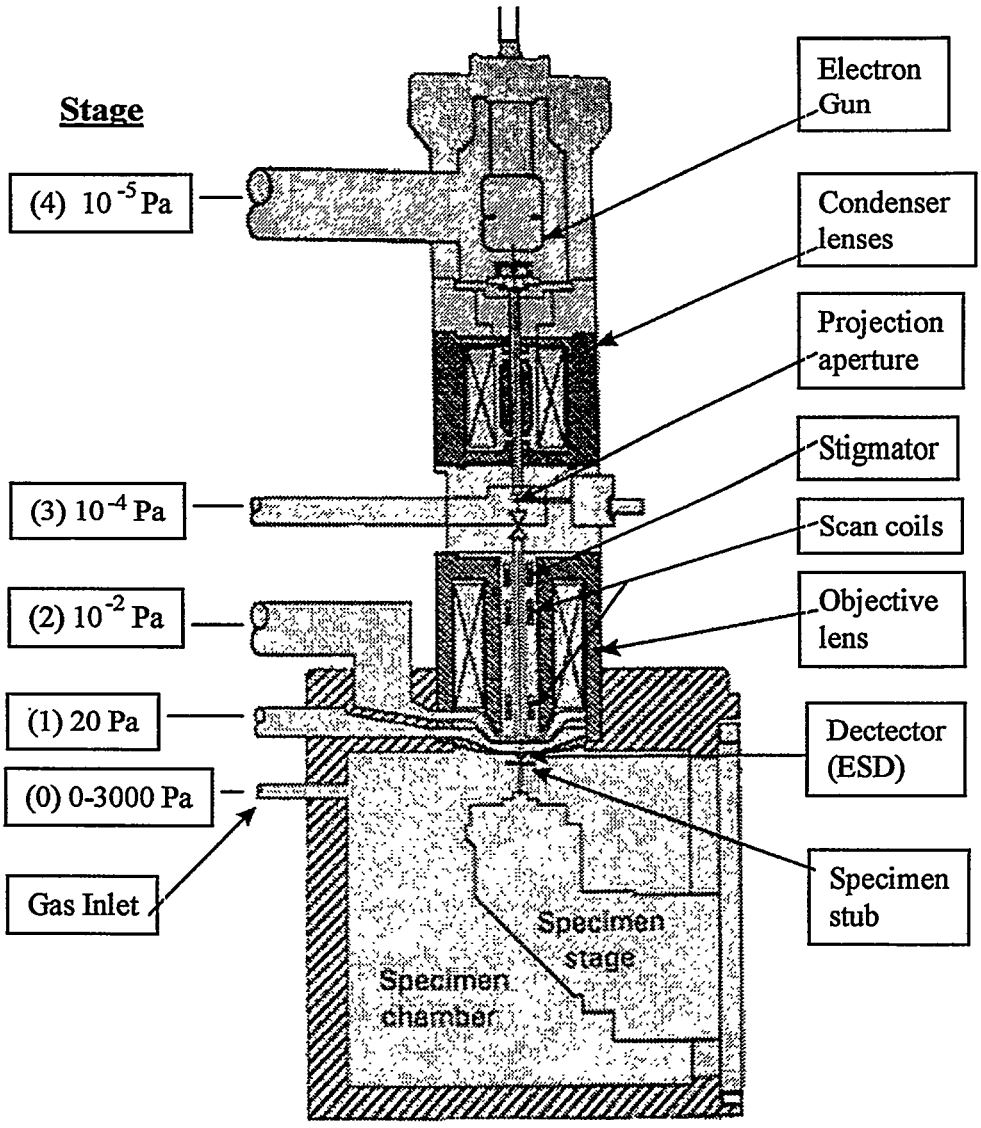

Figure 6. Water droplet formation on coalescer fibres after soaking in a clay-treated Jet A-1 fuel. Note the wide variation in droplet contact angle

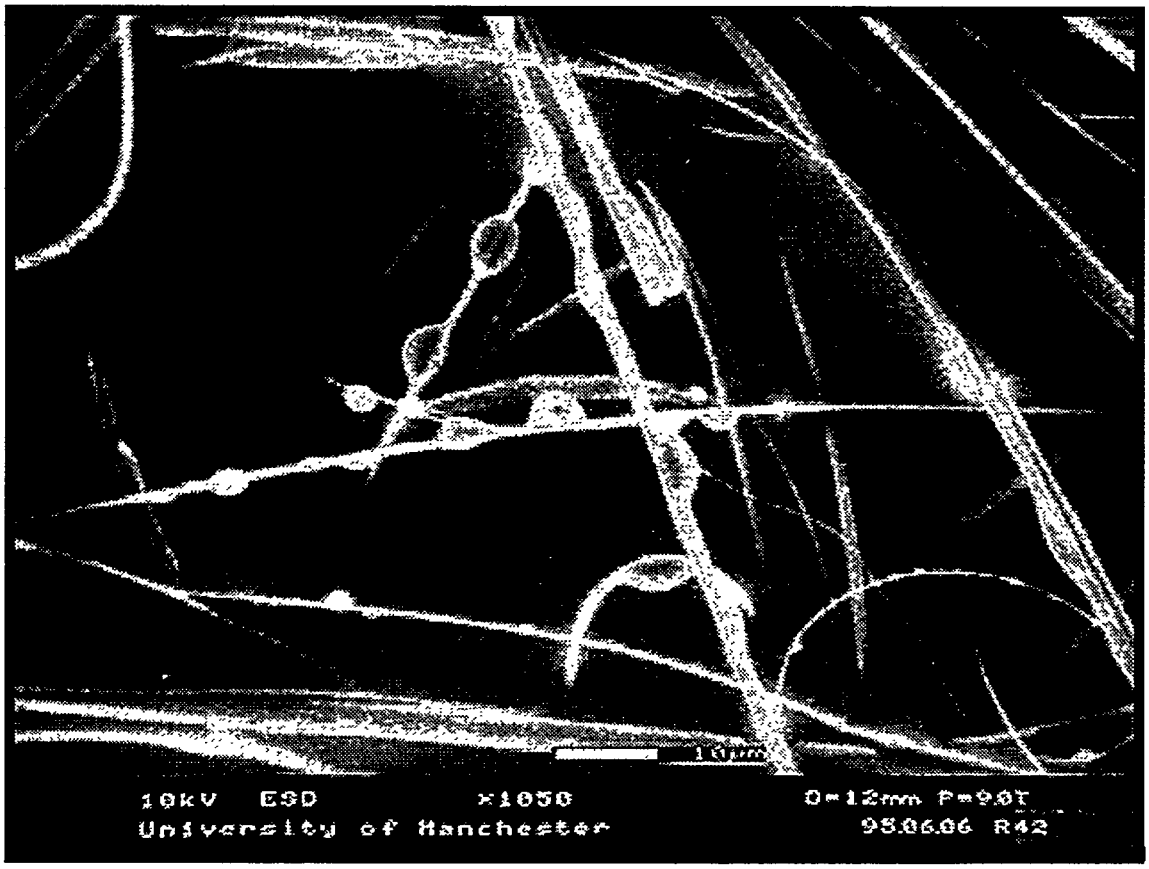

Figure 7. Water film formation on coalescer fibres after soaking in a Jet A-1 containing SNS. The sequence shows the progressive evaporation of water from the system.

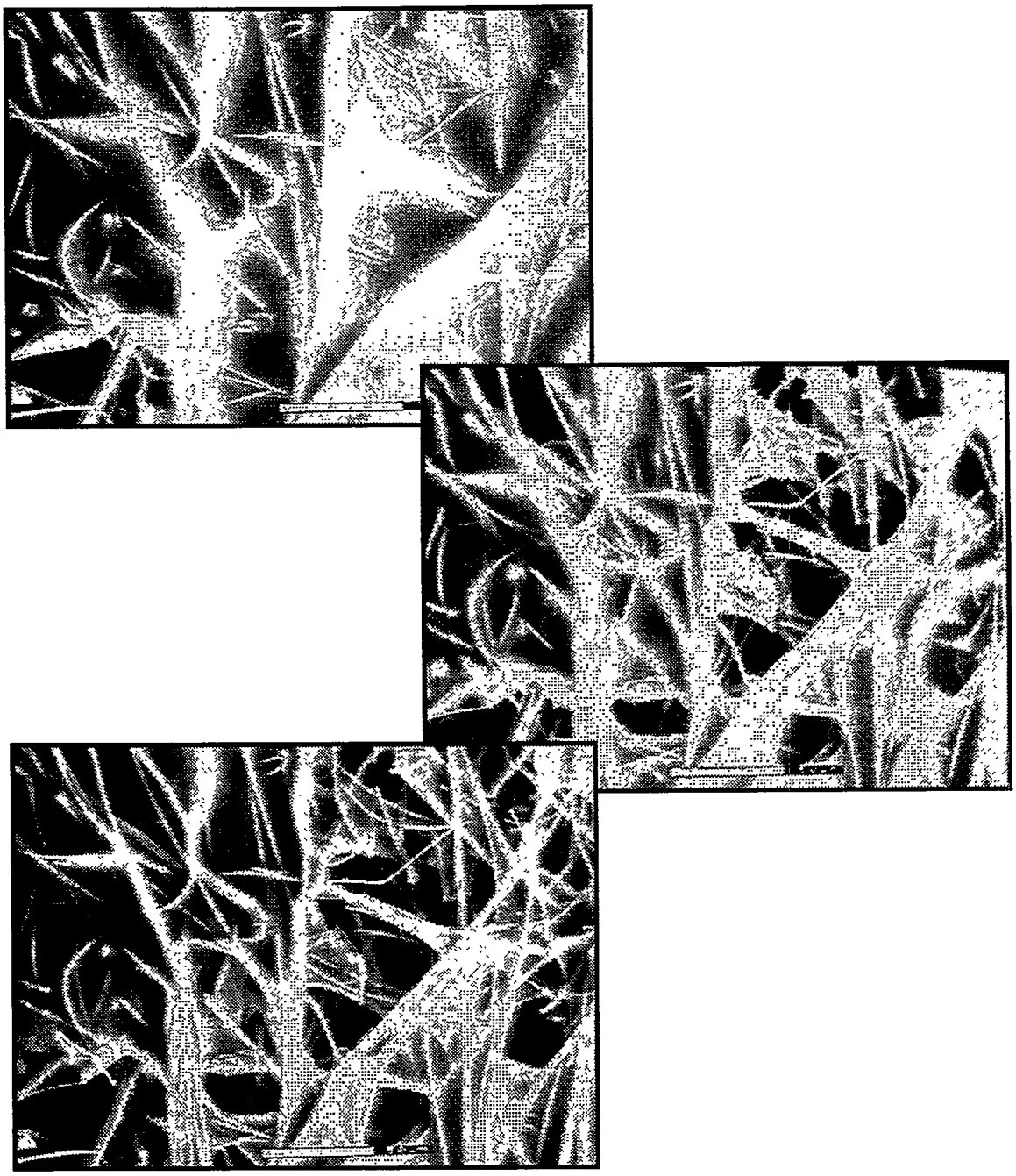

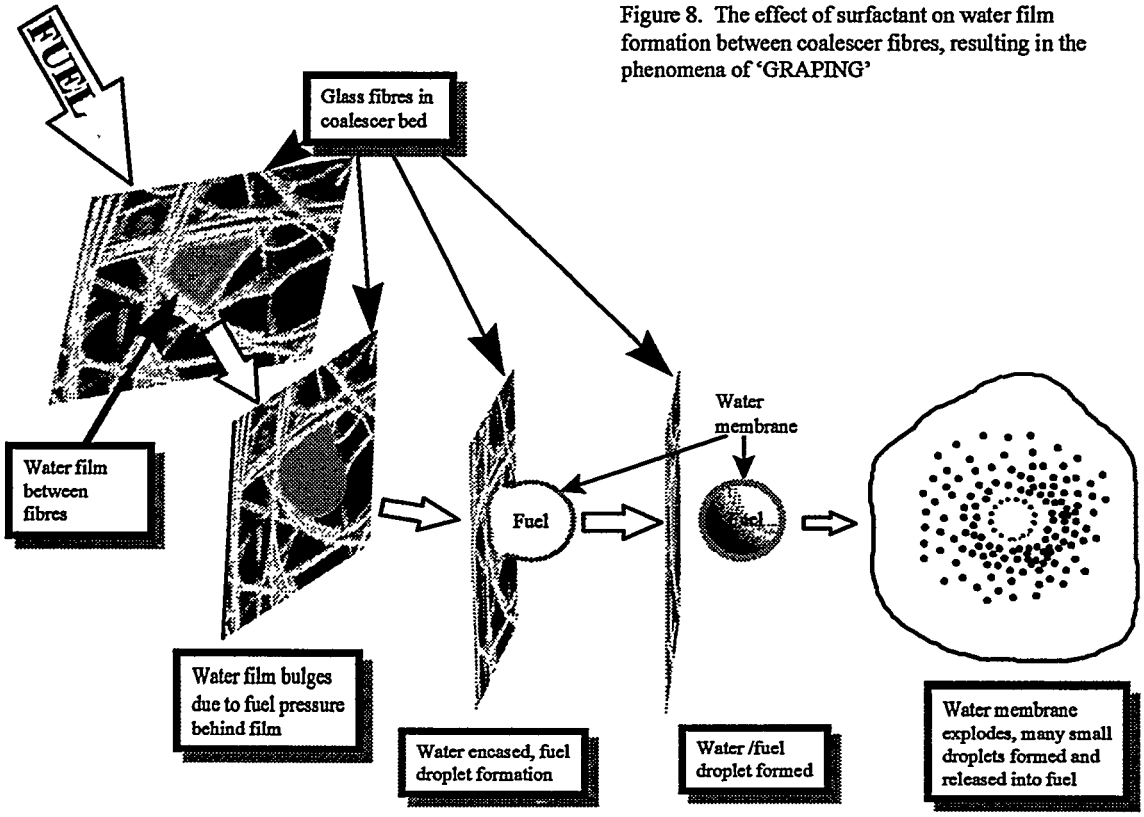

Figure 8. The effect of surfactant on water film formation between coalescer fibres, resulting in the phenomena of 'GRAPING'

6th International Conference
on Stability and Handling of Liquid Fuels
Vancouver, B.C., Canada
October 13-17, 1997

AN ANALYTICAL APPROACH TO WATER SEPARATION FROM JET FUELS AND COALESCER DISARMING

Peter David, Spencer E. Taylor* and Andy J. Woodward

BP Oil, Chertsey Road, Sunbury-on-Thames, Middlesex TW16 7LN, UK

Abstract

An analysis is presented of some aspects of fibre wetting and the possible implications for the operation of filter-coalescers. Two experimental approaches have been adopted in the present work. In the first, pre-treatment of single fibres by a Merox fuel and by a JP8+100 dispersant additive was followed by dynamic wetting measurements in water. The second approach, which is more representative of the practical situation, involves a "dual-liquid" system, in which the fibre first passes through an oil phase directly into water, *via* an oil/water interface. Specific wetting-related features arising from these single-fibre experiments have been identified.

Introduction

The operation of fibrous filters for removing dispersed water from jet fuels involves several distinct stages:[1]

1 Interception of the dispersed droplets by the fibrous media;
2 Droplet-fibre attachment as a result of wetting of the fibres following fuel displacement;
3 Coalescence between attached and incoming droplets;
4 Passage of coalesced drops through the bed; and
5 Release of coalesced droplets.

The interception process by which the droplets become physically attached to the fibrous media requires that *droplet-fibre contact* occurs, which will be dependent on physical factors such as the relative sizes of the droplets and fibres and the fibre

packing density, as well as the system hydrodynamics, controlled by fluid density and viscosity. Whether attachment of the droplet to the fibre occurs will necessarily be dependent on *wetting* of the solid fibre by the water (*ie* requiring that a *contact angle* of less than 90° is made with the fibre). The contact angle defines the wetting properties of a system, and relates to the *equilibrium* angle made by a liquid on a solid surface, as illustrated in Figure 1.

From a fundamental viewpoint, the wetting properties of individual fibres will govern the behaviour of a packed coalescer bed. However, the fibrous nature of coalescence media does not readily lend itself to an analysis of wettability in a bulk form. In the present study, therefore, a single-fibre approach has been taken to the analysis of the water wettability of glass fibres that have been exposed to a Merox-treated fuel and to a thermal stability dispersant additive. Whilst it is appreciated that coalescer action will be determined to some extent by the nature of packing of the fibre beds, the principal objective of this preliminary investigation was to identify general features of single-fibre wettability by fuel/water systems which could be important during the action of fibrous coalescers.

Experimental

Single-fibre wettability was determined using a Cahn Dynamic Contact Analyser (DCA) operating in the fibre balance mode. Two types of glass fibres have been used in the present work, one hydrophilic (denoted as type I) and one hydrophobic (denoted as type II). The type I fibres were from glass wool, obtained from BDH, Poole, whilst the type II fibres were extracted from heat-resistant insulation material and shown by scanning electron microscopy (SEM) and Electron Dispersive X-ray analysis (EDX) to be calcium-rich. Fibres suitable for examination were approximately 6 cm in length and had small wire loops secured to one end with epoxy resin for ease of attachment to the DCA. Optical microscopy was used to determine the fibre diameter. The DCA allows fibre immersion into the wetting liquid, whilst simultaneously monitoring the force exerted on the fibre and its immersion depth.

Two types of single-fibre wetting experiment were performed at ambient temperature (20 ± 2°C). The first, termed the *single-liquid* approach, involved pre-treating the fibre by immersion in appropriate liquids, either a Merox-treated jet fuel or (alumina-treated) *n*-heptane solutions of a JP8+100 dispersant additive. The force exerted on the fibre is given by

$$f = 2\pi r\gamma\cos\theta \qquad 1)$$

where γ is the surface tension of the test liquid and θ is the *dynamic* contact angle made by the liquid on the fibre, and a typical trace for *n*-heptane wetting is shown in Figure 2. Both *advancing* and *receding* dynamic contact angle behaviour can be studied in this way by immersing and withdrawing the fibre. During this process, adsorption of surface-active species can occur directly on to the fibre surface. This then allows the consequences of surface treatment on water wettability of the fibre to be determined.

The second approach, the *dual-liquid* method, which more accurately represents the practical situation, involves immersing the fibre attached to the DCA into an oil/water interfacial system. This is depicted in Figure 3. The attraction of this approach is that the fibre is pre-wetted by the oil phase before contacting the water, such that oil displacement is necessary before water wetting occurs, as in the "real" situation. As shown in Figure 4, a force is exerted on the fibre during immersion, first, from the effect of the oil (fuel) surface, which is then followed by the oil/water interface. Deconvolution of the effects of the surface and interfacial components is then possible with care. Analysis of the system is as follows.

The initial force exerted on the fibre is given by

$$f_{oil} = 2\pi r\gamma_{oil} \qquad 2)$$

where γ_{oil} is the surface tension of the oil phase and r is the fibre radius. The contact angle here is assumed to be zero, since hydrocarbons are regarded as completely

wetting liquids. Upon reaching the interface, the measured force is modified, such that the total force exerted on the fibre is given by

$$F_{total} = f_{oil} + f_{interface} = 2\pi r\gamma_{oil} + 2\pi r\gamma_{OW}\cos\theta \qquad 3)$$

where θ is now the contact angle for the oil/water/fibre system and $\gamma_{oil/water}$ is the interfacial tension. This latter situation exactly mimics the wetting interaction expected between a dispersed water droplet and a fuel-wetted fibre in the practical system. From equation 1, a knowledge of either r or γ_{oil} will enable the other parameter to be determined.

Results

Single-liquid systems

In Figure 2 are shown typical force-immersion depth traces for fibre wetting by hydrocarbon liquids. The traces can be seen to be relatively smooth in these cases, with the behaviour during immersion and withdrawal being almost identical, indicating that this type of liquid completely wets the fibres. Under these conditions, a knowledge of the surface tension of *n*-heptane (20.4 mN m^{-1}) allows the fibre radius to be calculated. For the fibres in the following example, the respective derived radii of 6.5 and 4.6 microns compare favourably with the microscopically-measured values (6.2 and 4.4 microns, respectively). The wetting behaviour found for hydrocarbons contrasts with the corresponding behaviour for water as the wetting liquid, shown for the same two fibres in Figure 5. Here, the wetting upon immersion (governed by the advancing contact angle) is seen to be erratic, which reflects the non-uniformity of the water contact angle along the length of each fibre. Figure 6 shows the corresponding advancing contact angle data for these two types of fibre which illustrates the essential difference between hydrophilic and hydrophobic fibres.

This is a typical finding for these types of fibre, and also suggests the difficulties which may arise when attempting to use other contact angle determination methods, *eg* direct observation of drops on fibres,[2] where, most likely, a range of values will be evident.

Upon retraction of the fibre, however, more uniform and larger forces are recorded, indicating that the receding contact angle is lower than the advancing angle, and in many cases, including the present examples, is almost zero. Also shown as dashed lines in Figure 5 are the expected retraction forces based on the zero contact angle hydrocarbon data and the ratio of the liquid surface tensions. Interestingly, it can be seen that the measured force is actually *higher* than the expected value, which has no physical significance in terms of the force due to surface tension. One explanation, however, is that a "wetting layer" is produced on the fibre, the weight of which contributes to the measured force. This is more evident in the case of the hydrophilic, type I fibre, as would be expected.

Figure 7 shows the average contact angle for the treated section of fibre as a function of the number of exposures to the Merox treated jet fuel. It can be seen that, although there is a relatively large increase in contact angle following the first treatment cycle, subsequent treatment cycles do not significantly affect the fibre wettability. From these data, this particular fibre radius is 6.1 microns (*cf* 6.5 microns by microscopy) and the Merox fuel surface tension is 25.5 mNm^{-1}.

However, pretreatment with different concentrations of the dispersant has a more dramatic effect on fibre water wettability. As shown in Figure 8, ppm levels of this surface-active additive cause a large effect on the advancing contact angle, which indicates that exposure of the fibre to approximately 10-20 ppm of the additive is sufficient to increase the contact angle to $\geq 90°$. Under these conditions, it would be expected that water droplets would not adhere to the fibres spontaneously upon contact. Correspondingly, the efficiency of coalescence by the fibrous media would be severely reduced.

Dual-liquid systems

In Figure 4, showing a typical force-immersion depth trace for type I fibres in the heptane/water system, the entry points into the oil phase and the oil/water interface can be clearly seen. From the oil surface data, the fibre radius in this case is determined as being 6.8 microns (*cf* 6.5 microns by microscopy). Upon retraction from the interface, and assuming a zero receding contact angle, the average heptane/water interfacial

tension is calculated to be 46.7 mN m^{-1} (*cf* 50.2 mN m^{-1}).[3] If the interfacial tension and fibre radius values are then used in analysing the immersion data, the contact angle profile for the interface shown in Figure 4 is produced, as shown in Figure 9, from which the heterogeneity of contact angle is evident, as also seen by the single-liquid approach. Surface-active materials can significantly affect the wettability in the dual-liquid systems also. In Figure 10 are shown advancing and receding contact angle data for successive immersion cycles in the Merox fuel, indicating the adverse effects of surface-active impurities in the fuel on wetting behaviour. More dramatic effects have been found in the *n*-heptane/water system in the presence of different concentrations of JP8+100 dispersant, again, leading to a decrease in fibre hydrophilicity.

Discussion

The two fibre wetting systems considered in the present work are contrasted by virtue of the predisposition of the surfactant with respect to interaction with the fibre. In the single-liquid situation, fibre surface modification by surfactant adsorption and subsequent water wetting are carried out in two separate stages. On the other hand, in the dual-liquid approach, oil wetting/surfactant adsorption and water wetting are consecutive processes occurring in the same system. The advantage of the latter approach, as far as understanding phenomena occurring during water coalescence is concerned, is that the fibre is pre-wetted by the oil (fuel) prior to contacting the water. Also, the measured contact angles reflect this situation, relating to the oil/water/fibre system, relevant to the practical application. From a surface chemical viewpoint the main difference between the two systems is the presence of the fuel/water interface in the dual-liquid situation. Such interfacial regions can often play important roles in surface chemical-dominated processes. Hitherto, little attention has been given to the fundamental aspects of the interfacial region during water coalescence processes. There are certain indications from the present work that the interfacial region is indeed playing an active role in influencing fibre wettability. For example, treatment with Merox fuel indicates that there is a greater effect on advancing contact angle data in the dual-liquid system compared with the single-liquid case, for which surfactant adsorption is the dominant mechanism. The presence of the interface is apparently

amplifying the influence of indigenous surfactants in the fuel. One mechanism for this is the more effective creation of a surface layer through surfactant *deposition* as opposed to adsorption. This is akin to the formation of Langmuir-Blodgett films on surfaces using well-defined surface-active molecules. As a consequence, it would be expected that fibre wettability would be adversely affected by such a deposition mechanism. The same general trends are true for the dispersant-treated fibres.

Conclusions

This work has identified some potentially important surface chemical features of the wetting of glass fibres by water. In addition, a new approach to water wetting in the presence of an oil phase in a dual-liquid situation is described for the first time. This has enabled the determination of a three-phase contact angle made with the fibre.

Acknowledgements

This project was funded by Air BP and the UK Ministry of Defence.

References

(1) Hazlett, R.N. *Ind. Eng. Chem. Fund.* **1969**, *8*, 625-632; *8*, 633-640

(2) (a) Taylor, S.E. unpublished observations; (b) Hughes, V. "Aviation Fuel Handling: New Mechanistic Insight to the Effects of Surfactants on Water Coalescer Performance", Presented at *6th International Conf. On Stability and Handling of Liquid Fuels*, Vancouver, 1997

(3) Ross, S.; Morrison, I.M. *Colloidal Systems and Interfaces*, Wiley-Interscience: New York, 1988; p 77

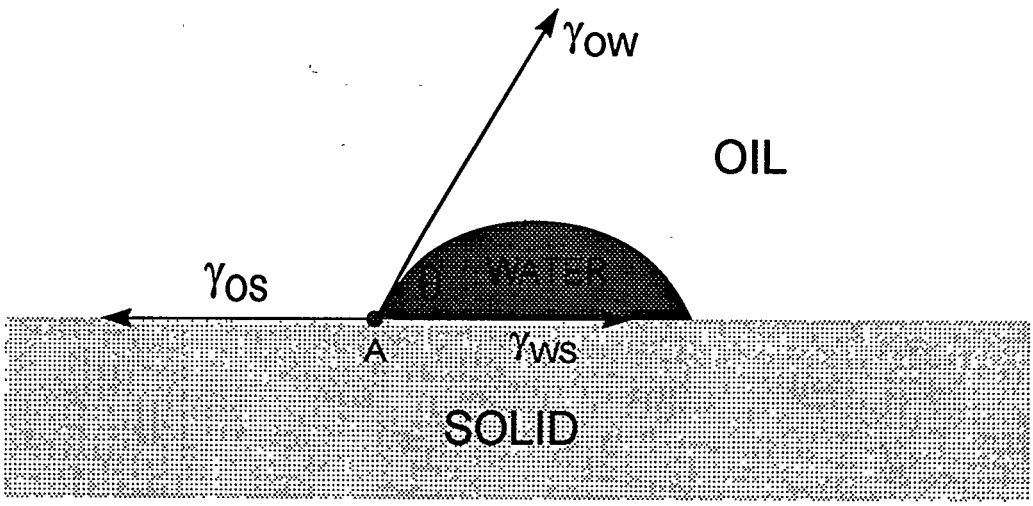

Figure 1. Schematic representation of a water drop at equilibrium on a solid surface, making a contact angle θ with the surface under the influence of the respective interfacial forces indicated.

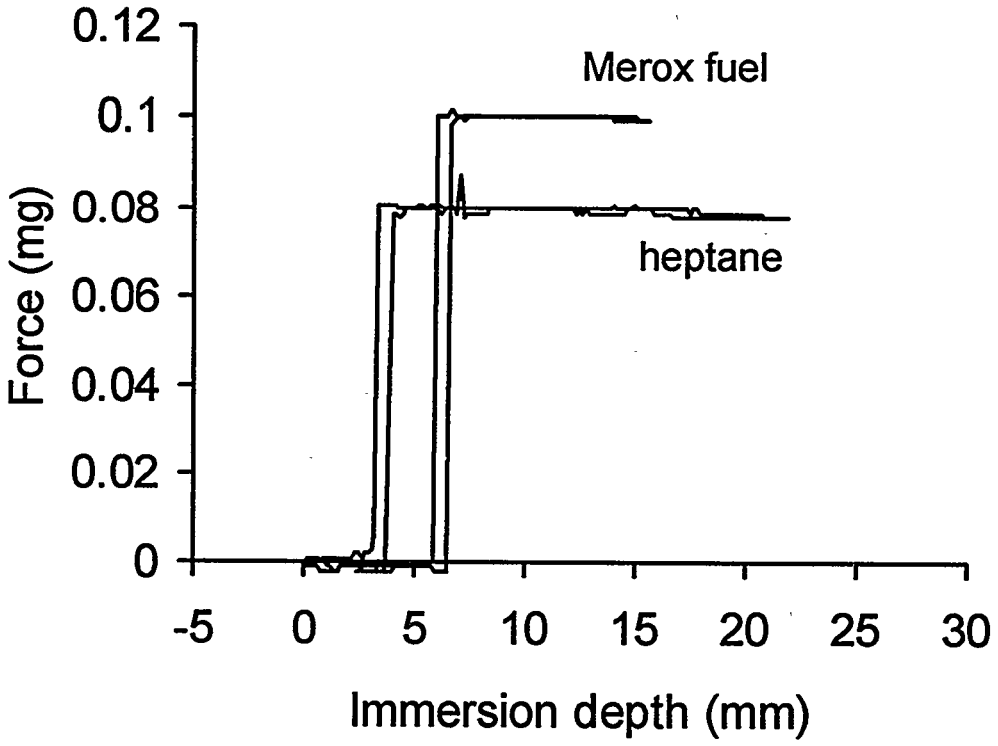

Figure 2. A typical force-immersion depth trace for fibre wetting by *n*-heptane and Merox fuel.

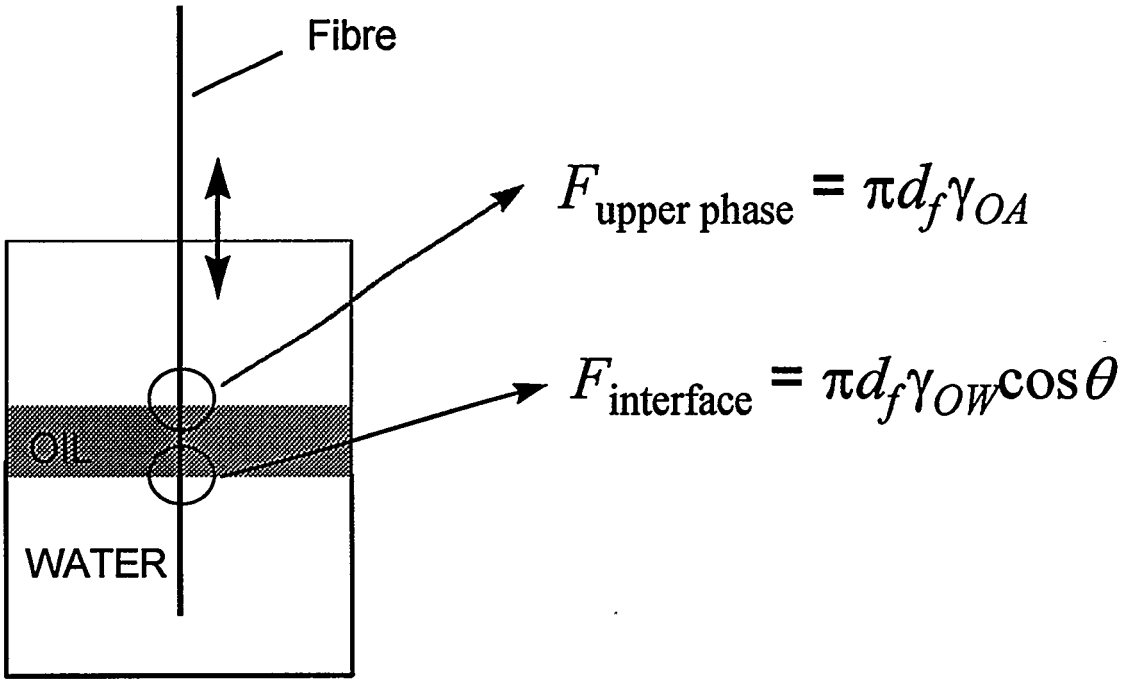

Figure 3. Schematic of the dual-liquid system.

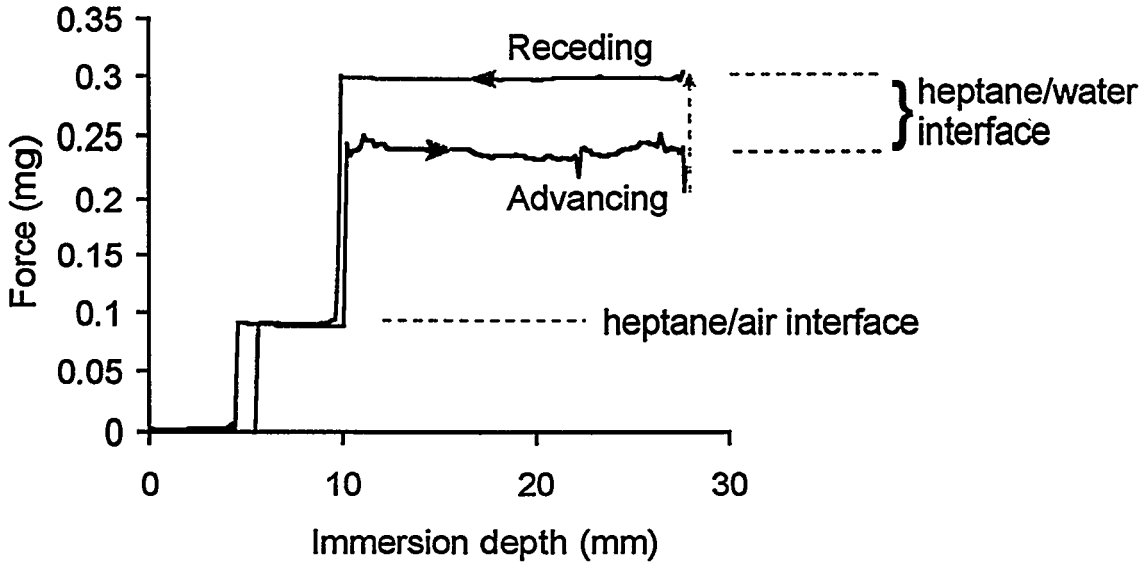

Figure 4. Typical form of fibre force-immersion depth profiles for an interfacial system in the dual-liquid approach.

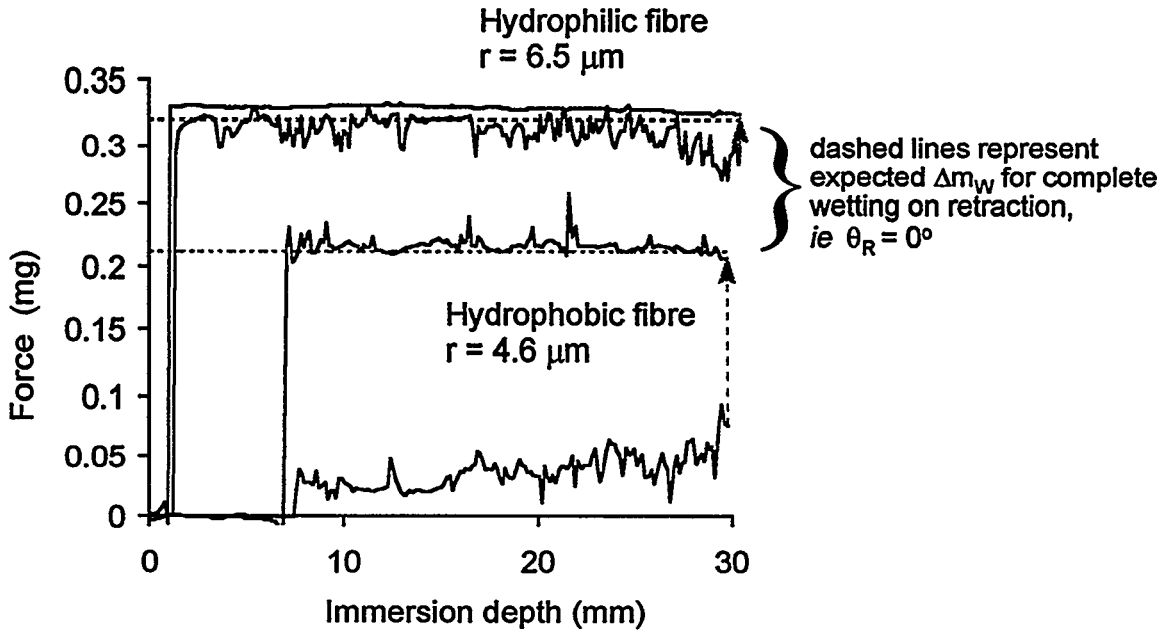

Figure 5. Force-immersion depth traces for types I and II fibres in water.

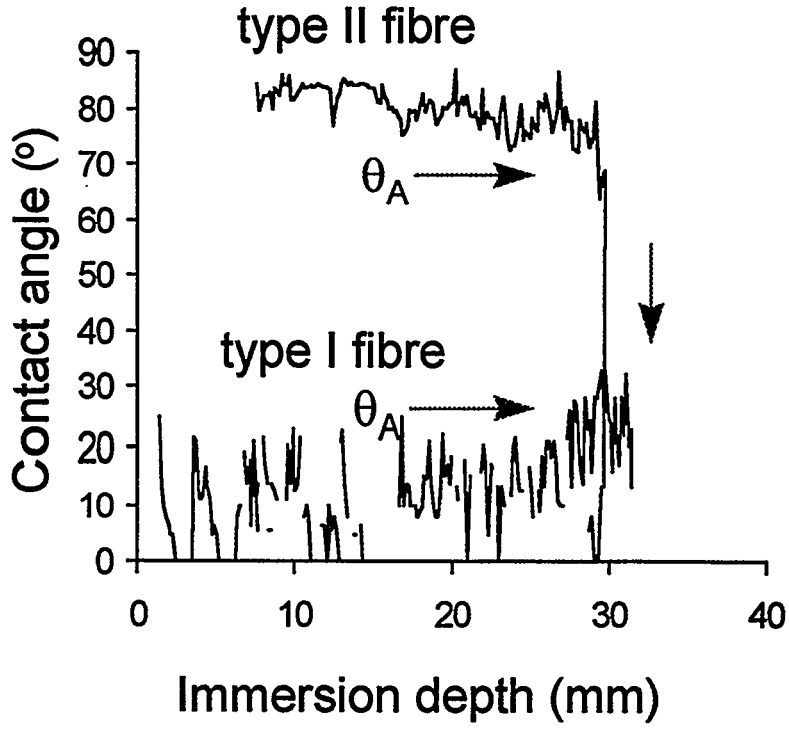

Figure 6. Advancing contact angle profile for types I and II fibres.

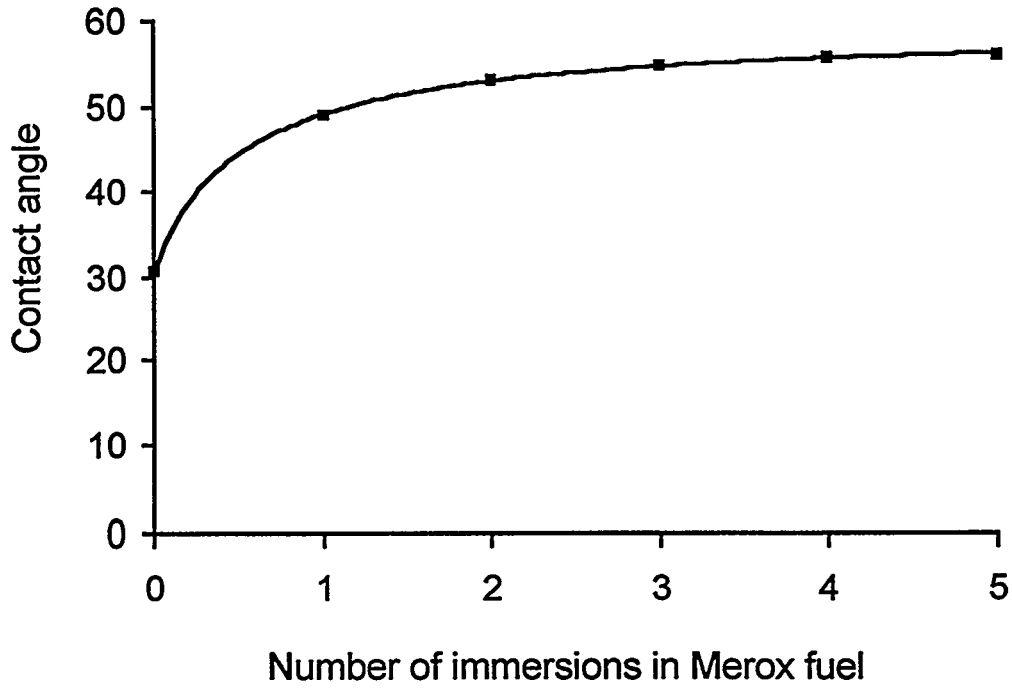

Figure 7. Effect of the number of immersion/drying exposures to Merox fuel on the resulting contact angle against water.

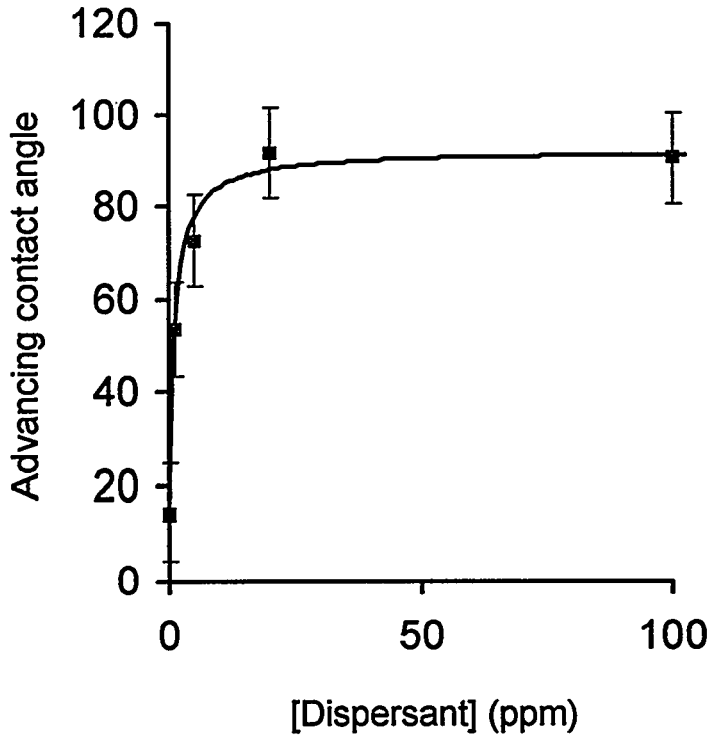

Figure 8. Effect of dispersant concentration on the mean advancing contact angle for a type I fibre.

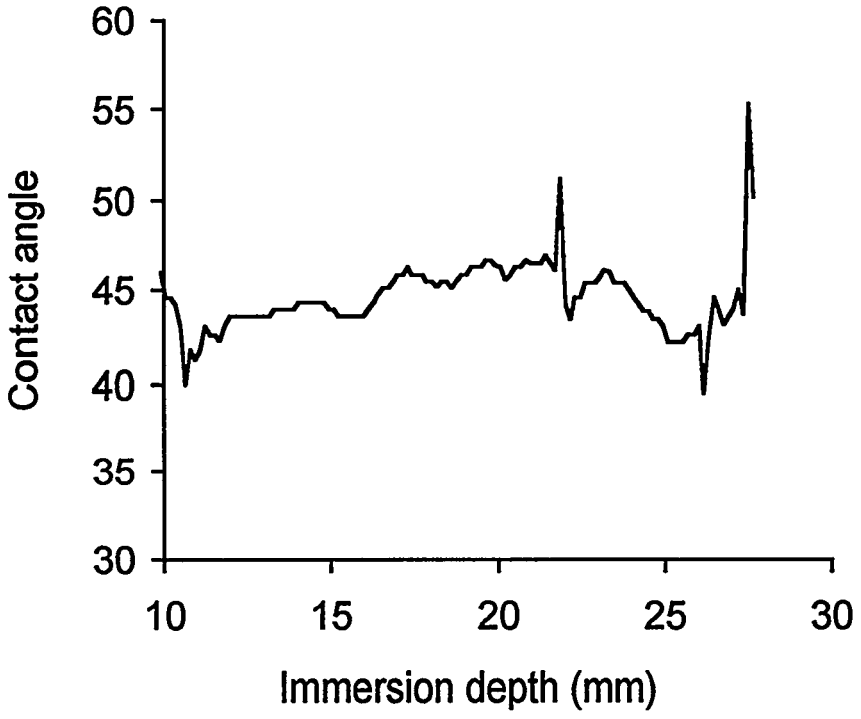

Figure 9. Example of an advancing contact angle profile along a type I fibre determined in the dual-liquid system.

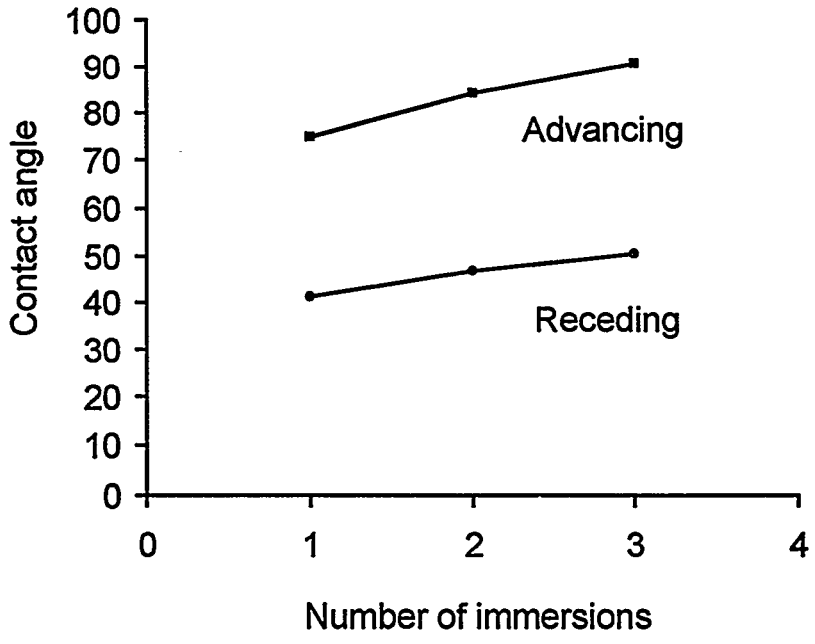

Figure 10. Effect of the number of immersion cycles in Merox fuel on the advancing and receding contact angles of a type I fibre.

6th International Conference
on Stability and Handling of Liquid Fuels
Vancouver, B.C., Canada
October 13-17, 1997

STADIS® 450 IN AVIATION FUEL APPLICATIONS - UPDATED

Cyrus P. Henry Jr.

Octel America, Inc., 200 Executive Drive, Newark DE 19702 USA

At the October, 1994 International Conference in Rotterdam, information was presented on the use of Stadis® 450 in certain fuels, mainly chemically sweetened, which contain interacting trace impurities resulting in several difficulties. A slightly modified product has now been introduced which overcomes a potential to form a precipitate containing a dodecylbenzene sulfonate. This modified additive has now been fully accepted by airframe and turbine manufacturers and is fully commercialized; production of the old formulation ceased in December 1996. The status of the transition to the modified product is reviewed. Additionally, progress has been made in understanding the relationship of the results from ASTM D 3948 water separation tests, and the actual performance of coalescers in the industry. This has lead to changes in aviation fuel specifications, and to a program in ASTM to better define an improved test method to predict coalescer performance. Overall, fewer difficulties are expected in the future.

INTRODUCTION

At the 5th International Conference on Stability and Handling of Liquid Fuels, a paper [1] was presented which detailed a number of concerns about Stadis® 450 in chemically sweetened aviation fuels, and efforts underway to understand and rectify them. Two fundamental problems and their various ramifications were discussed. The first dealt with disarmed coalescers found at the Munich airport, which was due to formation of an insoluble dodecylbenzene sulfonate in the fuel. This accumulated on coalescers while operating with dry fuel, but led to a failing result when a coalescer was removed from the fuel system and evaluated in the single element test. This was caused by the dodecylbenzenesulfonic acid component in Stadis® 450. A modification of Stadis® 450 was developed and discussed which overcame this problem, and consideration of changing over to its use was discussed. That has now been completed, and is reviewed.

The second problem was more general in nature; some Merox™-sweetened fuels containing Stadis® 450 show conductivity loss during storage. Stadis® 450 also tends to have a greater effect on the D 3948 [2] MSEP rating of these fuels. The combination of these effects

makes it difficult to assure supply of fuel to airports which meets both conductivity and water separation requirements. That work led to the conclusion that the fundamental aspects of testing to simulate coalescer performance needed to be addressed, and is also reviewed. This paper is a general review of the activities leading to resolution of these problems, and of other recent activities.

"DINNSA" STADIS® 450 INTRODUCED

The concept of replacing dodecylbenzenesulfonic acid (DDBSA) with dinonylnaphthylsulfonic acid (DINNSA) in the Stadis® 450 formulation was discussed at the last conference[1]. At that time the concept was shown viable in small scale testing, but a full-scale demonstration had not yet been carried out; a great deal of work was needed to fully verify suitability, and steps needed to implement a transition had not been defined. This has all been completed, as follows.

First, data were developed comparing performance of the two formulations. These results included properties of the modified additive, relative conductivity-improving performance, electrostatic charging properties, various aspects of water separation, effects on thermal stability, compatibility with other jet fuel additives in fuels and aircraft fuel system materials, and compatibility of the old and new additives. This was completed in July, 1995 and a report is available detailing the findings [3]. Lot 1 of modified Stadis® 450 was produced in September, 1995. Feasibility of manufacturing was demonstrated thereby, and an adequate store of material obtained for general testing and trial purposes, but not released for general use in aviation fuels.

Next, large-scale tests were carried out at the OMV refinery in Berghausen, Germany. These demonstrated that the modified product was indeed useful and solved the problem. On two occasions, 5,000 m^3 batches of Jet A-1 fuel containing the modified Stadis® 450 were circulated through a coalescer vessel then elements were removed and evaluated in the single element test. These were successful, and showed no signs of coalescer deactivation. These fuel batches were downgraded and not used as jet fuel, since the modified product was not fully accepted.

These results provided the necessary motivation for aircraft and turbine manufacturers to consider the acceptability of the modified product. Acceptance was requested from Boeing, Airbus Industries, Fokker, Lockheed, McDonnell Douglas, British Aerospace, General Electric,

Pratt & Whitney, Pratt & Whitney Canada, Rolls Royce, Garrett (Allied Signal), the United States Air Force, the British Ministry of Defence, CAA, and indirectly, FAA. All of these parties had accepted the use of DINNSA in place of DDBSA in the Stadis® 450 formulation by May, 1996. In the meantime, members of ASTM Subcommittee J on Aviation Fuels, the IATA Aviation Fuel Working Group, the Canadian General Standards Board Aviation Fuel and Related Products Committee, and the MOD Aviation Fuel Committee, and the CRC Coalescer Deactivation Panel were all fully apprised of the work in progress.

It was also agreed that the name of the additive would not be changed, and the modified product would still be identified as Stadis® 450; this resulted in no need to revise any specification or document which referred to "Stadis® 450". It was not possible to develop a satisfactory laboratory test to determine whether this form of coalescer deactivation might occur with DDBSA Stadis® 450. Because it was determined unsatisfactory to have two different forms of Stadis® 450 in use, Octel America agreed to a complete transition to DINNSA Stadis® 450 upon completion of trials.

During the period May to December 1996, these acceptances were the basis for limited use of the DINNSA Stadis® 450 in aviation turbine fuel at several sites where performance was carefully monitored. Commencing in October, 1996 modified Stadis® 450 was used in fuel produced at the OMV Burghausen refinery and sent to Munich airport. On two occasions during the period October – December 1996, coalescers were removed from the fuel distribution system and evaluated in the single element test; excellent results were obtained. The second testing was after 57,000 m^3 (approximately 360,000 barrels) of fuel had flowed through the coalescer vessels. The success of these trials fulfilled the final requirement to begin a complete transition to the modified product.

The last lot of DDBSA Stadis® 450 was manufactured in December 1996 and all customers were notified. Early in 1997 all supplies of DDBSA at Octel America, Inc. were exhausted, save a small reserve for non-aviation applications. We anticipate that it will take some time before all supplies of DDBSA Stadis® 450 are depleted in customers' hands. Further information is available on the transition [4]. No difficulties related to the modification have been reported as of this date.

IMPROVING THE CONDUCTIVITY/MSEP RATING TRADEOFF IN MEROX-SWEETENED FUELS

In the previous paper we noted that some, but not all, chemically-sweetened jet fuels exhibit loss of conductivity during storage following treatment with Stadis® 450. Results from several treatment options were discussed. These have been more extensively evaluated, and have not proven generally successful for refineries which have varied crude slates. These included filtration through alumina, acid washing, reduction of filming amine additive in the processing equipment, and improved water washing. At several refineries, conductivity retention and D 3948 MSEP test results were shown to vary substantially depending on the crude oil slate in use. This demonstrated that frequent changeout of the attapulgus clay tower is, in many cases, not a satisfactory solution. While absorbent clay removed interacting species, some are apparently not strongly absorbed and are quickly eluted. Strong surfactants, on the other hand, are very polar and absorbed permanently. Fuels were examined where each of these options gave acceptable improvement, but additional fuel samples from the same refinery often did not respond the same way. For a refinery producing 10,000 bbl/day of jet fuel, installing an additional absorbent tower for alumina, or an acid washing step, represents significant investment which might be acceptable if known to be a consistent solution – but not otherwise.

This led to a conclusion that a general solution to the conductivity/MSEP tradeoff difficulties could not be identified, mainly because the variable nature of the interacting trace materials in jet fuel. In the meantime, we were aware that API Publication 1581 "Specifications and Qualification Procedures for Aviation Jet Fuel Filter/Separators", 3rd Edition [5] had been amended to allow use of 3.5 mg/L of Stadis® 450 in place of 0.75 mg/L of ASA-3 during qualification testing. This level was set by determination of water coalescing performance in modern coalescers, and was intended to provide the same level of severity for coalescer vessel qualification purposes. Yet, we were well aware that most fuels containing these levels of conductivity additives would show vastly better D 3948 MSEP test results with ASA-3 than with Stadis® 450! Overall, this led to two conclusions which were discussed at the April 1997 meeting of the Coordinating Research Council (CRC) Aviation Fuel, Lubricant and Equipment Research Committee meeting [6].

- *The only universal remedy for the conductivity/MSEP problems encountered for Merox sweetened jet fuels produced at many refineries was to replace with hydrogen*

treating sweetening processes. Since there are about 150 jet fuel Merox units world-wide, the cost would be formidable.

- *The results of API / IP studies leading to the API 1581 amendment suggested that this was not necessary: a better remedy was to find a water separation test method which had a better correlation with field performance of coalescers.*

As a consequence of these discussions, several initiatives were quickly undertaken. At the June ASTM meeting, a Task Force on Water Separation Test Methods was established to determine if an improved D 3948 Test Method could be developed, or an alternative method could be defined which would better predict water separation properties of fuels in full scale coalescers. A CRC report was assembled which reviewed available literature and data and concluded that "the customary minimum MSEP of 70 can be relaxed when a drop in rating is ***specifically due to the addition of Stadis® 450"*** [7]. This led to a relaxation of MSEP requirements in Canadian and British aviation turbine fuel specifications [8,9]

The work of the Task Force on Water Separation Test Methods led to development of an improved version of the D 3948 Test Method, which is being evaluated. The modified method uses a mini-coalescer for the test which better mimics modern filter coalescer media, and is a promising lead toward providing a test method to assure jet fuel remains adequately free of coalescer-disarming surfactants during distribution. The modified test coalescer reflects current trends toward using a fiberglass-containing filter media, which initiates coalescence prior to flow through the outer fiberglass wraps. This material is much finer, and intercepts smaller water droplets. Other test work indicates that Stadis® 450 tends to cause smaller water droplets to form when water is emulsified with fuel. However, when the modified test coalescer is challenged with fuel containing Aerosol OT surfactant, it gives similar results to the current test coalescer. It is, however, necessary to re-evaluate the ratings obtained with the two versions of the method to establish correlation. This is especially important to assure that the aviation fuel industry knows what rating with the new method correlates with the 85 rating value traditionally thought to be the borderline for "surfactant-free" fuel.

OTHER RELATED ACTIVITIES

The changes which have been implemented in specifications which note MSEP requirements, and the ongoing D 3948 MSEP test method activities have reduced worries about

conductivity loss and MSEP effects for fuels containing Stadis® 450. We still view these problems as serious concerns which need further work to help refiners deal with any difficulties involving use of Stadis® 450, but the these are now reduced to the inconvenience of re-doping when necessary.

Conductivity and Light Exposure

Studies have shown that exposure to sunlight can cause dramatic, permanent loss in the conductivity of fuels containing conductivity improving additives. This has been demonstrated in borosilicate glass and in polytetrafluoroethylene bottles, and probably occurs in other transparent or UV transparent containers. Glass containers are frequently used on refineries to obtain quality control samples for laboratory measurement. The data in Table 1 were obtained for three kerosine jet fuel samples with conductivities of 385 - 550 pS/m obtained by treatment with Stadis® 450, in 500 mL borosilicate glass or in polytetrafluoroethylene (PTFE) containers after exposure to Mid-Atlantic Summer sunlight. Slower loss is expected from fluorescent lights or other uv sources. Similar effects were found with various other conductivity additives. An Octel Additive Brief has details of these findings [10].

Table 1. Conductivity Loss from Sunlight Exposure

Container	% Conductivity Loss at designated exposure interval		
	5 min	20 min	95 min
Amber Glass	0	0-16	1-47
Clear Glass	0-58	66-71	78-89
PTFE	22-70	76-80	81-90

These conductivity losses occur only with parts per million solutions of these additives in fuels. Thirty days daylight exposure of concentrated Stadis® 450 as supplied, or of a 5% solution in kerosine, did not result in a measurable conductivity loss when these were then used to treat fuels. Modification of D 2624 Conductivity Test Method and Practice D 4306 on containers for jet fuel has been recommended commensurate with these findings.

Fuel Temperature and Conductivity Loss

Some time ago we studied chemically sweetened jet fuel from a refinery in Canada which tended to exhibit rapid conductivity loss after treatment with Stadis® 450, but it was observed that such losses were especially troublesome during hot summer months. This led us to evaluate the rate of conductivity loss exhibited by jet fuels as a function of temperature. Five Jet A and Jet A-1 fuels were chosen, several of which were known to exhibit conductivity loss problems. These were treated to obtain a moderately high conductivity. Half-liter samples in Teflon™ bottles were then stored at 4.4°C, 21°C, and at 43°C, and conductivity measured at the stored temperature over time [11]. Rate of conductivity loss generally showed a temperature relationship which is typical for slow chemical reactions. The one exception was Fuel B when stored at 4.4°C. This was from a refinery which has typically low aromatics content (12-14%) jet fuel, and the results indicate that some degree of micell formation or other phenomena may play a role. Results are in Tables 2, 3, 4, 5, and 6. We then prepared fresh samples of four of these fuels at 21°, determined conductivity after Stadis® 450 doping, and stored them 16 hours at 79°C. The samples were cooled for 3 hours back t[illegible]C, and conductivity re-measured. Results were in good agreement with data obtained after 4 t[illegible] weeks at 43°C. This technique needs additional work, however, to assess the reliability of the correlation. Prior to this work, we believed that the trend of conductivity stability would be apparent after two weeks storage at ambient temperature. These results indicate longer storage is needed to fully assess the potential for conductivity loss. We plan further work to fully develop this methodology, which will help to determine an appropriate initial conductivity, and to assess the possible need for further re-doping to assure minimum conductivity requirements are met.

Table 2. Fuel A (Jet A, processing unknown; 1 mg/L Stadis® 450)

Storage Temp °C	Initial PS/m, 21C	3 Hr pS/m at Temp	% Conductivity Change During Storage (Compared to 3Hr Result)				
			1 wk	2 wk	3 wk	4 wk	5 wk
4.4	274	179	+2	-4	+18	0	+7
21	268	248	-5	-9	-14	-22	-30
43	269	434	-20	-30	-32	-24	-31

Table 3. Fuel B (Jet A-1, Merox sweetened, 2 mg/L Stadis® 450)

Storage Temp °C	Initial PS/m, 21C	3 Hr pS/m at Temp	% Conductivity Change During Storage (Compared to 3Hr Result)				
			1 wk	2 wk	3 wk	4 wk	5 wk
4.4	285	235	-43	-55	-48	-60	-66
21	282	253	+7	-9	-14	-22	-30
43	294	547	-3	-15	-36	-54	-69

Table 4. Fuel C (Jet A-1, Merox sweetened, 2.5 mg/L Stadis® 450)

Storage Temp °C	Initial PS/m, 21C	3 Hr pS/m at Temp	% Conductivity Change During Storage (Compared to 3Hr Result)				
			1 wk	2 wk	3 wk	4 wk	5 wk
4.4	297	188	-13	--	-3	-15	-11
21	322	272	0	-8	-14	-21	-29
43	305	618	-19	-68	-66	-64	-65

Table 5. Fuel D (Jet A-1, Merox sweetened, 2 mg/L Stadis® 450)

Storage Temp °C	Initial PS/m, 21C	3 Hr pS/m at Temp	% Conductivity Change During Storage (Compared to 3Hr Result)				
			1 wk	2 wk	3 wk	4 wk	5 wk
4.4	329	216	-4	-4	-2	-9	-8
21	340	321	-30	-11	-17	-27	-39
43	330	636	-16	-77	-75	-77	-76

Table 6. Fuel E (Jet A-1, Merox sweetened, 2 mg/L Stadis® 450)

Storage Temp °C	Initial PS/m, 21C	3 Hr pS/m at Temp	% Conductivity Change During Storage (Compared to 3Hr Result)				
			1 wk	2 wk	3 wk	4 wk	5 wk
4.4	438	260	-2	+23	+7	0	0
21	450	399	+5	-18	-22	-28	-45
43	430	816	-27	-84	-85	-87	-85

Table 7. Conductivity of Jet Fuels After Heating 16 Hours at 79°C, and Cooling

Fuel	S450 Conc., mg/L	Initial Cond., 21°C	Cond. After 16 Hr 70°C Aging, and cooling 3 Hr to 21°C
A - Jet A	1	262	172 (-34%)
B – Jet A-1	2	315	137 (-57%)
D – Jet A-1	1.5	328	80 (-76%)
E – Jet A-1	1.5	371	67 (-82%)

Based on these results, we suggest the following.

- *Conductivity loss in Merox-sweetened jet fuels will be minimal when fuel is stored at low temperature. Loss can be further minimized by delaying treatment with Stadis® 450 during cold weather until after the fuel has cooled.*
- *Under most conditions, the likely maximum loss in conductivity during extended storage of jet fuel can be estimated by storing samples at 80°C for 16 hours, cooling to room temperature, and re-measuring conductivity.*

CONCLUSIONS

The possibility that insoluble sulfonates will form in jet fuel resulting in disarming of coalescers has been successfully addressed by introduction of a slightly modified Stadis® 450 with a new sulfonic acid stabilizer. The transition to this modified product has proceeded smoothly with no known difficulties.

Difficulties with the conductivity – MSEP tradeoff have been successfully addressed. Work is progressing to improve or develop test methods to better predict coalescer performance. Data suggest that the rate of conductivity loss which occurs during storage of some fuels follows a temperature relationship. This relationship predicts fewer problems at low fuel temperatures, and suggests that conductivity loss can be predicted with an accelerated test method.

Octel America, Inc. maintains information on Stadis® 450 in aviation fuels on the world wide web; address is www.octel-petadd.com.

ACKNOWLEDGEMENTS

Many individuals contributed to the success of the work reported above. The author wants to especially acknowledge the efforts of Ed Matulevicius, Exxon R&E and Vic Hughes, Shell Research who co-chaired the CRC Panel on Coalescer Deactivation; Udo Lauks, OMV – Berghausen, whose full cooperation and expert handling was crucial to the refinery trials with modified Stadis® 450; and finally, Andy Holden of British Airways who was a great help in obtaining the necessary aviation equipment manufacturers' acceptance of modified Stadis® 450.

REFERENCES

1. Henry, C.P., *Proceedings of the 5th International Conference on Stability and Handling of Liquid Fuels,* Giles, H.N. (Ed); U.S. Department of Energy, Washington DC, **1995**, 59-73.

2. ASTM D 3948-93 "Standard Test Method for Determining Water Separation Characteristics of Aviation Turbine Fuels by Portable Separometer", *Annual Book of ASTM Standards Vol. 5.02,* American Society for Testing and Materials, West Conshohocken, PA.

3. Henry, C.P. "Modified Stadis® 450 – Supporting Information on Composition and Performance", PLMR-7-95, Octel America, Inc., Newark DE, **1995.**

4. Henry, C.P. "Transition Underway for Modified Stadis® 450 in Aviation Fuels", Octel America Additive Brief 97-01, Octel America, Inc., Newark DE, **1997.**

5. API *Specifications and Qualification Procedures for Aviation Jet Fuel Filter/Separators,* API Publication 1581, 3rd Edition, May 1989 and amendment, API, Washington DC.

6. Minutes of the Aviation Fuel, Lubricant and Equipment Research Committee of the Coordinating Research Council, April 27, **1995.**

7. "The Effect of Stadis® 450 on MSEP Rating and Coalescence – Technical Basis of Re-doping Turbine Fuels with Stadis® 450", CRC Report No. 601, CRC, Atlanta GA, **1996.**

8. Defence Standard 91-91/Issue 2, "Turbine Fuel, Aviation Kerosene Type, Jet A-1", Ministry of Defence Directorate of Standardization, Glasgow, UK, **1996**.

9. CAN/CGSB-3.23-93 "Aviation Turbine Fuel – Kerosine Type", Amendment No. 4, Canadian General Standards Board, Ottawa CANADA, **1997**.

10. Henry, C.P., "Conductivity of Fuels After Exposure to Sunlight", Octel America Additive Brief 97-07, Octel America, Inc., Newark DE, **1997**.

11. Henry, C.P., Garcia, A.W. , Montgomery, N.E., and Horack, J.J. "Guidelines for Laboratory Evaluations of Stadis® 425 and Stadis® 450 Conductivity Improver Additive", Octel America Additive Brief 96-09, **1996**.

6th International Conference
on Stability and Handling of Liquid Fuels
Vancouver, B.C., Canada
October 13-17, 1997

THE EFFECT OF PHENOLIC IMPURITIES IN JET FUEL ON THE BEHAVIOUR OF CONDUCTIVITY IMPROVERS

Brian Dacre and Janice I. Hetherington*.

Rutherford Laboratory, Royal Military College of Science, Cranfield University, Shrivenham, Swindon, Wiltshire,
SN6 8LA, United Kingdom.

ABSTRACT

The conductivity improver Stadis 450 is known to give a variable conductivity response in jet fuels which come from different crudes and refinery processes. The present work shows that certain phenolic impurities in the jet fuel may be responsible for these variations and that fuels with a high phenolic content could be particularly prone to poor conductivity response with Stadis. Conductivity measurements on Stadis in model systems have shown that certain phenols interact with Stadis to cause considerable reductions in the conductivity. The magnitude of the effect is highly dependent on the concentration and the structure of the phenol and especially on whether the phenol is hindered or unhindered. Unhindered simple phenols such as m-cresol, p-cresol and phenol, at concentrations above 50ppm, cause a large reduction in the conductivity response with Stadis. Highly hindered phenols, such as the types used as antioxidants (2,6-di-tert-butyl-4-methylphenol), cause almost no reduction in the conductivity. This confirms the findings of the antioxidant suppliers. Partially hindered phenols such as 2-tert-butyl-4-methylphenol are intermediate in their effect on the reduction of the conductivity. Jet fuels analysed by BP revealed total phenol concentrations as high as 700ppm, which is considerably higher than had previously been expected. Of these phenols, 80% were found to be of the simple, low molecular weight, unhindered type, such as m-cresol, which were found in the model systems work to have the most damaging effect on the conductivity of Stadis. The conductivity of Stadis was measured in fuels of known phenolic content. The response was found to be lower in fuels of high phenolic content, thus confirming the behaviour predicted from model phenol systems. The role of the phenols on the conducting mechanism of Stadis is discussed. It is proposed that the phenol is involved in a proton donor interaction with a component of the Stadis, possibly the sulphone and that this interferes with the normal ion producing mechanism which imparts conductivity to Stadis-doped fuels.

1 INTRODUCTION

Jet fuel has a very low natural electrical conductivity, normally less than $5pSm^{-1}$. It is well known that dangerous levels of electrostatic charge can accumulate during the high speed pumping and filtration of jet fuel[1,2]. This can be overcome by increasing the electrical conductivity of the fuel which is achieved by the use of a static dissipator additive. Only one static dissipator additive is approved for this purpose, namely Stadis, supplied by Octel America. However, considerable variation is observed in the conductivity response of fuels from different crude oils when doped with the same amount of Stadis.

In earlier papers[3,4,5] we have reported the influence of a wide range of possible fuel components on the performance of Stadis. Sodium salts of acid impurities in the fuel were found[4] to have a complex effect on the conductivity. The salts at low concentrations were found to reduce, by as much as 50%, the conductivity performance of Stadis, with a minimum value of the conductivity occurring when the ratio (in ppm) of sodium salt to Stadis was approximately unity. At higher concentrations of the salts the conductivity response was enhanced. The sodium salts have a significant, but complex, effect on the water separation characteristics of model systems.

Preliminary work on phenols[4] indicated that some phenolic impurities also caused considerable conductivity loss, as great as 70%, in Stadis. The conductivity decreased non-linearly with phenol concentration but did not exhibit the conductivity minimum found with the sodium salts. The magnitude of the effect was dependent on the type of phenol and appeared to contradict the well documented knowledge that commercial phenolic antioxidants such as BHT (2,6-di-tert-butyl-4-methyl phenol) had no effect on the conductivity response of Stadis.

2 AIMS OF THE WORK

This work continues the theme of our earlier published work[3,4,5] with the aims of:

- investigating the influence of fuel components on the performance of the static dissipator additive Stadis 450,

- attempting to understand the nature of the intermolecular interactions occurring in Stadis 450 which impart conductivity to a fuel,
- attempting to understand, in terms of the intermolecular interactions occurring, the role of fuel components and impurities in assisting and obstructing that mechanism.

Our earlier work on phenols suggested that Stadis was sensitive to some types of phenolic impurities. The effect was greater and showed a different concentration dependence to the sodium salt impurities which we have studied in detail[4]. These findings appeared to conflict with the knowledge that antioxidants of the hindered phenolic type had no effect on the conductivity response of Stadis.

It was to clarify these points that a comprehensive study has been made of the influence of a range of unhindered, partially hindered and highly-hindered phenols on the conductivity of Stadis in dodecane solutions. The parameters studied are: (a) phenol type, (b) phenol concentration, (c) time effects, (d) comparison of response of Original Stadis 450 and Reformulated Stadis 450, (e) pK_a of the phenol.

The study of phenols in model systems is compared with the role of phenols in jet fuels doped with Stadis. To support this work BP has supplied fuels, analysed for phenol concentrations, phenol type and sources of phenolic impurities. The conductivity behaviour of Stadis in these fuels is characterised for the effects of: (g) fuel phenol levels, (h) fuel viscosity, (g) methods of removal of phenolic impurities.

These results are used to support a theoretical treatment of the equilibria for the interactions of the phenols with the Stadis. By elucidating the nature of the reaction it is hoped to increase the understanding of the conducting mechanism of Stadis and the sensitivity to impurities which could destroy or enhance the conductivity.

3 EXPERIMENTAL

3.1 Materials

Original Stadis 450 was supplied by Octel. Reformulated Stadis 450 was supplied by DuPont. *m*-cresol (3-methylphenol) was purchased from BDH Chemicals. The following phenols were purchased from Aldrich Chemical Company: 2,6-dimethylphenol, 2,4,6-trimethylphenol, 2-*tert*-butyl-4-methylphenol, 2-*tert*-butyl-6-methylphenol, 2,6-di-*tert*-butyl-4-methylphenol, o-cresol (2-methylphenol), *p*-cresol (4-methylphenol), phenol, 2-nitrophenol, 3-nitrophenol, 4-nitrophenol.

Dodecane was supplied by BDH Chemicals / Merk and purified as described previously[3]. Toluene (Analar) and acetone (Analar) were supplied by BDH Chemicals / Merk.

Jet fuels were supplied by BP.

3.2 Conductivity Equipment and Conditions

Conductivity measurements were made at 25C using the apparatus and experimental procedures described in previous work[3,4]. The uncertainty in the conductivity measurements with the laboratory built apparatus is estimated to be ±4%.

Concentrated stock solutions (~2000ppm) of each of the phenols listed above but excluding the nitrophenols, were made up in toluene and these were added to the Stadis solutions in the conductivity cells at the concentrations indicated in Section 4. The effect of toluene on the conductivity of the Stadis solutions is negligible at the concentrations employed. In the case of the nitrophenols concentrated stock solutions were made in acetone due to their limited solubility in toluene. The contribution to the conductivity from the nitrophenol / acetone system alone was always below 15pSm^{-1}.

4 RESULTS AND DISCUSSION

4.1 Effect of Model Phenolic Impurities on the Conductivity of Stadis 450 in Dodecane

The effect of a range of phenols on the conductivity of a 3ppm solution of Stadis 450 in dodecane is given in Figure 1. The most significant feature is the difference in the effect of the hindered and unhindered phenols on the conductivity response of Original Stadis 450.

The highly hindered phenol 2,6-di-*tert*-butyl-4-methylphenol has no effect on the conductivity of the Stadis 450 solution. This supports the general view in the industry that the antioxidant 2,6-di-*tert*-butyl-4-methylphenol (BHT) does not affect the behaviour of Stadis 450. It suggests that any similarly hindered phenol with large groups on the 2-, 6- positions will have no effect on the performance of Stadis.

The unhindered, simple phenols, by contrast, greatly reduce the conductivity of the Stadis solution. Phenol and *m*-cresol show the most pronounced effects with concentrations of 100ppm causing reductions of 50% in the conductivity and higher concentrations of 750ppm causing reductions of 80% in the conductivity. The analysis of the BP fuels indicated that levels of 100ppm of simple phenols regularly occur in fuels and that levels as high as 750ppm have been found.

The partially hindered phenols reduce the performance of Stadis, with the magnitude of the effect being as expected from the steric restrictions imparted on the -OH group or the phenoxide ion by groups in the 2- and/or 6- position. For example, the effect of 2-*tert*-butyl-4-methylphenol on the conductivity is intermediate between that for phenol and 2,6-di-*tert*-butyl-4-methylphenol.

The same trends are apparent when equimolar concentrations of the phenols are considered.

It should be noted that where there is a decrease in the conductivity for a phenol, the effect is nonlinear with the concentration and that there is no minimum in the conductivity versus concentration plot as was reported for sodium salt impurities in the previous paper in this

series[4]

4.2 Time Effects on the Conductivity of Stadis Solutions Containing Phenols

The conductivity of Stadis solutions in dodecane containing 650ppm of *m*-cresol and 2,6-di-*tert*-butyl-4-methylphenol remained unchanged from the values in Figure 1 when measured over a period of seven days. This confirms the lack of response of the conductivity of the Stadis solutions to highly hindered phenols and rules out the possibility of mobility or diffusion effects accounting for the difference in behaviour compared with simple unhindered phenols such as *m*-cresol.

The phenol concentrations of 650 ppm in these model systems were chosen to be representative of the level of phenolics measured in a fuel identified as exhibiting a drop in conductivity over a period of several days. These data indicate that although a poor response of Stadis in some fuels may be attributed to high levels of simple phenols, the phenols are unlikely to be responsible for any long term drop in conductivity.

4.3 Comparison of the Effect of Model Phenolic Impurities on the Conductivity of Reformulated Stadis 450 and Original Stadis 450 in Dodecane

In the presence of phenolic impurities the Reformulated Stadis 450 shows the same conductivity behaviour as the Original Stadis 450. Figure 2 for the Reformulated Stadis and Figure 1 for the Original Stadis show that simple phenols such as *m*-cresol at concentrations of 100ppm and above, greatly reduce the performance of both types of Stadis. Hindered phenols, even at concentrations as high as 1000ppm, have very little effect or no effect on either type of Stadis.

4.4 Dependence of Conductivity on Stadis Concentration at Constant Phenol Concentration

The poor conductivity response of Stadis even at relatively high concentrations in the presence of unhindered or partially hindered phenols is illustrated in Figure 3. The phenol concentration of 550ppm is typical of that found in fuels with high levels of phenolic impurities.

The data for *m*-cresol are particularly significant by showing that increasing the concentration of Stadis from 1ppm to 5ppm, the maximum level used in the industry, produces very little increase in the conductivity. This mimics the poor conductivity response reported for some fuels on increasing the Stadis concentration. These results suggest that the fuels in question had a high level of phenolic impurities.

Partially hindered phenols also depress the response of Stadis, but the effect is intermediate between that for the unhindered phenols and that in the absence of any phenols, as illustrated by the data for dodecylphenol.

The previous paper in this series[4] discussed the effects of sodium salts on the conductivity of Stadis solutions. The depression of Stadis performance is considerably greater in the presence of unhindered phenols than sodium salts when each are considered at the concentrations likely to be encountered in fuels.

4.5 Effect of pKa of Phenolic Impurities on the Conductivity Perform ance of Stadis 450

The magnitude of the effect of a phenol in relation to its pK_a is unclear from the data presented in Figure 1. There the magnitude of the effect is in the order:

phenol > *m*-cresol > *o*-cresol > *p*-cresol

whereas the relative order expected from consideration of the pK_a values would be:

phenol (9.95) > *m*-cresol (10.08) > *p*-cresol (10.19) > *o*-cresol (10.28)

The previous paper[4] in this series,postulated a proton transfer process for the ion producing mechanism of Stadis. The interference with this mechanism by a phenol must involve the -OH group and consideration of the effect of pK_a is significant in this context since it provides a means of quantifying its proton donor ability albeit in aqueous media.

Nitrophenols were used to extend the range of pK_a and degree of hindering. Although they are not found in fuels, their effect on the behaviour of Stadis is nevertheless interesting and suggestive in elucidating the mechanism of the interaction of the phenols in general. Figure 4 shows the effect of some Nitrophenols on the conductivity of a solution of Stadis. By simply

considering the pK_a of the Nitrophenols, the magnitude of the suppressing effect on the Stadis conductivity is expected to be:

4-nitrophenol (pK_a 7.14) > 2-nitrophenol (pK_a 7.2) > 3-nitrophenol (pK_a 8.35) > *m*-cresol (pK_a 10.8)

The order found experimentally is:

4-nitrophenol ≥ 3-nitrophenol >> *m*-cresol >> 2-nitrophenol

This suggests that the pK_a does relate to the effect on Stadis performance, but where groups are introduced in the 2-, 6- positions on the benzene ring then steric and other effects predominate over the effects of pK_a. The phenolic compounds appear to be acting as proton donors in the absence of such neighbouring groups.

Relying on pK_a data to interpret the behaviour of phenolic compounds in a hydrocarbon solvent is open to question, although some data[6] show a parallel between acidity in aqueous and non-aqueous systems.

4.6 Effect of Fuel Phenol Levels on the Conductivity Response of Stadis 450

A useful way of comparing the work on model phenol systems with the effects of phenol levels in real fuels is required. Figure 5 presents the data in terms of a ratio R, where R is a measure of the performance degradation of the Stadis due to the presence of phenols. R is the ratio of the conductivity of the Stadis solution (in dodecane or fuel) *with phenol present* to the maximum possible conductivity for an ideal Stadis solution in dodecane *without phenols*. Incorporated into Figure 5 is the performance degradation of Stadis in a number of fuels analysed by BP for phenol content. In Figure 5 a correction has been made for the difference in viscosity of the fuels and the dodecane as outlined in Section 4.7.

The fuels show a significant degradation in Stadis performance as the levels of phenolic impurities become higher.

4.7 Significance of Fuel Viscosity when Comparing Conductivity Response to Stadis 450

A two or threefold variation in viscosity is not uncommon in fuels[7] and the subsequent effect

on the conductivity response to Stadis must be taken into account when comparing fuel properties or performing standard tests. Work by Henry[8] and subsequent analysis by Dacre[9] shows that the relationship between the conductivity κ and the viscosity ν can be approximated by:

$$\kappa \propto 1/\nu^{0.7}$$

This relationship is used as the viscosity correction in Figure 5.

4.8 Removal of Phenolic Impurities from Fuels

The change in response of Reformulated Stadis to fuels at different stages in the refining process is shown in Figure 6. The fuels were supplied by BP. The conductivity response of the Stadis increases with each stage in the refining process. The largest change occurs after the Merox unit, suggesting that the efficiency of this process is paramount in determining the performance of Stadis.

The phenolic impurities from the caustic wash were isolated by BP and redoped into BP fuels and dodecane. The response of Stadis to this phenolic extract at different concentrations is given in Figure 7. The similarity with the response to the model phenolic impurities is striking. The agreement is excellent, both in the magnitude of the effect and the concentration of the phenolic impurity required to produce a given fall in the conductivity. These results highlight the importance of changing the caustic wash frequently to prevent problems with Stadis.

Filtering through fresh clay is found to remove phenolic and polar impurities from the fuel and to improve the response to Stadis. However impurities extracted from a 'spent' refinery clay bed do not cause a reduction in the conductivity of fuel doped with Stadis (in fact a small increase in conductivity was found) but they do have a large effect on the water separation characteristics. This supports the idea that the caustic wash is the critical stage in the refining process for removing the phenolic impurities and preventing problems with the conductivity response of Stadis.

5 SPECULATION ON THE ROLE OF PHENOLS IN DESTROYING THE CONDUCTION MECHANISM OF STADIS

5.1 General Comments

In earlier papers[3,4] we have discussed a possible mechanism for ion production in Stadis 450 solutions. In this mechanism an activated sulphone group $-SO_2$ plays a central role as a proton acceptor for carbonyl hydrogen from another molecule. Any interaction which interferes with this process will change the ion concentration and hence the conductivity. We suggest that the antagonistic effect of phenolics is caused by their complexation with sulphone which is then not available for interaction with ion-producing carboxyl groups. We have considered several alternative mechanisms, but the one outlined below combines simplicity with ability to represent observed behaviour as described in the following paragraph.

5.2 Equilibrium Model

If P represents a phenol and S the sulphone group in Stadis, then the association interaction between them can be written :

$$\begin{array}{ccccc} P & + & S & \leftharpoondown & PS \\ (a-x) & & (b-x) & & x \end{array}$$

where PS is a phenol/sulphone complex and a and b are the weighed-in molar concentrations of P and S respectively. If the solutions are sufficiently dilute to be ideal then the equilibrium constant can be written :

$$K = \frac{[PS]}{[P][S]}$$

$$= \frac{x}{(a-x)(b-x)}$$

If we assume that the measured conductivity, κ, is proportional to the free sulphone concentration [S], then in the absence of phenol the conductivity, κ_0 is given by:

$$\kappa_0 = Ab \quad \textit{where } A \textit{ is a constant}$$

also

$$\kappa = A(b-x)$$

$$Let\ F = \frac{\kappa}{\kappa_0}$$

$$then \quad b-x = bF$$

$$so \quad x = (1-F)b$$

$$(a-x) = [a-(1-F)b]$$

$$Thus\ K = \frac{(1-F)}{[a-(1-F)b]\ F}$$

$$so \quad \frac{(1-F)}{F} = K\ [a-(1-F)b]$$

and so in principle from conductivity and concentration data it is possible to obtain the equilibrium constant K. Unfortunately b, the molar concentration of sulphone groups is not known with any certainty since the information required for its calculation is not available. However for a given fixed sulphone concentration and for low phenol concentrations such that (1-F) is less than ~0.15, then b(1-F) << a and (1-F)/F plotted against a should be linear and have a slope equal to K. Plots have been obtained in this way for all the phenols and values of K have been derived.

5.3 K Values and Their Dependence on Phenol Type

If this simple model has any validity then we expect the K values to depend on phenol structure and in particular to depend on the influence of ring substituents. To check this we have used

the Hammett equation[10] which quantifies the ability of ring substituents to influence a reaction centre, which in this case is phenolic -OH. One form of the Hammett equation can be written

$$\log K = \rho\sigma$$

in which K is an equilibrium constant, the substituent effect is expressed in terms of a σ-value and the reaction type is characterised by ρ. We have calculated total σ-values for the combinations of substituents present using published data[10] and these are shown in Table 1. Figure 8 is the Hammett plot of logK against Σσ. The plot, which spans a thousandfold range of K values is encouraging and is consistent with a complexation process involving the -OH group and which is assisted by electron-withdrawing substituents. One further point is that it is possible to assess the behaviour of molecules of the antioxidant type 2,6-di-tert-butyl-4-methylphenol by extrapolating the Hammett line to the appropriate value of Σσ, which is equal to -1.04. The predicted K value is ~3 and is clearly consistent with the absence of antagonistic effects observed with this compound.

The magnitude of antagonistic effects observed at higher phenol concentrations may require further elaboration of the simple equilibrium model to include association of a second phenol molecule at a sulphone site. This will be reported in full when more information is available.

6 SUMMARY AND CONCLUSIONS

6.1 Simple phenols such as *o*-cresol, *m*-cresol, *p*-cresol and phenol, at concentrations above 50ppm, greatly *reduce* the conductivity of Stadis 450 and Reformulated Stadis.

6.2 Highly hindered phenols have no effect on the conductivity of Stadis.

6.3 Both the *type of phenol* and the *concentration of the phenol* affect the performance of Stadis.

6.4 Analysis of fuels by BP has indicated phenolic levels as high as 750ppm, with 80% of the phenols being of a simple low molecular weight type such as cresols.

6.5 The response of Stadis was found to be poorer in fuels of high phenolic content.

6.6 The behaviour of Stadis in a limited number of fuels of known phenolic content fits with the behaviour of Stadis in model phenol systems. Further work on reliably characterised fuels is required to confirm the types and concentrations of phenols in the fuel which will give rise to problems with Stadis.

6.7 Phenolic extract from the caustic wash of the refinery behaved in a very similar manner to the model simple non-hindered phenol impurities.

6.8 To remove phenols from fuels effectively, the caustic wash should be replaced regularly to prevent high levels of phenols accumulating and being reincorporated into the fuel.

6.9 Where the conductivity response of fuels is being compared, the viscosity-corrected conductivity should be used.

6.10 It is speculated that phenols interact with sulphone groups present in Stadis 450 and that the resulting complexed sulphone has less ability to activate the ion production mechanism.

6.11 A model for complexation is suggested and is successfully treated by simple equilibrium theory. This permits the calculation of equilibrium constants.

6.12 The variation of the equilibrium constant with phenol structure, as represented by the Hammett σ-value, is consistent with a complexation model in which the phenol group is an interaction centre. As a consequence the equilibrium constants also correlate with the phenol pK_a values.

6.13 Some anomalous effects are observed for phenols with substituents adjacent to the phenolic group.

7 ACKNOWLEDGEMENTS

The authors wish to thank additive manufacturers and oil companies for there helpful cooperation and supply of additives and fuels. In particular they would like to thank BP for the analysis of the fuels and for many helpful and enjoyable discussions during the course of this work. They would also like to express their gratitude to the sponsors of this work, LSF4, DERA, Pyestock, Farnborough, UK, under contract LSF/E20093.

8 REFERENCES

(1) Klinkenberg,A; van der Minne,J.L. *Electrostatics in the Petroleum Industry*; Elsevier,1958.

(2) Bustin,W.M,:Dukek,W.G. *Electrostatic Hazards in the Petroleum Industry*; Research Studies Press, 1983.

(3) Dacre,B; Abi Aoun,W.G. The Effects of Fuel Components on the Behaviour of Conductivity Improvers in Jet Fuel, 4th International Conference on Stability and Handling of Liquid Fuels, Orlando, Florida, USA, November 1991.

(4) Dacre,B; Hetherington,J.I. Behaviour of Conductivity Improvers in Jet Fuel, 5th International Conference on Stability and Handling of Liquid Fuels, Rotterdam, The Netherlands, October 1994.

(5) Dacre,B; Abi Aoun,W.G. Effects of Fuel Components on the Performance of Conductivity Improvers in Hydrocarbons, *Journal of Electrostatics*, 1997, *39*, 89-110.

(6) US Department of Commerce NBS Monograph 105, *Acid-Base Behaviour in Aprotic Organic Solvents*, August 1968.

(7) Annual Reports by DQA/TS and DRA, *Quality of Aviation Turbine Fuels Available in the UK,* 1983 to 1992.

(8) Henry,C. CIT/MOD Seminar on Aviation Turbine Fuel Specification - History and Future Development, Bath, UK, September 1988

(9) Dacre,B, Unpublished Work

(10) Perrin,D.D.; Dempsey,B.; Serjeant E.P. *pK_a Predictions for Organic Acids and Bases*, Chapman and Hall, 1981.

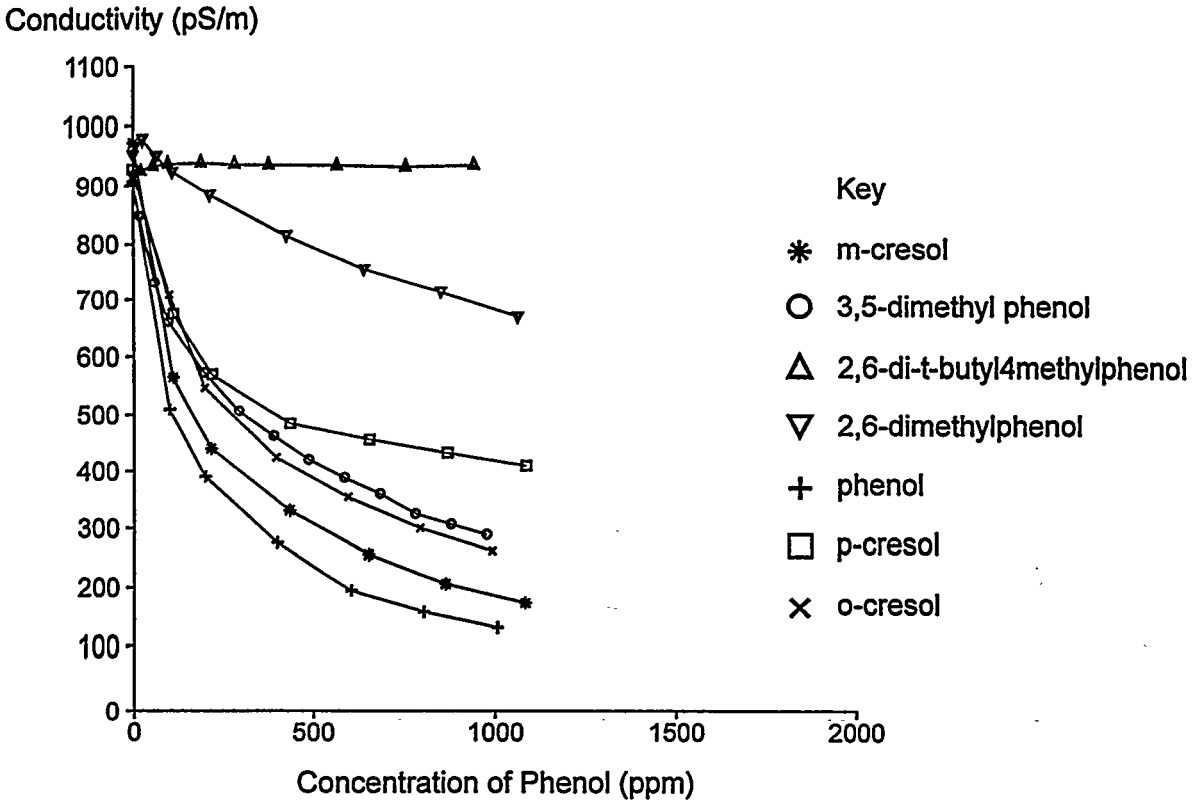

Fig. 1 Effect of Phenol Type on the Conductivity of 3ppm Original Stadis 450 in Dodecane

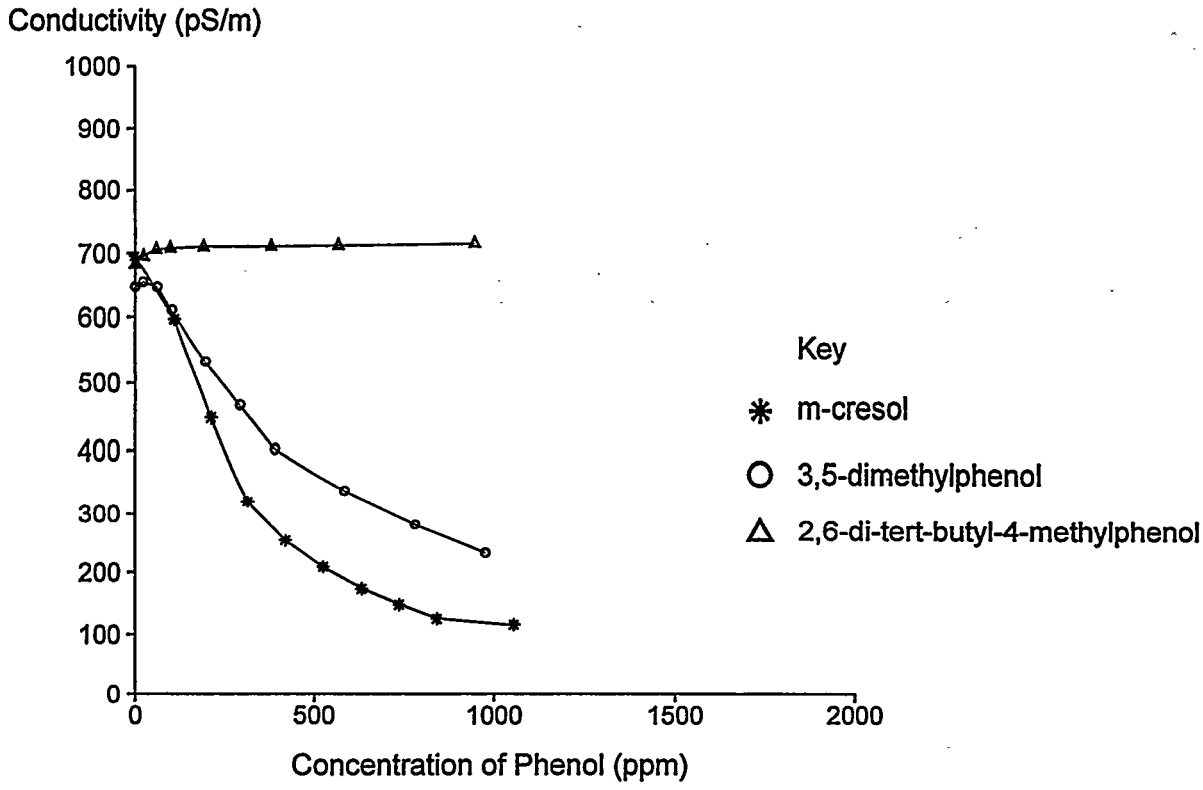

Fig. 2 Effect of Phenol Type on the Conductivity of 3ppm Reformulated Stadis 450 in Dodecane

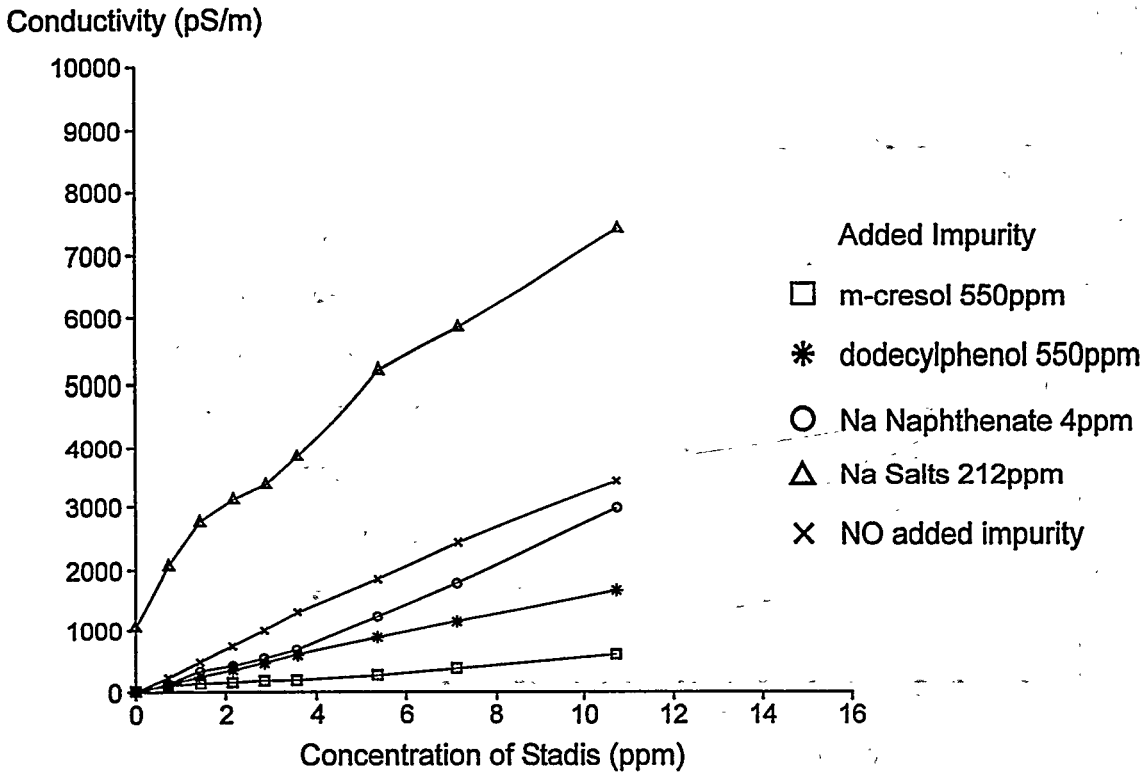

Fig. 3 Conductivity Response of Original Stadis 450 in Dodecane Containing Sodium Salt and Phenolic Impurities

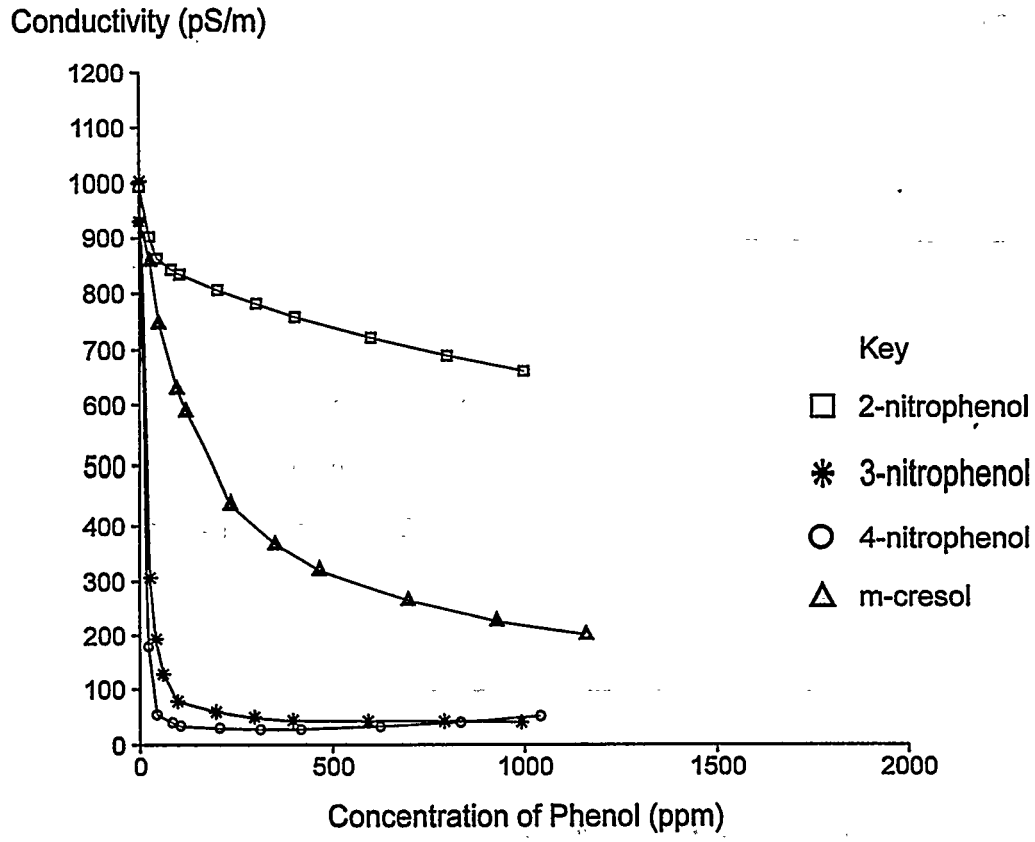

Fig. 4 Effect of Phenol Type on the Conductivity of 3ppm Original Stadis 450 in Dodecane

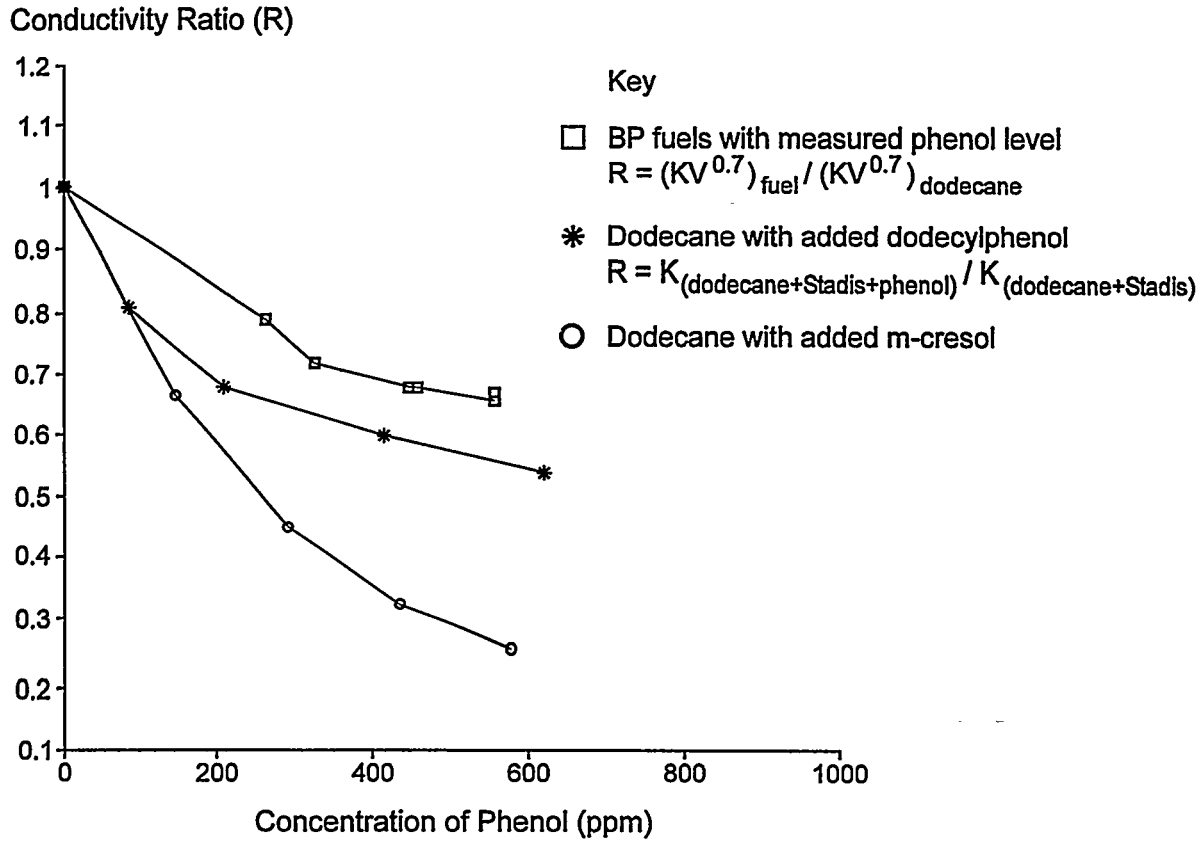

Fig. 5 Effect of Phenols on the Conductivity of 4.8ppm Original Stadis 450 in Fuels and Dodecane

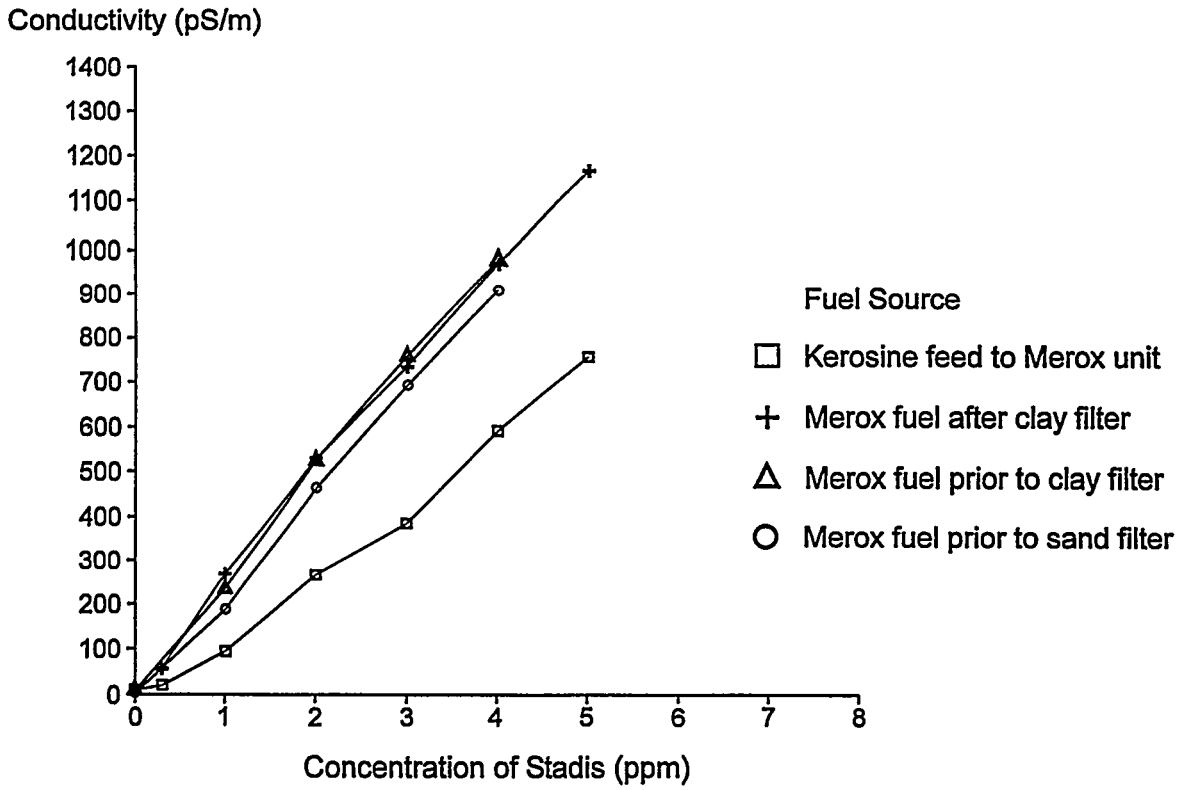

Fig. 6 Conductivity vs. Concentration for Reformulated Stadis 450 in Fuel from Different Stages in the Refining Process

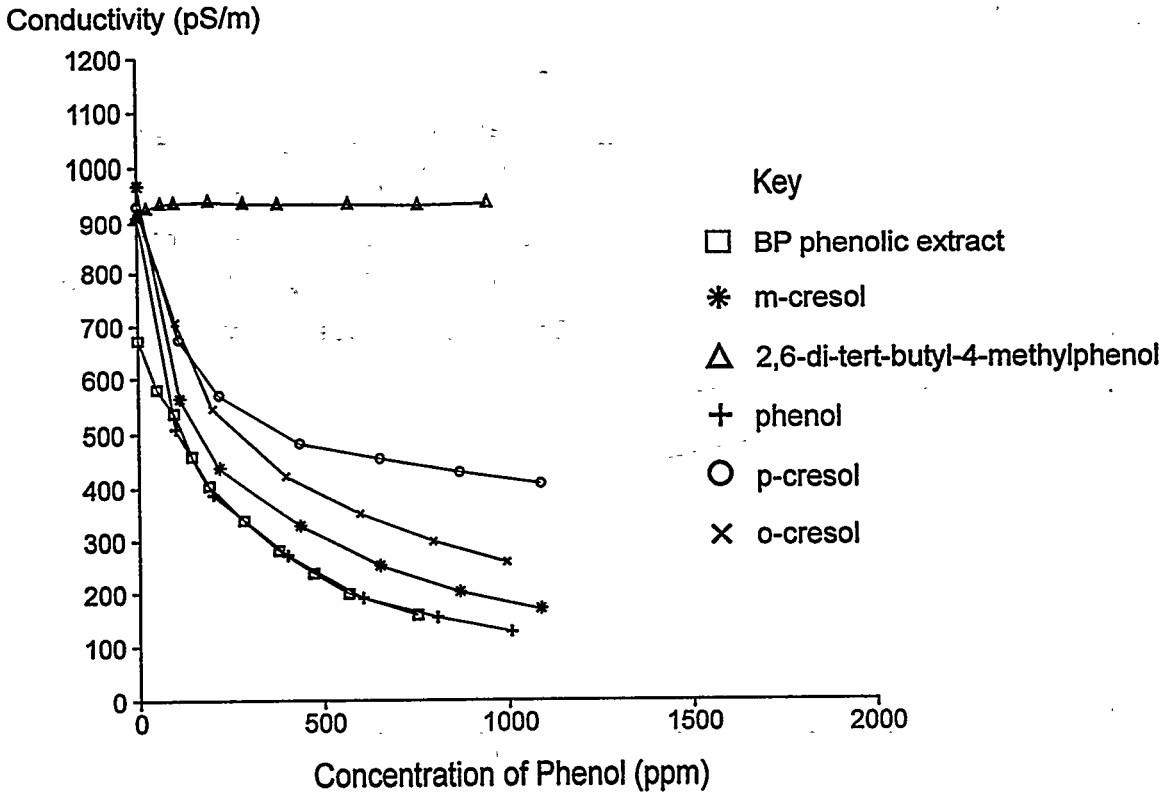

Fig. 7 Effect of Phenol Type on the Conductivity of 3ppm Original Stadis 450 in Dodecane

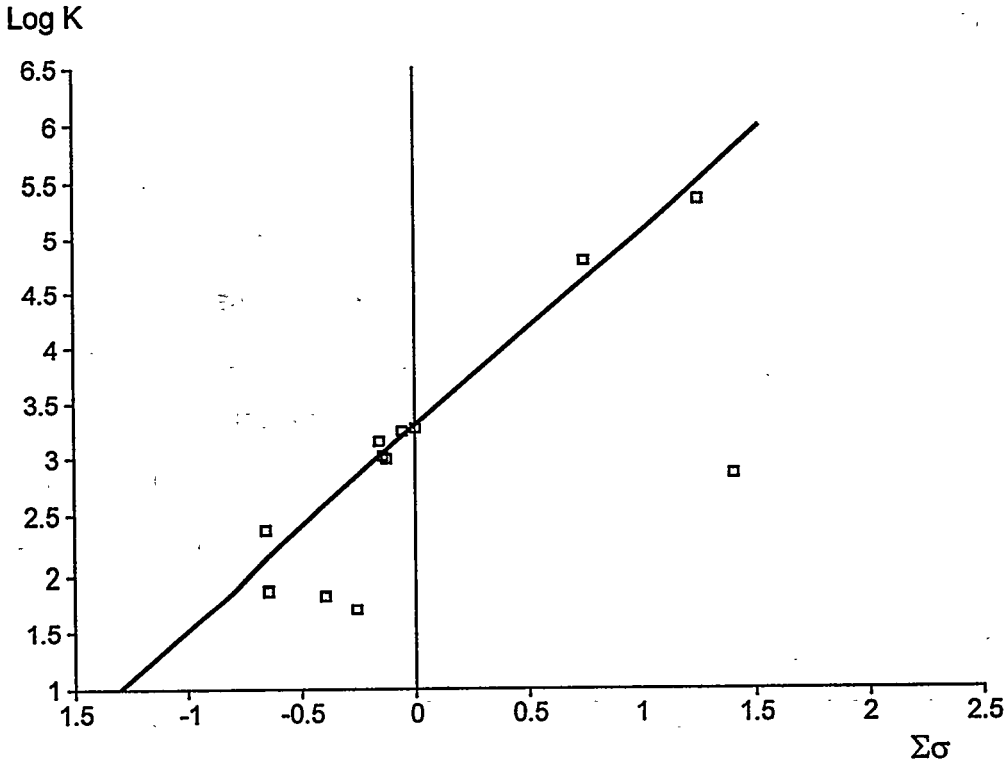

Fig.8 Variation of Equilibrium Constant (K) with Substituent Constant (σ)

Substituents	Σσ	Substituents	Σσ
4-methyl	-0.14	2,6-terbutyl	-1.04
3-methyl	-0.06	2-terbutyl,6-methyl	-0.65
2-methyl	-0.13	2,4,6-trimethyl	-0.4
4-dodecyl	-0.16	4-nitro	1.24
2,6- dimethyl	-0.26	3-nitro	0.74
2-terbutyl,4-methyl	-0.66	2-nitro	1.4

Values have been calculated from tables A1,A4 and A5 in reference 10. The value for 4-dodecyl has been assumed to be equal to that for butyl.

Table 1 Total Substituent Constants for Substituted Phenols

6th International Conference
on Stability and Handling of Liquid Fuels
Vancouver, B.C., Canada
October 13-17, 1997

COPPER CONTAMINATION OF JET FUEL FROM SHIPS' HEATING COILS

Peter David*, Alan Goddard, Spencer E. Taylor and Andy J. Woodward

BP Oil, Chertsey Road, Sunbury-on-Thames, Middlesex, UK, TW16 7LN

Abstract

Metal contamination of aviation fuels can sometimes occur during distribution to the extent that the fuel is rendered off-specification with respect to thermal stability. Such problems can occur during sea transportation and the effects can often be traced to on-board copper dissolution from ship's heating coils, employed for shipment of more viscous cargoes, such as residual fuel. Verification of the metal-leaching propensity of fuels has been based for the most part on the results from tests involving controlled storage of fuels over specimens of representative metallurgies, followed by metal analysis to determine the levels of contamination. Often these experiments are lengthy and by the time the results of the extended tests are known, failures in the JFTOT or other indicators of contamination are also known. There is therefore a requirement for a method which will rapidly determine a fuel's propensity for copper leaching, especially in cases where it is known that the likelihood is high of the fuel coming into contact with copper alloys. A simple laboratory test based on copper strip immersion with determination of fuel copper by a new in-house colorimetric method has been devised to predict the aggressive nature of fuels towards copper alloys. The relationship with fuel composition and processing route has been investigated. The quartz crystal microbalance (QCM) with copper crystals has also been used to study copper dissolution from fuel systems; results are generally in agreement with the immersion tests. Details of the studies are presented in the paper, together with recommendations on test implementation.

Introduction

Metals contamination of aviation fuels can sometimes occur during distribution to the extent that the fuel is rendered off-specification with respect to thermal stability. Such problems can occur during sea transportation and the effects can often be traced to on-board copper dissolution from ship's heating coils, employed for shipment of more viscous cargoes, such as residual fuel. The detrimental effects of copper on JFTOT breakpoint are well known[1].

In a recent example, a batch of Merox treated jet fuel was transported from Sardinia to the UK. The fuel satisfied specification requirements on loading, but after discharge, failed

JFTOT at 260°C. Upon investigation, the fuel had been carried on a ship with copper alloy heating coils in the product tanks and the copper content of the jet fuel had increased from 6ppb (μg/kg) to in excess of 60ppb. Not all the tanks contained heating coils, and the copper content of samples taken from these tanks indicated no uptake of copper. On this occasion, the fuel was treated with metal deactivator additive (MDA) in accordance with specification requirements, prior to release. The whole episode created considerable operational difficulties, which could have been minimised, or even avoided, if there had been some forewarning that copper contamination might have occurred. The incident prompted a study at the BP Oil research laboratories at Sunbury-on-Thames to investigate the propensity for fuels to leach metals from ships' heating coils and to develop a laboratory predictive test, details of which are given in this paper.

The study covered three areas of activity:

- Long term fuel storage over representative heating coil sections
- Laboratory short-term copper strip immersion tests
- Evaluation of quartz crystal microbalance (QCM) to study copper dissolution.

Long term fuel storage over heating coil sections

To simulate carriage of jet fuel in ships' tanks with heating coils, controlled laboratory immersion tests were performed. Test sections of typical heating coils were immersed in a range of Merox and hydrofined fuels contained in 1 litre glass bottles at 43°C for 12 weeks and the copper content monitored during the storage period. The composition of the heating coils is shown in Table 1. These analyses were obtained using X-Ray Fluorescence rubbing techniques and the data shown thus represent surface composition.

The heating coil sections were cut to size to give surface areas of *ca* 22cm^2, giving a surface area:fuel volume *ca* 100 times greater than in practice. This high ratio was chosen to allow ease of reproducing the same surface area sizes for the different heating coils and also to accelerate the metal leaching process to enable laboratory assessment. The test sections were lightly rubbed with emery paper to remove any surface oxides present, and thoroughly solvent washed beforehand.

Uptake of copper, zinc and iron was monitored using Inductively Coupled Plasma-Mass Spectrometry (ICP-MS). Only copper measurements are presented here; similar trends were observed for iron and zinc uptake.

Figure 1 shows that there was significant leaching of copper from the aluminium/brass and copper/nickel/iron heating coils by the Merox treated fuel which occurred within a matter of days and continued throughout the storage period. For the tests with the galvanised steel and stainless steel coils, there was no increase in copper content, as expected from the coil composition. The galvanised steel coil gave significant increases in iron and zinc contents; the stainless steel coil was the most inert of the coils examined, although even here there was a slight increase in iron content.

In contrast, Figure 2 shows that the hydrofined fuel was far less aggressive towards the coils, with no significant increase in copper uptake during storage. It is not precisely known how metal contamination of the fuels occurs, although it is suspected that polar species present in trace amounts may be aggressive to metals. Fuels are known to contain low residual levels of species which vary in acidity, such as phenates, naphthenates, sulphonates, and such species are likely to be present at higher levels in the Merox treated fuel than in the hydrofined fuel.

In Figure 3, the effect of MDA in the two fuels is shown; results are shown for the aluminium brass coil tests. The presence of the additive leads to a significant increase in uptake of copper compared with the base fuels. It is interesting to note that the copper level in the MDA treated Merox fuel after 12 weeks storage is at a higher level than might be anticipated on the basis of metal chelation alone. On a stoichiometric basis, 5.7 mg/l MDA will chelate with *ca* 1300 ppb copper, coincidentally the level in the MDA treated hydrofined fuel after 12 weeks. With hindsight, it would have been worthwhile continuing the storage period for this fuel beyond 12 weeks. These data indicate that under the conditions of the tests performed, there would have been high levels of unchelated copper present especially for the Merox treated fuel, suggestive of poor thermal stability. Unfortunately, JFTOT tests were not performed on the fuels during this study, the original purpose of which was to define the potential for copper uptake from heating coils.

It is recognised that differences in heating coil surface finish will strongly influence the metal leaching process. No attempt was made in the investigation to characterise the surface finish of the heating coil sections and thus comparisons of absolute metals content observed should be treated with caution. For the same reasons, no attempts are made to predict the extent of metal leaching which would occur in practice with full size heating coils. However, the trends observed between the various fuels and heating coils are likely to be valid and indicate that some fuels will be aggressive towards heating coils. On the evidence of field experience, such fuels may be rendered off-specification in terms of their thermal stability.

Laboratory short term screening tests

The metal leaching propensity of fuels can be established by controlled storage of fuels over specimens of representative metallurgies, followed by metal analysis to determine the levels of contamination. However, these experiments are lengthy, and by the time the results of the extended tests are known, failures in the JFTOT or other indicators of contamination are known. Such tests cannot therefore be used practically to predict the potential for copper contamination. On the basis of the results from the coil immersion tests, consideration was given to development of a laboratory test to predict the aggressive nature of fuels to heating coils. Such a test could find use to establish the acceptability of transporting fuels in product carriers with heating coils in situations where no other carrier is available.

A simple laboratory test based on the Copper Strip Corrosion test (IP 154/ASTM D130) was devised. The fuel is subjected to the standard test for jet fuels of 2 hours at 100°C with additional copper content measurement before and after strip immersion. The premise is that the extent of copper pick-up will be indicative of the propensity of the fuel to leach metals from heating coils.

Initially, copper contents were measured by atomic absorption spectroscopy, but it was recognised that such equipment might not be available in less well-equipped laboratories. Accordingly, a simple, laboratory test method for copper was developed. The method is based on:

- Ignition of the fuel remaining after the standard copper strip immersion test in the presence of sulphuric acid
- Ashing of the material remaining after ignition at 500°C
- Dissolution in sulphuric acid
- Complexation with 2,2-biquinoline
- Extraction into iso-amyl alcohol
- Measurement of absorption at 545 nm

Results for a hydrofined and Merox treated fuel are shown in Figure 4 and show that the Merox fuel was more aggressive in terms of copper pick-up than the hydrofined fuel. The trend is similar to that observed for the heating coil immersion tests, although comparison between absolute levels of copper pick-up cannot be made.

In blends containing both hydrofined and Merox components, the extent of metal leaching is dominated by the presence of the Merox component, and within the limits of experimental error, the relationship is linear (see Figure 5). The copper measurements are given in Table 2 where results by atomic absorption and the colorimetric method are compared. There is generally good agreement. The lower limit of detection of the colorimetric method is *ca* 25 ppb, restricted by the volume of fuel (30ml) arising from the standard copper strip corrosion test. By increasing the sample volume, the lower limit of detection may be reduced.

In order to compare the role of individual acidic species in determining the metal leaching propensity of fuels, copper strip immersion tests were performed on fuel containing various individual acidic reagents representative of those naturally occurring in fuels. These included:

- Phenols, as p-cresol, at levels up to 100 mg/l
- Naphthenic acids, molecular weight 190, at levels up to 100 mg/l
- Sulphonate as Aerosol OT (dioctyl ester of sodium sulphosuccinate) at levels up to 0.1 mg/l.

The effect of these reagents at the maximum addition rate given above on the copper strip immersion test is shown in Figure 6. The base fuel selected was a hydrofined jet fuel and the additional effect of MDA is also shown. In these tests, when added singly, the p-cresol and

AOT had little effect on copper pick-up, whereas the naphthenic acids were aggressive to some extent, resulting in levels of copper comparable with those observed for Merox fuels. MDA added singly had a similar effect. In contrast, very high levels of copper extraction occurred when the MDA was added in combination with the acidic reagents, with apparent synergism being observed. Definite conclusions cannot be drawn from the limited data available; a separate study at the BP Oil laboratories at Sunbury is currently underway to help clarify matters. The data do suggest that the presence of MDA can have a pronounced effect on the leaching of metals from heating coils. Unfortunately, as with the heating coil immersion tests described earlier, no assessment of the fuel thermal stability was made, and no conclusions regarding the state of the metal ions (whether chelated or not) can be drawn.

Finally, samples of Merox treated and hydrofined fuels were taken from the market and subjected to the copper strip immersion test. Whilst recognising that the quality of such fuels will be dependent on processing conditions and crude source, it is clear from Figure 7 that the three hydrofined fuels examined were not aggressive to copper, whereas the six Merox treated fuels showed varying degrees of propensity to leach out copper. The effect of approved jet fuel additives (added at the maximum permitted addition rate) is also shown in the Figure 7. As expected, the additives had little effect on copper corrosion, although it is possible that any effect might have been swamped by the corrosive properties of the base fuel.

Application of QCM to study copper dissolution

QCM offers the sensitivity to determine rapidly a fuel's propensity for copper leaching through ready detection of the dissolution of very small (ng) masses of copper. Previous experience with QCM has largely been directed at the use of "inert" metal electrodes (usually gold Au-QCM) for following deposition in jet fuel thermal degradation experiments. In the present study, copper dissolution was studied using copper electrodes (Cu-QCM).

QCM employs the piezoelectric resonant properties of a quartz crystal which change proportionately with small mass changes, either through deposition or dissolution on/from the active electrode surface. By measuring the change in frequency of the quartz crystal oscillator, a mass change can be quantitatively detected. The theory of QCM and practical details of QCM operation may be found elsewhere[2].

The fuels examined in this study comprised Merox treated and hydrofined basestocks and blends thereof. The QCM experiments were performed at 105+/-1°C. Whilst extremely small reductions in mass resulting from dissolution can be readily detected, any deposition from thermal degradation which may also be occurring may serve to complicate the observed behaviour. Thus both Cu-QCM and Au-QCM experiments were performed. It is assumed that results from the Cu-QCM will comprise contributions from both dissolution and deposition, whereas the Au-QCM results reflect deposition only.

For the Cu-QCM, there was a frequency change consistent with mass loss from the crystal. For the Au-QCM experiments performed under identical conditions, the frequency change was consistent with crystal mass increase, ie through deposition. Changes of frequency with time as a function of blend composition are shown in Figure 8. Positive values are indicative of mass loss; negative values indicate mass gain. The behaviour is interesting in that there is an apparent maximum rate of dissolution at approximately a 50:50 Merox:hydrofined blend. For the Au-QCM experiments, there is roughly a linear decrease in deposition rate with increase in hydrofined component, suggesting that the Merox component is the major contributor to the deposition behaviour. (This agrees with the results from the copper strip immersion tests described earlier.)

From the measured rates of frequency change given in Figure 8, an estimate of the dissolution rate in which deposition effects have been accounted for can be obtained. The resultant behaviour is shown in Figure 9 and is believed to be a more realistic measure of copper dissolution. Treated in this manner, the results suggest that as with deposition, the level of Merox component dictates the propensity for copper dissolution. Also shown in Figure 9 are results of copper strip immersion tests on the same samples as the Cu-QCM tests. The same general features are exhibited by both series of results providing strong support for the interpretations of the QCM approach.

Whilst recognising that a number of assumptions have been made in interpretation of the QCM data, these preliminary findings confirm the potential of QCM for the assessment of the copper dissolving propensity of aviation fuels towards heating coils. In particular, it has been

assumed that deposition rates will be identical on the gold and the copper crystals and no account has been made of the destabilising effect the dissolved copper will have on the fuel stability.

Conclusions

- Metal contamination from ships' heating coils can make fuels off specification in terms of their thermal stability. Heating coils comprising copper alloys are particularly hazardous; stainless steel coils are inert.
- In general, Merox fuels are more aggressive than hydrofined fuels in their propensity to leach metals from heating coils. Differences are related to the levels of trace acidic species present in the fuels.
- Laboratory strip immersion tests with copper determination can be used to identify potentially aggressive fuels.
- QCM is sufficiently sensitive to study copper dissolution.

Recommendations

- Whenever possible, ships with copper alloy heating coils should be avoided, especially for MDA treated fuels.
- If unavoidable, JFTOT tests should be performed before and after shipment.
- The fuel leaching potential of the fuel may be assessed by the copper strip immersion test.
- If deterioration in JFTOT performance has occurred through metal contamination, consideration may be given to the use of MDA after discharge to restore the fuel quality in accordance with specification requirements.

Acknowledgements

This project was funded by Air BP and UK Ministry of Defence.

References

(1) Hazlett, R.N.; Thermal Oxidation Stability of Aviation Turbine Fuels; ASTM, Ann Arbor, MI, 1991.

(2) Bruckenstein, S.; Shay, M.; Experimental Aspects of Use of the Quartz Crystal Microbalance in Solution, *Electrochim. Acta*, **1985**, 30, 1295-1300.

TABLE 1

HEATING COIL COMPOSITION

(%m, surface analysis)

	Al / Brass	Copper / Nickel / Iron	Galvanised Steel	Stainless Steel
Copper	75.4	86.1	-	0.7
Zinc	22.1	0.13	97.7	-
Iron	0.08	1.7	1.8	65.5
Aluminium	1.9	-	-	-
Nickel	-	10.7	-	11.6
Chromium	-	-	-	17.2
Others	0.5	1.37	0.5	5.0

Table 2

COPPER STRIP IMMERSION TEST RESULTS (µg/kg)

	AA COPPER	COLORIMETRIC COPPER
Merox treated Jet A-1	520	490
Hydrofined Jet A-1	40	40
80/20 v/v Merox/hydrofined	500	470
60/40 v/v Merox/hydrofined	360	340
50/50 v/v Merox/hydrofined	300	280
40/60 v/v Merox/hydrofined	280	250
20/80 v/v Merox/hydrofined	130	120

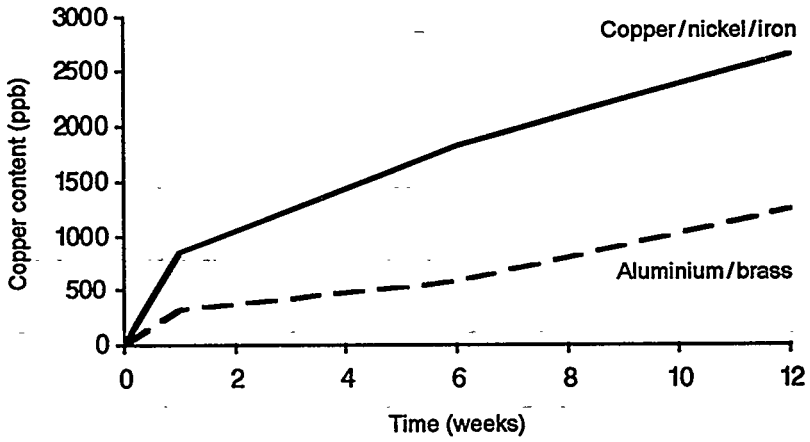

Figure 1. Heating coil immersion tests – Merox fuel

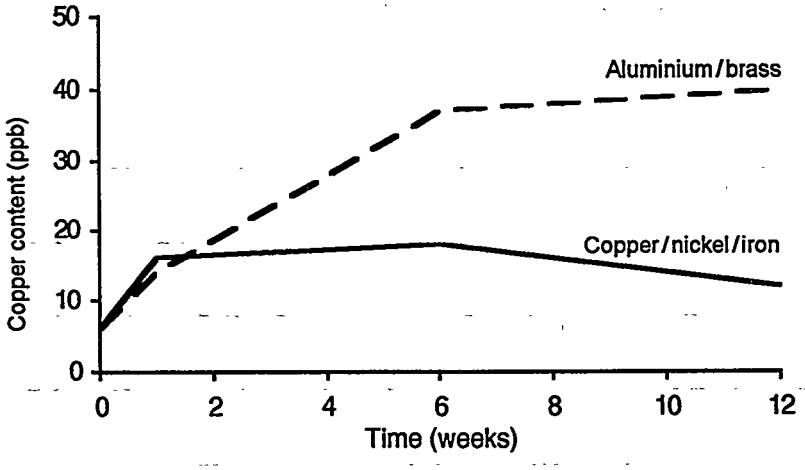

Figure 2. Heating coil immersion tests – Hydrofined fuel

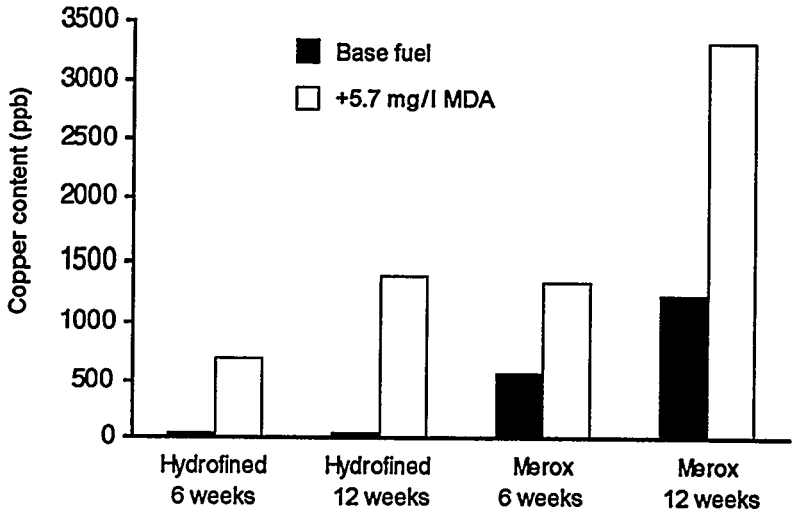

Figure 3. Heating coil immersion tests – Effect of MDA

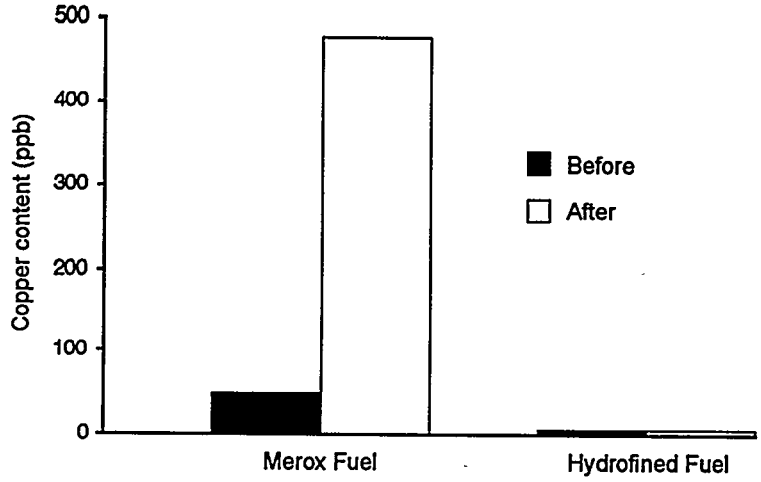

Figure 4. Laboratory copper strip immersion tests

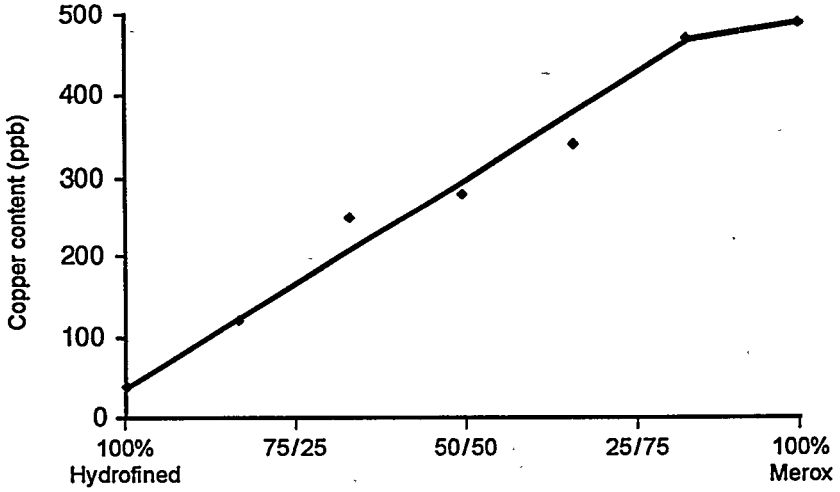

Figure 5. Copper strip immersion tests effect of blend composition

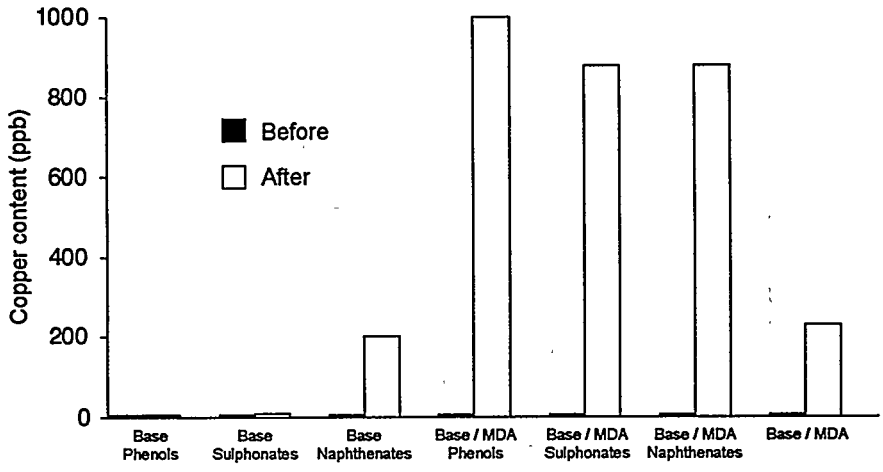

Figure 6. Copper strip immersion tests: Hydrofined fuel with acidic species / MDA

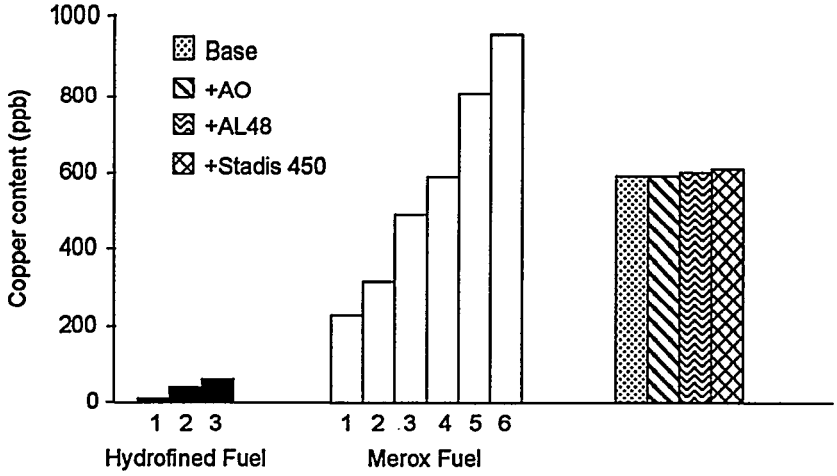

Figure 7. Copper strip immersion tests market samples / additive effects

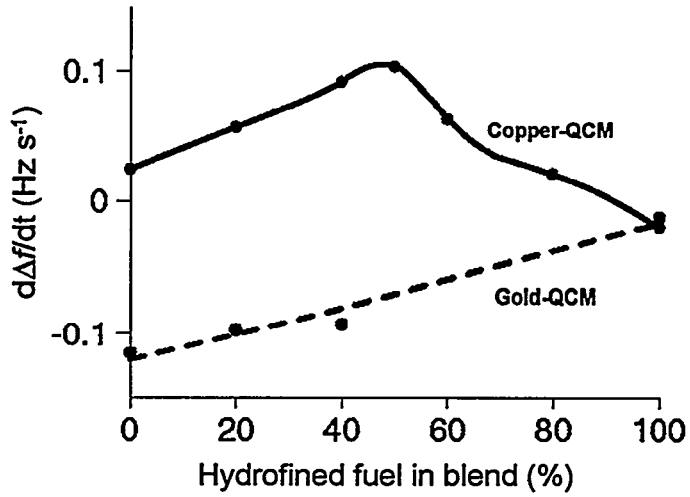

Figure 8. Frequency change rates – Copper and Gold QCM

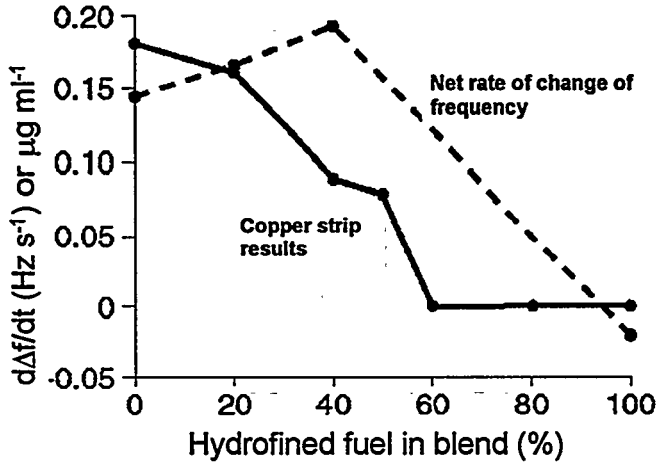

Figure 9. Copper dissolution results – QCM and strip immersion

6th International Conference
on Stability and Handling of Liquid Fuels
Vancouver, B.C., Canada
October 13-17, 1997

CHARACTERISATION AND QUANTIFICATION OF DEPOSITS FROM THERMALLY-STRESSED AVIATION FUELS

Clive Baker, Peter David, Ian Love, Robin Mogford, Spencer E. Taylor*
and Andy J. Woodward

BP Oil, Chertsey Road, Sunbury-on-Thames, Middlesex TW16 7LN, UK

Abstract

Using a combination of the Ellipsometric Tube Analyser (ETA), SEM/EDX analysis and the Jet Fuel Thermal Oxidation Tester (JFTOT), three aspects of thermally-induced deposit formation in jet fuels have been studied. These are (i) the quantification of surface deposits and bulk insolubles generated in the JFTOT test, and the extent to which metal deactivator additive affects deposition rates; (ii) the feasibility of characterising fuel thermal stability from single JFTOT runs; and (iii) a preliminary analysis of the composition and nature of *abnormal* deposits generated in JFTOT tests and the mechanism by which they are formed. The analyses have been based on results from a variety of fuel types.

Introduction

The action of thermally stressing jet fuels is well-known under operational conditions, and research to understand the phenomena involved is well-documented in the literature.[1] The laboratory study of these aspects of fuel thermal breakdown is restricted to a few specialised approaches. Traditionally, the Jet Fuel Thermal Oxidation Tester (JFTOT) is a laboratory device for evaluating the thermal oxidative stability of a jet fuel under a standard set of operating conditions. The device is used to identify the extent of fuel thermal breakdown through the formation of *surface deposits* on a heated metal tube, and also indicates the formation of particulates which cause an increase in pressure differential across a test filter. The ASTM D1655 specification for jet fuel takes into account both types of deposit formation through an assessment of the tube surface coloration and the differential pressure. In a previous

report,[2] the analysis of filterable deposits generated in the JFTOT was achieved by replacing the conventional *ca.*17 micron Dutch-weave filter with a 0.45 micron Millipore membrane and analysing the deposits gravimetrically. This approach usefully complements data provided by more labour-intensive rig testing, and thereby provides additional information on the mechanism and chemistry of fuel degradation under *quasi-dynamic* conditions of laminar flow. Results of previous work along these lines has shown that the rate of bulk particulate formation decreases with increasing JFTOT test time.[2]

Until very recently, routine quantification of JFTOT tube surface deposits was only possible under specific conditions, such as when sufficient deposit was present to allow its combustion and determination of the evolved CO_2, or through dielectric breakdown measurements. These approaches require that deposition occurs over relatively long periods in order to obtain measurable deposit levels, with the mean rates of deposition over the particular time period being quoted. Generally, it has been observed with the carbon burn-off technique that the quoted *deposition rates* initially increase with time, suggesting that different deposition processes are occurring during the experimental timescales. The disadvantage of this methodology, however, is its relative insensitivity to the *early stages of deposition*, which are likely to be formative for the overall course of deposition. One approach to overcome this problem has been through the use of ellipsometry for the analysis of the dimensions of surface films on JFTOT tubes. A description of the basic principles of the ellipsometric approach for characterising surface deposits was presented at the Rotterdam IASH meeting.[3] Since that time, an Ellipsometric Tube Analyser (ETA) dedicated to the handling and deposit quantification of JFTOT tubes has been developed in conjunction with Plasmos GmbH (Munich). This device is able to determine typical surface film thicknesses in the range 0 - 300nm, and is therefore able to characterise the early stages of deposition.[4]

The overall aim of the present study is therefore to quantify fuel breakdown and the formation of different types of deposits in the JFTOT. In particular, examples are described in which a combination of ellipsometric tube analysis, gravimetry and scanning electron microscopy (SEM) are used to investigate different aspects of fuel thermal oxidative stability. These include (i) the relationship between surface and bulk

deposits generated in the JFTOT test, and the extent to which these are affected by the presence of metal deactivator additive; (ii) characterisation of fuel breakdown in terms of the temperature-time course of deposition in the JFTOT; and (iii) a study of the chemical composition and physical nature of *abnormal* deposits produced in JFTOT tests, and the mechanism by which they are formed.

Experimental

Materials

The main fuels used in this study are listed in Table 1. The approved metal deactivator additive (MDA), *N,N'*-disalicylidene-1,2-propanediamine, was obtained from Octel. *n*-Dodecane was purified by passing it through an alumina column prior to use. *n*-Hexane thiol was obtained from Aldrich. The deposits formed on 6061 aluminium JFTOT tubes were largely freshly-generated, although in some cases older, retained tubes were used as illustrative examples.

Methods

A Hot Liquid Process Simulator (HLPS), modified to include a 0.45 micron filter downstream of the fuel outlet from the aluminium JFTOT tube, was used for the surface and bulk deposition studies. Temperature and time have been the two main variables used for any given fuel in the present work. Analysis of surface deposits was effected using the Ellipsometric Tube Analyser, ETA, described elsewhere.[4] Briefly, this method allows tube surface deposit thickness profiles to be measured, and integration under these profiles provides the total deposit volume. Typically *maximum* deposit thickness and deposit volume are the two parameters currently used to characterise the deposit.

JFTOT tube surface (compositional) analyses have been made using Scanning Electron Microscopy (SEM) in a grazing incidence mode at relatively low applied voltages of 3 kV and Electron Dispersive X-ray (EDX) analysis.

Results and Discussion

Comparative Production of Bulk Insolubles and Surface Deposits

A typical ellipsometric deposit thickness profile derived using ETA is shown in Figure 1 as a single slice for a typical fuel. Such profiles illustrate the increasing deposit thickness as the hottest position of the tube is reached (at a point 39.5mm from the inlet).[1] The deposit thickness then decreases beyond this point. ETA routinely measures 12 such longitudinal slices, enabling integration under the resultant surface profile to provide a measure of total deposit volume, V_{dep}. Deposit thickness, t_{dep}, and volume can therefore be used as quantification of the deposits. The time courses for deposit formation for fuel M1 are shown in Figure 2 and for fuel H at two temperatures in Figures 3 and 4; each figure includes data for particulates and surface deposits. Here, data are presented as deposition rates, either for the bulk insolubles (k_b) or surface deposits (k_s), and are based on the volume of fuel treated during a given test time and the residence time τ that the fuel is exposed to the heated tube region (*ie* 11.4s). The latter is calculated from the flow-rate f of 3 ml min^{-1} and the JFTOT test time t and the free volume between the tube and its holder calculated from the tube dimensions. Expressing the data in this way is consistent with other measures of deposit formation based on dynamic testing methods. This serves to normalise the data throughout a given JFTOT experiment, recognising that fresh fuel is being continuously passed over the heated tube, *ie*

$$k_s = \frac{V_{dep}}{ft\tau} \qquad 1)$$

and

$$k_b = \frac{w_{dep}}{ft\tau} \qquad 2)$$

for surface and bulk deposits, respectively, where V_{dep} and w_{dep} are the corresponding ETA deposit volume and weight of filtered bulk insolubles. In Figure 5 are results for M1 fuel containing (added) copper(II) naphthenate (CuM1) in the presence and absence of MDA to modify the thermal stability.

It is apparent from the deposition rate data shown in Figures 2 to 5 that complex behaviour occurs in both surface and bulk deposition regimes. For example, the bulk

insoluble deposit formation rate is seen to decrease during the early stages of the JFTOT experiments for all the fuels studied. For later JFTOT test times, the deposition rate for CuM1 shows signs of increasing. This appears to correspond reasonably well to an increase in surface deposits. These effects are illustrated for M1 and CuM1 fuels in Figure 6 in which the ratio of the rates of formation of surface deposits to bulk insolubles are presented.

It can be seen that, in the case of the highly-depositing CuM1 fuel (in the absence of MDA), the ellipsometric analyses show a steady rate of surface deposition, up to *ca.* 100 minutes into the test. Thereafter, an increase becomes apparent. Interestingly, this region coincides with the "secondary production" of bulk filterable deposits (Figure 5). Even allowing for the uncertainties associated with the quantification of the low levels of filterable deposits, the correspondence between these two sets of data is evident. It is tempting in this case to suggest that the increases in the two sets of deposits have a common origin. In the case of the corresponding MDA-treated fuel, there is little evidence for an increase in surface deposition rate over the time-scale of the experiments, with bulk particulate formation also being retarded. Deposit formation in all the fuels studied so far has been characterised by a high initial rate of bulk particulate formation, suggestive of an involvement of the clean tube surface. The reduction in the bulk deposition rate (Figure 6) appears to be accompanied by the slower rate of formation of surface deposits. The activity of the fresh tube surface may be influenced by surface metallurgical factors discussed later in this paper.

Single-run Thermal Stability Analysis

The JFTOT test is a non-isothermal method. Fuel flowing over the electrically-heated tube produces a temperature gradient as detailed in ASTM D3241. As a consequence, surface deposition generally approaches a maximum thickness at or around the "hot spot", some 40mm from the fuel inlet. Although attempts had been made with varying degrees of success in the past to quantify deposit thicknesses, only now does ETA analysis make this routine. In particular, it is now possible to determine deposit thicknesses at given positions along the tube surface which can be correlated with tube temperature profiles, thereby generating deposit thickness-tube temperature profiles from single JFTOT runs. An example of this transformation is given in Figure 7, from

which the asymmetry of the temperature profile is evident, with the upstream side of the deposit being thinner than the downstream side for the same temperature. This has been found for all of the tubes analysed in this way to date, and confirms previous SEM/EDX analyses,[2] and possibly arises from the finite kinetics of the surface deposition process. If this is indeed the case, it would seem appropriate that effects on the upstream side of the maximum deposit thickness will be indicative of the direct effects of temperature on the formation of depositing species and of deposition, and hence fuel thermal stability in general. The reproducibility of this portion of the deposition profile is illustrated in Figure 8 in which deposit thickness profiles for a single fuel at several different JFTOT operating temperatures are presented. It is evident that data on the fuel inlet side of the maximum tube temperature position are highly reproducible, whilst deviations are apparent on the outlet side. This type of analysis therefore creates the possibility of determining *from a single JFTOT run* a temperature which corresponds to a given deposit thickness *on the inlet side of the maximum deposit*. This has been done for a number of different fuels systems, and temperatures corresponding to a thickness of 120 nm (as an illustration of the approach only) are compared with the conventional visually-rated "breakpoint temperature", in Table 2. From these data, it can be seen that there is good directional agreement between results from "conventional" determinations and this new approach based on a single JFTOT run.

Analysis of "Abnormal" Deposits

The visual appearance of many abnormal deposits results from the scattering of light, suggesting the presence of some surface particulate material. Moreover, the consistent formation of abnormal deposits using fuel systems has been difficult to achieve in the laboratory. In view of the latter, in order to satisfy the requirement for reproducible abnormal deposits, a model system was developed. This comprised dodecane + 100ppm hexane thiol run at typically >300°C, for which the appearance of the deposits was similar to those observed for a sample of M1 fuel (at the lower temperature of 260°C). ETA and SEM/EDX analyses were carried out on each system. In each case, in the "abnormal" regions of the respective tubes, a high concentration of particulates in the size range 1-5 microns, comprising, predominantly magnesium and oxygen was

observed, as shown in Figure 9. Additionally, some carbon was often also found to be associated with these particles.

Figure 10 shows the "abnormal" ETA thickness profiles for a sample of fuel M1, in which the abnormal and normal regions are clearly distinguishable. Figure 11 shows comparative EDX spectra for a typical particle and the adjacent background for the M1 fuel. In this region, there is little carbon seen to be associated with the deposit, although in the background spectrum there is evidence for the presence of contaminant metals. (Cu or Zn in this instance). By way of contrast, Figure 12 shows a corresponding particle in the "normal" region at approximately 40mm from the fuel inlet, in which it can be seen that the level of carbon is substantially increased, in accord with the ellipsometric profile.

Figure 13 shows the deposit profile for the dodecane/*n*-hexane thiol system at three temperatures. The presence of magnesium-rich particles was confirmed by SEM/EDX, as above, and a representative EDX spectrum is shown for the 40mm position from the fuel inlet in Figure 14. On the basis of these observations, it is concluded that the presence of magnesium in particulate form on the tube surface must originate from the tube itself. The 6061 aluminium JFTOT tubes contain *ca.* 1% magnesium which is initially uniformly distributed throughout the aluminium matrix. Previous studies led to the conclusion that, under JFTOT conditions, magnesium "migration" to the surface occurred.[1] Although at a relatively early stage, results of recent SEM/EDX analyses, confirm changes to the surface metallurgy of aluminium tubes as a consequence of thermal/fuel treatment. A tentative explanation of the observed features of the process involves an initial redistribution, akin to a coalescence process, of the minor magnesium component of the 6061 alloy into Mg-rich surface domains, observable at the inlet end of the tube. Further along the tube, where the local surface temperatures are higher, these domains give way to pronounced Mg-rich particulates, as described above. Although initially located in the surface region, the particulates appear to be depleted further along the tube, only to be concentrated in specific regions, where their increased concentration results in an "abnormal" appearance. At the present time it is not clear whether the observations and interpretations of this part of the work is

related in any way to the increased rates of bulk particulate formation discussed earlier. These aspects are being addressed in continuing studies.

Conclusions

The present study has demonstrated the use of a combination of JFTOT/HLPS techniques and ellipsometric (ETA) analysis for characterising jet fuel thermal stability and breakdown mechanisms. The rate of formation of bulk insolubles is found to decrease as the volume of fuel treated is increased. Profiling JFTOT tube surfaces by ellipsometry has been shown to offer potential for determining fuel thermal stability from a single test. Abnormal deposits have been found to comprise mainly inorganic particulates, which have been found to be magnesium-rich in many instances. In the present work, the formation of magnesium-based abnormal deposits in a model fuel system which is devoid of magnesium, strongly implicates the JFTOT tube as the magnesium source. If this finding is confirmed during ongoing studies, this indicates that this thermal stability fail code may be an artefact of the test procedure using aluminium alloy tubes.

Acknowledgements

This project was funded by Air BP and the UK Ministry of Defence.

References

(1) Hazlett, R.N. *Thermal Oxidation Stability of Aviation Turbine Fuels*; ASTM, Ann Arbor, MI, 1991

(2) Baker, C.; David, P; Hall, D; Swatridge, R. *Proc. 4th International Conf. on the Stability and Handling of Liquid Fuels*, Orlando, FLA, 1991, 316-328

(3) Baker, C; David, P; Taylor, S.E.; Woodward, A.J. *Proc. 5th International Conf. on the Stability and Handling of Liquid Fuels*, Rotterdam, 1994, 433-447

(4) David, P.; Mogford, R.; Paduschek, P.; Taylor, S.E.; Woodward, A.J. "Development of an Ellipsometric JFTOT Tube Analyser (ETA)", Presented at *6th International Conf. On the Stability and Handling of Liquid Fuels*, Vancouver, 1997

Table 1. Fuels used in the present work.

Fuel (abbreviation)	Comments
Merox 1 (M1)	< 10ppb metals
Merox 2 (M2)	< 10ppb metals
Cu-doped Merox 1 (CuM1)	30ppb Cu added as copper naphthenate
Hydrofined (H)	< 10ppb metals

Table 2. Comparison between visually-rated breakpoints and single-run T_{120nm} values for several systems.

Fuel system	Tube number (JFTOT temperature /°C; VR)	T_{120nm} /°C	VR breakpoint /°C
M1 + 150ppb Fe naphthenate	1989 (255; <4)	238	-
Kerosene	2023 (250; <4)	250	245
CuM1	1988 (260; <4)	260	-
M1	96/113 (260; <4)	257	255
M2	2154 (290; <4P)	272	265
Jet A1/6% diesel	2016 (295; >4P)	293	285
JP8	3982 (296; <4)	296	291

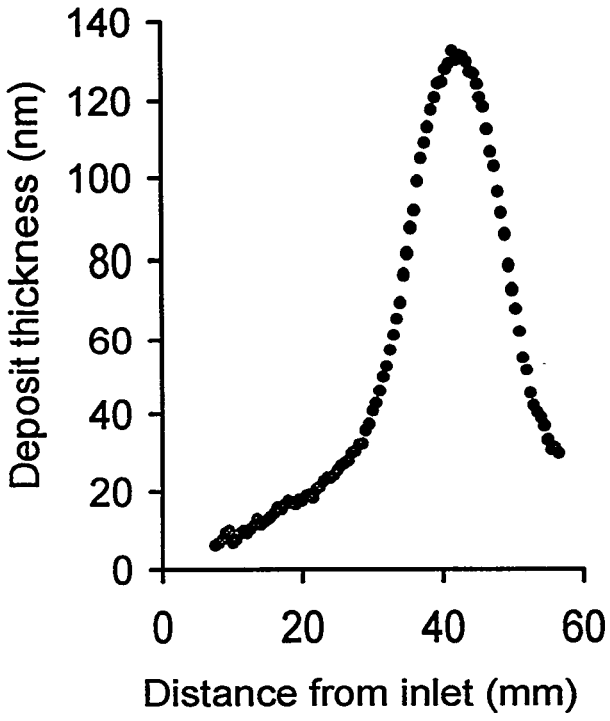

Figure 1. A typical single slice surface deposit profile for a coloured deposit.

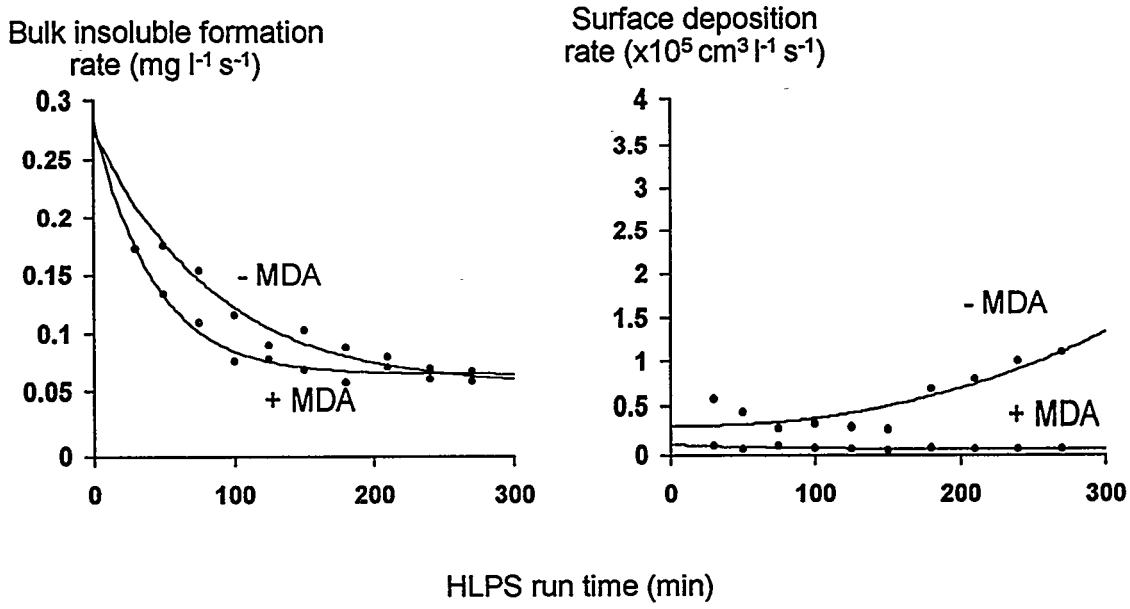

Figure 2. Surface and bulk deposition rates for Merox fuel M1 in the presence and absence of 5.7 mgl^{-1} MDA (255°C).

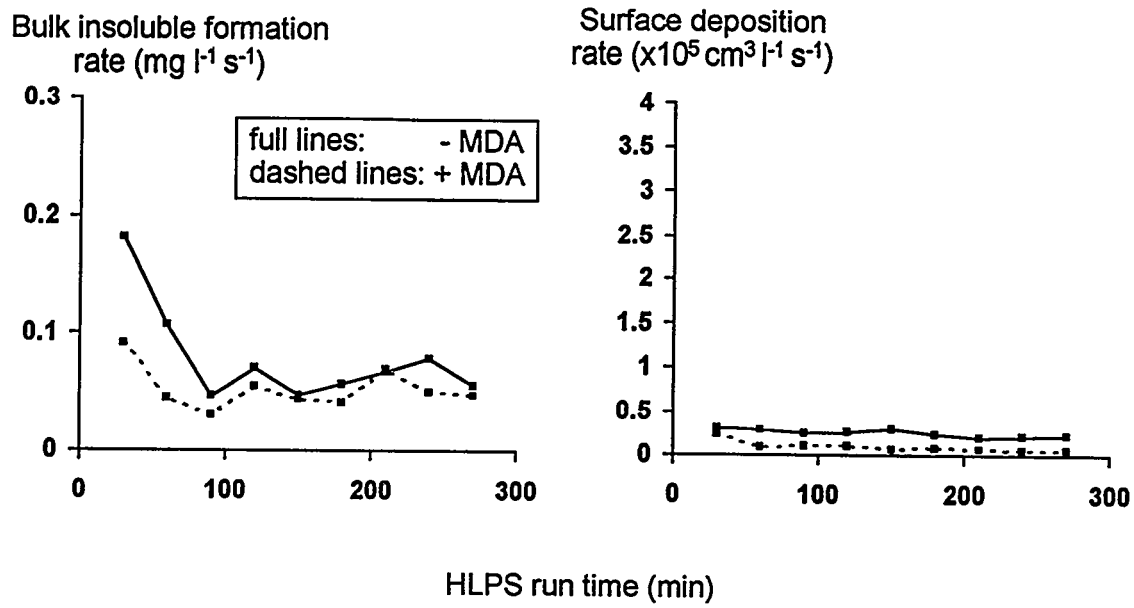

Figure 3. Surface and bulk deposition rates for hydrofined fuel H in the presence and absence of 5.7 mgl^{-1} MDA (280°C).

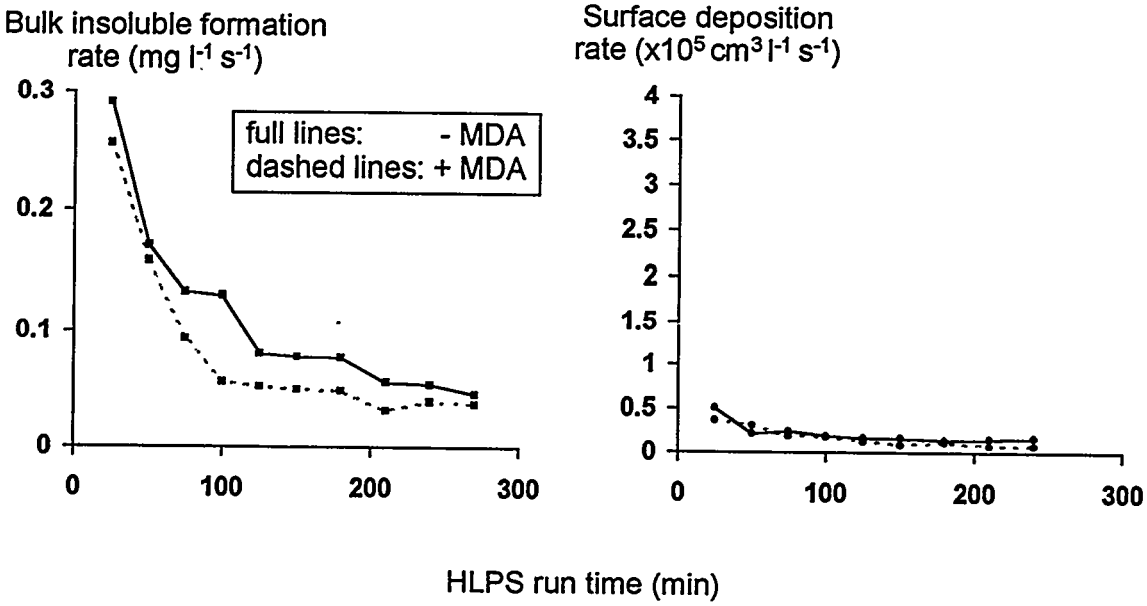

Figure 4. Surface and bulk deposition rates for hydrofined fuel H in the presence and absence of 5.7 mgl^{-1} MDA (340°C).

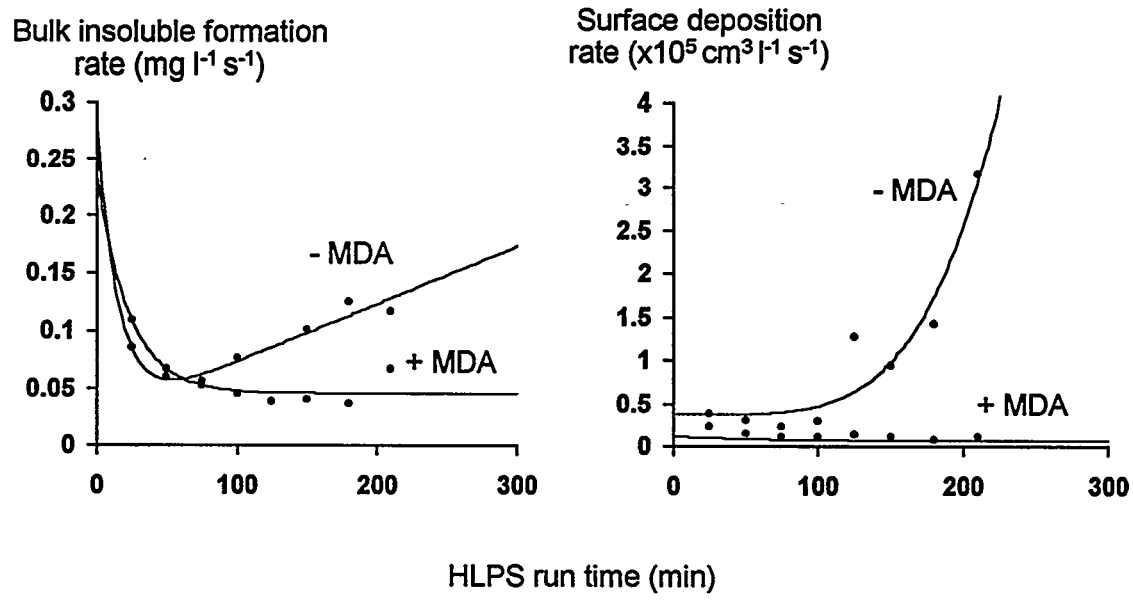

Figure 5. Surface and bulk deposition rates for CuM1 fuel in the presence and absence of 5.7 mgl^{-1} MDA (245°C).

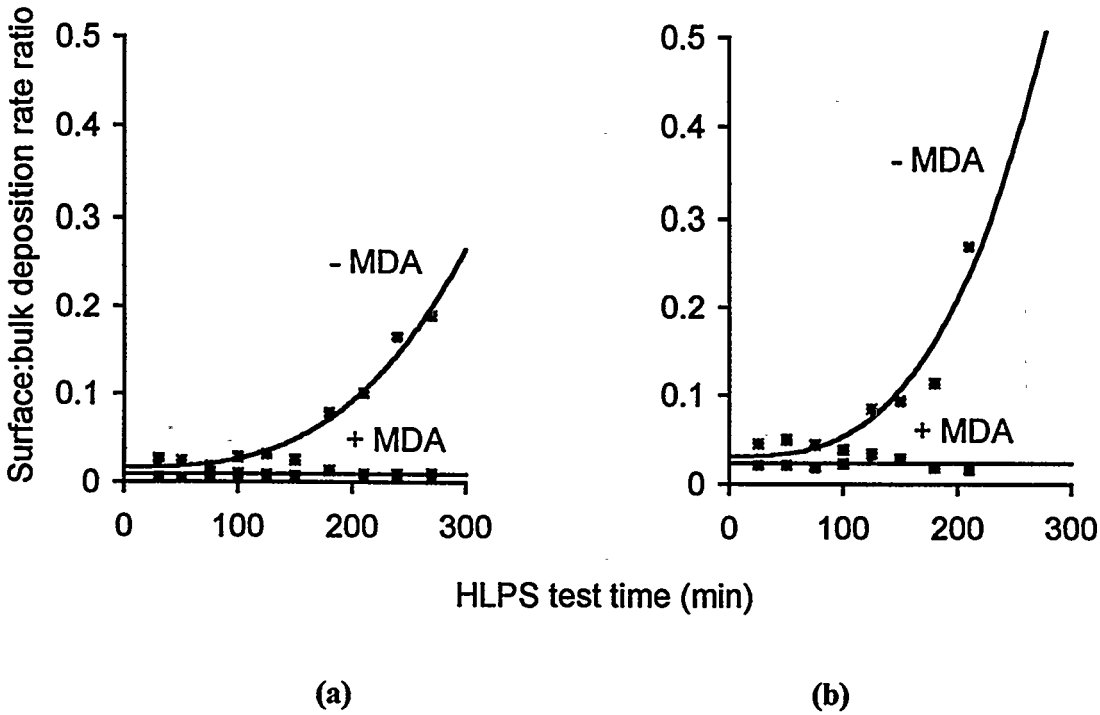

Figure 6. Ratio of surface to bulk deposition rates for (a) M1 at 255°C and (b) CuM1 at 245°C, in the presence and absence of 5.7 mgl^{-1} MDA

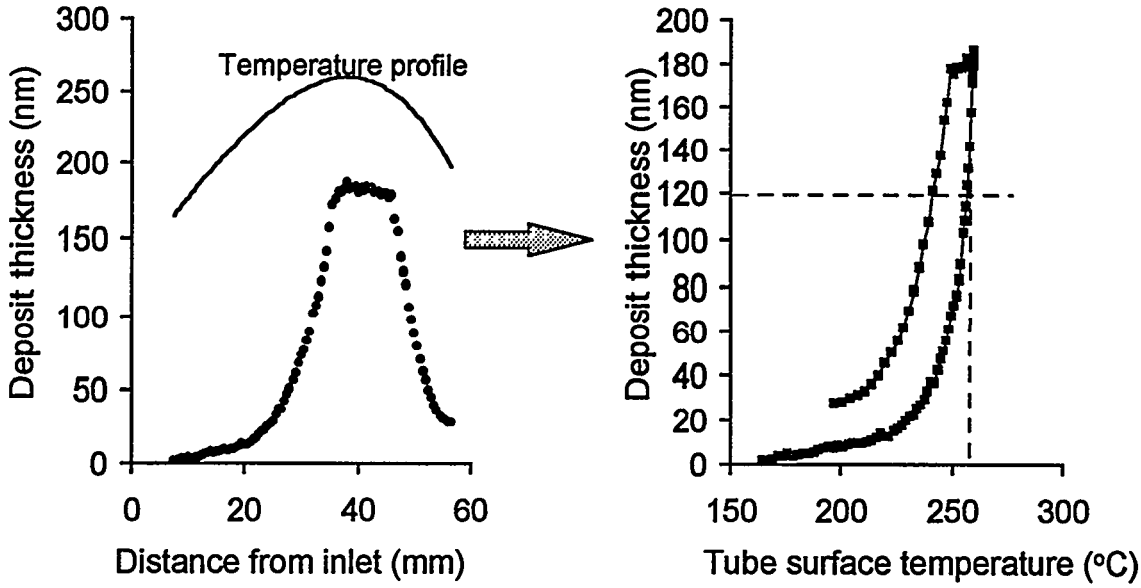

Figure 7. An illustration of the transformation between deposit thickness-distance data to thickness-temperature data for fuel M1 run at a JFTOT temperature of 260°C, indicating the "critical" temperature T_{120nm}.

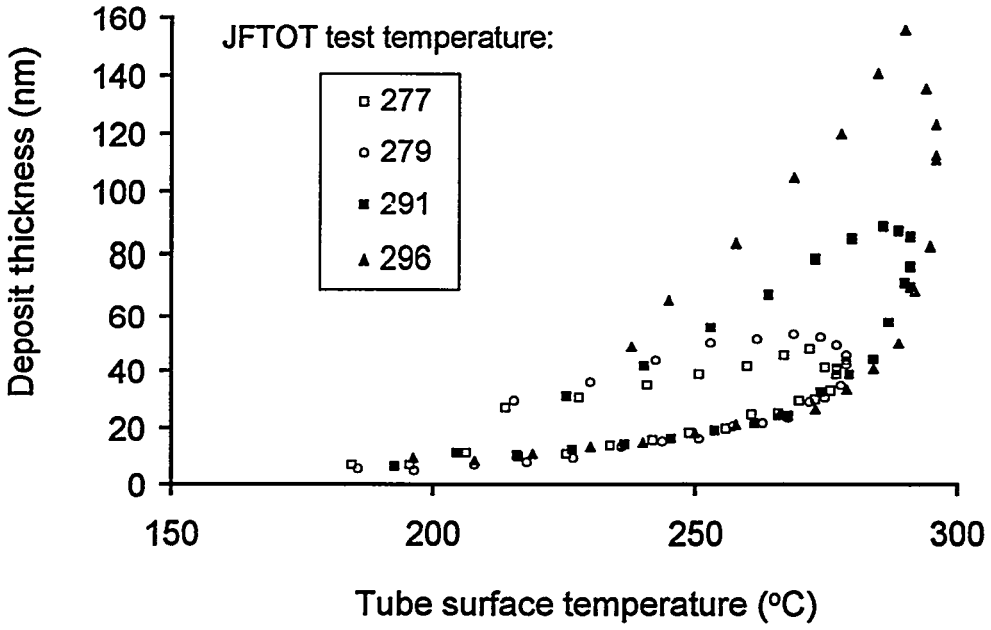

Figure 8. Deposition profiles for different JFTOT temperatures as a function of tube surface temperature.

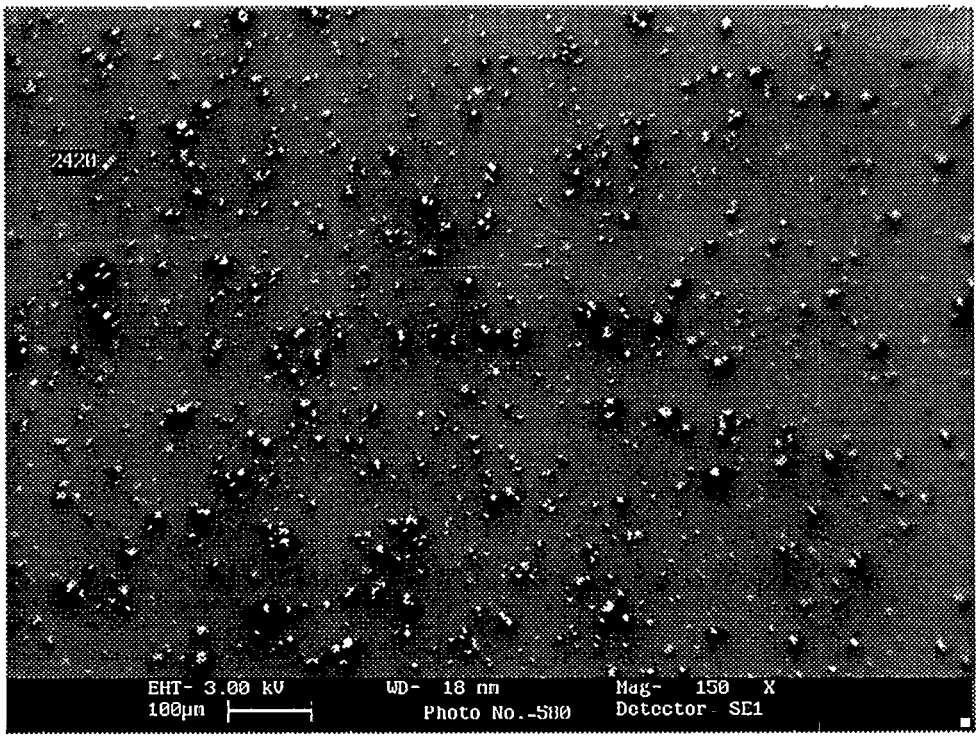

Figure 9. A scanning electron micrograph showing magnesium-rich particles in the "abnormal" region.

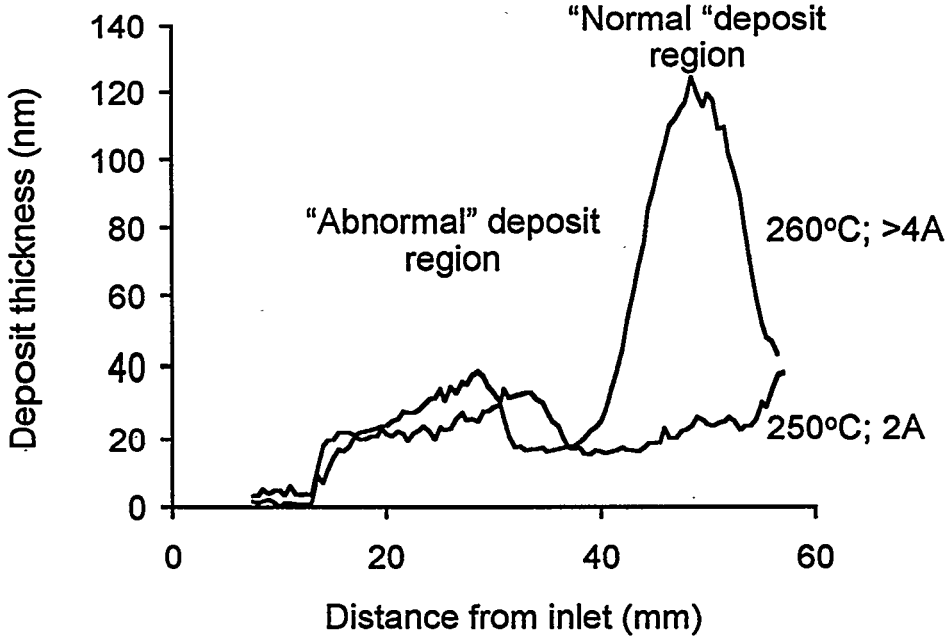

Figure 10. ETA thickness profile for a sample of fuel M1 at two different (indicated) temperatures.

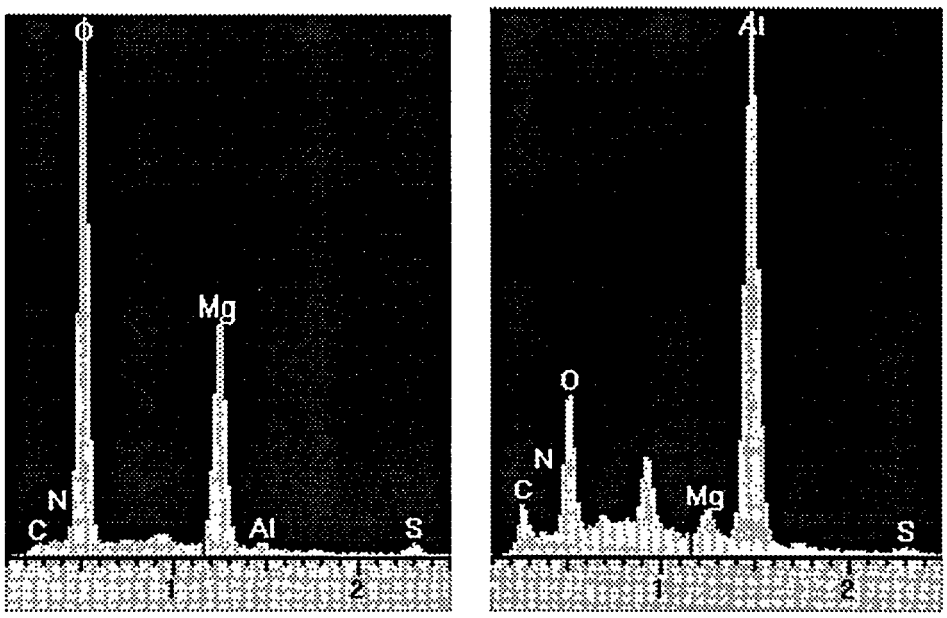

(a) (b)

Figure 11. EDX compositional analysis of (a) a particle in the "abnormal" region at 30mm from the fuel inlet and (b) the adjacent background region for fuel M1 at 260°C.

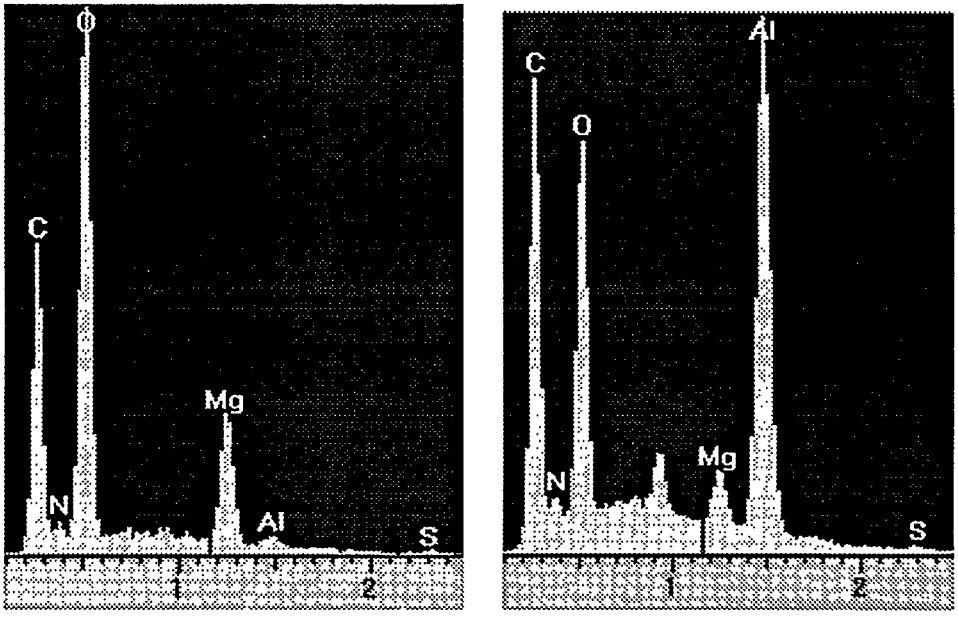

(a) (b)

Figure 12. EDX compositional analysis of (a) a particle in the "normal" region at 40mm from the fuel inlet and (b) the adjacent background region for fuel M1 at 260°C.

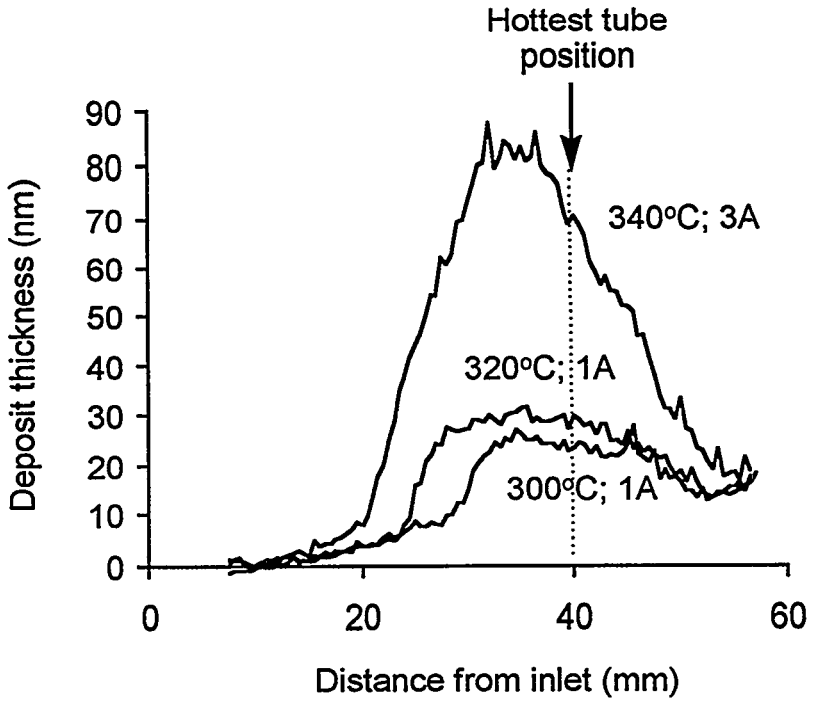

Figure 13. ETA thickness profile for dodecane + 100ppm *n*-hexane thiol at three different (indicated) temperatures. Visual ratings are also indicated.

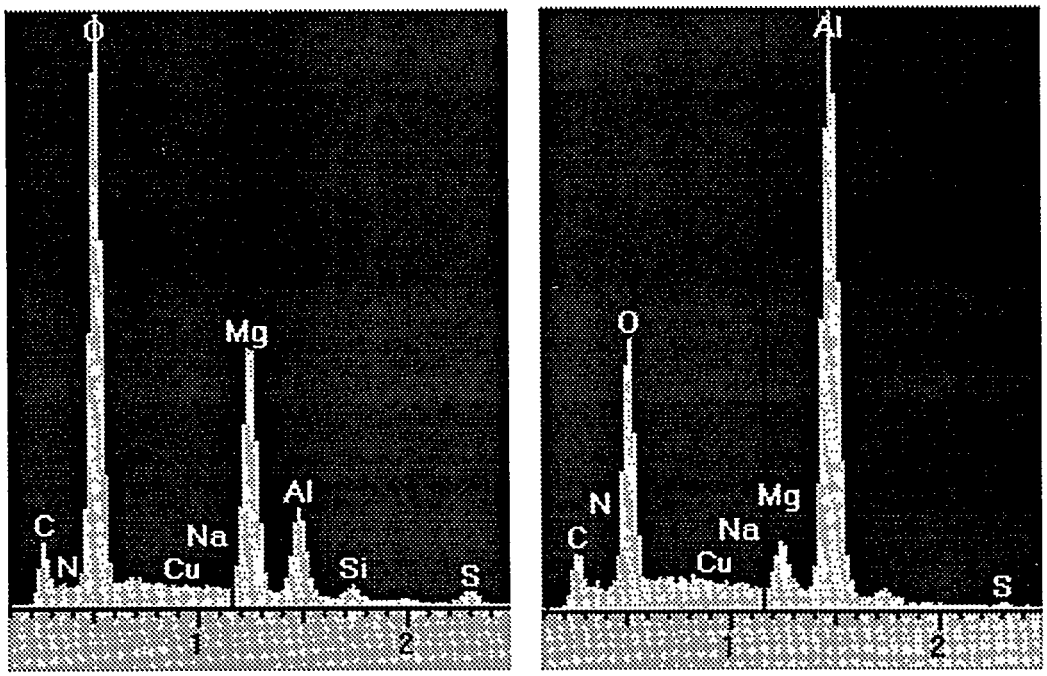

(a) (b)

Figure 14. EDX compositional analysis of (a) a particle in the "abnormal" region at 40mm from the fuel inlet and (b) the adjacent background region for the dodecane/*n*-hexane thiol system at 320°C.